COMPLEXATION OF DIVALENT COPPER, ZINC AND CALCIUM IONS BY PHOSPHATE ESTERS IN AQUEOUS SOLUTION

Ulrike Kramer

Thesis submitted in fulfilment of the requirements for the degree of

Doctor of Philosophy
at the
University of Cape Town

June 1988

The University of Cape Town has been given the right to reproduce this thesis in whole or in part. Copyright is held by the author.

The copyright of this thesis vests in the author. No quotation from it or information derived from it is to be published without full acknowledgement of the source. The thesis is to be used for private study or non-commercial research purposes only.

Published by the University of Cape Town (UCT) in terms of the non-exclusive license granted to UCT by the author.

University of Cape Town

Abstract

The role of metal ions as catalysts for numerous biochemical reactions has been the subject of many investigations. One of the most important classes of ligands are phosphate esters. In this thesis I describe the investigation of some phosphate ester-metal ion equilibria. Formation constants for the complexation of p-nitrophenyl phosphate, phenyl phosphate, 1-naphthyl phosphate, α-D-glucose-1′-phosphate, glycerol-2-phosphate, methyl phosphate, 8-quinolyl phosphate, 8-quinolyl methyl phosphate, triphosphate and fluorotriphosphate with protons, copper, zinc and calcium ions were determined by potentiometry. In addition, the complexation of 1-naphthyl phosphate, 8-quinolyl phosphate and 8-quinolyl methyl phosphate with nickel and cobalt ions was also studied. Protonation enthalpies and copper complexation enthalpies of p-nitrophenyl phosphate, phenyl phosphate, 1-naphthyl phosphate, α-D-glucose-1′-phosphate, glycerol-2-phosphate and methyl phosphate were determined by calorimetry.

A correlation between the nucleophilicity of the ester group and the magnitude of the stability constants of the proton, copper and zinc complexes of p-nitrophenyl phosphate, phenyl phosphate, 1-naphthyl phosphate, α-D-glucose-1′-phosphate, glycerol-2-phosphate and methyl phosphate is found and explained in terms of electronic induction effects, i.e. by polarisation of the phosphate oxygens by the ester group. The calorimetric results show that the desolvation of ligand and metal ion during the complexation plays an important role. The possibility of similar correlations for complexes of triphosphates is also discussed.

Acknowledgements

I would like to thank

Professor Peter W. Linder, my supervisor, for his tremendous support and encouragement throughout the course of this work

Professor Tomasz A. Modro for the help with the synthetic work

Professor Johannes J. Cruywagen of the University of Stellenbosch for permission to use their calorimeter and for many interesting discussions about calorimetry

Professor Fabrizio Marsicano of the University of Natal for many stimulating discussions and useful hints

I also like to thank all my colleages at the University of Cape Town for their continuous interest and support.

Special thanks go to Allard Schnabel for his invaluable help.

A Junior Research Fellowship from the University of Cape Town for 1985-1987 and a bursary from the South African Council for Scientific and Industrial Research for 1988 are gratefully acknowledged.

Notations

Symbols

$[x]$	concentration of x
$\{x\}$	activity of x
γ	activity coefficient
$L_pM_qH_r$	complex consisting of p ligands, q metal ions and r protons
$\beta_{L_pM_qH_r}$	overall formation constant of the complex $L_pM_qH_r$
pK	negative logarithm of a stepwise formation constant
pK_{ROH}	pK value of an alcohol
pK_a	negative logarithm of the acid dissociation constant
pH	negative logarithm of the free hydrogen ion concentration
pA	negative logarithm of the free ligand concentration
$\bar{Z}$	average number of ligands bound per metal ion
$\bar{Z}_H$	average number of protons bound to the ligand
$\bar{Q}$	average number of protons displaced per metal ion upon complexation
ΔG	free energy of a complexation reaction
ΔH	enthalpy of a complexation reaction
ΔS	entropy of a complexation reaction
T	temperature
I	ionic strength
z	charge of an ion
n	number of moles
E_0	electrode intercept
R	Hamilton R factor
emf	electromotoric force
k	hydrolysis rate constant
δ	nmr chemical shift

List of abbreviations used in tables

std.dev.	standard deviation
n_t	number of titrations
n_p	number of data points
I	ionic strength in mol/l
K	kind of titration: A: titration with acid solution
	B: titration with hydroxide solution
	M: titration with metal ion solution

Terminology

protonation constant: equilibrium constant for the reaction $pL+rH \rightleftarrows L_pH_r$

formation constant: equilibrium constant for the reaction $pL+qM+rH \rightleftarrows L_pM_qH_r$

stability constant: formation constant

protonation curve: plot of $\bar{Z}_H$ against pH

deprotonation curve: plot of $\bar{Q}$ against pH

formation curve: plot of $\bar{Z}$ against pA

speciation plot: plot of the concentrations of the various complexes formed by a ligand with metal ions and protons against pH

Contents

Structures of the ligands investigated in this thesis

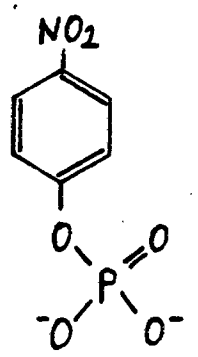

p-Nitrophenyl phosphate

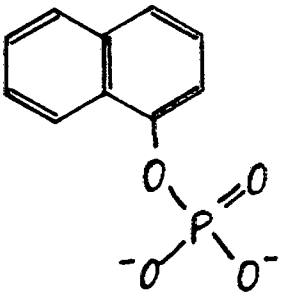

1-Naphthyl phosphate

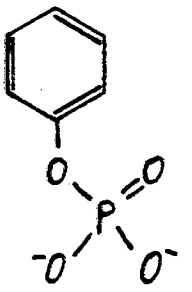

Phenyl phosphate

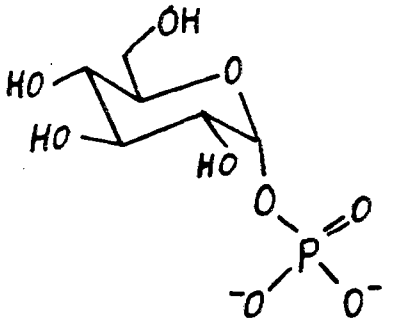

α-D-Glucose-1'-phosphate

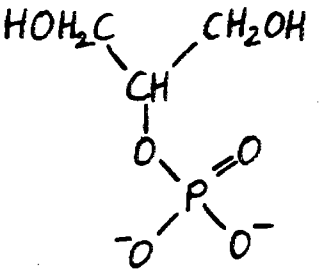

Glycerol-2-phosphate

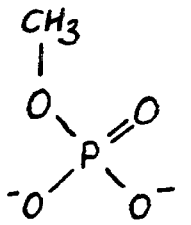

Methyl phosphate

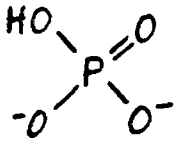

Hydrogen phosphate

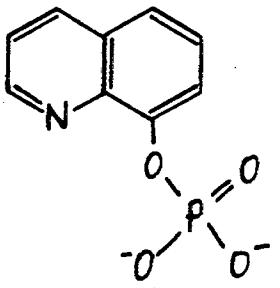

8-Quinolyl phosphate

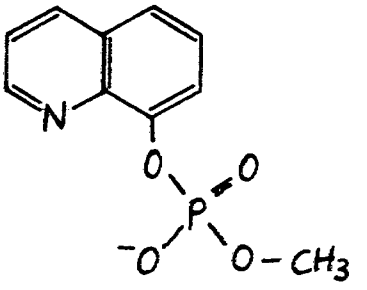

8-Quinolyl methyl phosphate

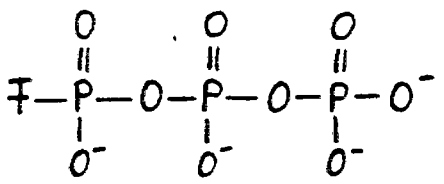

Fluorotriphosphate

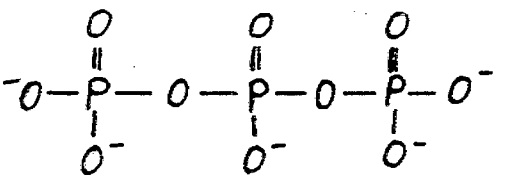

Triphosphate

1. INTRODUCTION

1.1 The role of metal ions and phosphate esters in biological systems

It has long been recognized that metal ions are very important to many vital functions of the living organism [1-4]. For example, they can form a metal complex which facilitates transport through membranes or induces a certain conformation which is more reactive than that species itself. Metal ions are essential in keeping up osmotic pressures on either sides of the cell walls, in transmitting nerve impulses and inducing muscle contractions. Many enzymatic and metabolic processes require the presence of metal ions as catalysts. Some metal ions can exist in different oxidation states and act as reducing or oxidising reagents. The role of some essential metal ions in the body is summarized in table 1.1.

Table 1.1: The role of metal ions in the organism [1]

metal ion	role
Na^+, K^+	Maintainance of osmotic pressure on either side of the cell wall, muscle contractions
Ca^{2+}, Mg^{2+}	transmission of nerve impulses, blood clotting, formation of bones and teeth, carbohydrate metabolism, phosphate transfer reactions
Mn^{2+}, Mn^{3+}	enzyme activation
Fe^{2+}, Fe^{3+}	redox reactions, oxygen transport, protein formation
Co^{2+}, Co^{3+}	vitamin B_{12} synthesis, enzyme activation
Cu^+, Cu^{2+}	production of haemoglobin, oxygen transport and storage
Zn^{2+}	enzyme activation

An imbalance of the metal ions in the body rapidly leads to malfunctions of essential processes. Wilson's desease, a disorder of the copper control mechanism, leads to an excessive deposit of copper in the liver,

brain and kidney resulting in liver cirrhosis, abnormal kidney function and progressive degeneration of the nerveous system. It is treated by the administration of copper complexing compounds, such as e.g. penicillamine or triethylenetetramine. In the treatment of inflamatory diseases, the administration of copper containing compounds has proved beneficial [5,2c,2d]. Zinc and copper compounds are also being used in the treatment of some skin diseases [2d, 2e]. The use of metal complexes as nmr imaging agents is the subject of many recent studies [6].

Among the most important ligands are amino acids, carbohydrates, carboxylic acids and phosphate esters. Phosphate esters act as phosphate group and energy transmitters as well as energy storage mediums both in animals and in plants. One of the most important phosphate esters is adenosine triphosphate (ATP). ATP is employed in enzyme activation and enzyme inhibition, and it is involved in nucleic acid structure, muscle contraction and shock production [7]. ATP is particularly important as energy storage medium because it contains an "energy-rich" phosphate bond. In the general reaction

$$ATP + H_2O \rightarrow ADP + MP + energy$$

one phosphate group of ATP is released to yield adenosine diphosphate (ADP), monophosphate (MP), and energy. The reaction is a phosphoryl transfer reaction, i.e. a phosphate group is transferred from ATP to a nucleophile (water). The released energy can then be used in the biosynthesis of other compounds, e.g. for the formation of glucose phosphate from glucose and phosphate.

Other phosphate esters have also been found to be of major importance. Glucose phosphate plays an important role in sugar metabolism where it is the immediate precursor of starch or glycogen. It is also found in calcifying cartilage. Glycerol phosphate is present in hydrolyzates of lecithins. p-Nitrophenyl phosphate is engaged in calcium transport. Many important lipids are phosphate diesters [8].

A lot of work has been published on the interactions of phosphate esters, especially nucleotides (adenosine-, guanosine-, cytidine-, uracil- and thymine mono, di, and triphosphates), with other compounds and on the activation of some of these reactions by metal ions. In view of the importance of phosphoryl transfer in biological systems, one of the most extensively studied reactions of phosphate esters are phosphoryl transfer reactions and phosphate ester hydrolysis, i.e. phosphoryl transfer to water. Numerous investigations have been carried

out on the hydrolysis of phosphate monoesters $ROPO_3(H)(H)$. In most of the systems studied [9], the monoanion was found to be the reactive species at pHs above 2, and the hydrolysis followed first order kinetics, i.e.

$$\text{hydrolysis rate} = \text{constant} * [ROPO_3H^-]$$

Thus, hydrolysis rates have a maximum at the pH where the concentration of the monoanion $ROPO_3H^-$ is highest. In the majority of cases the P-O bond is exclusively broken while the O-R bond remains intact [10]. At low pH, the neutral acid and its conjugate acid $H_3^+PO_4R$ also undergo hydrolysis, and in contrast to the hydrolysis of the monoanion, C-O and P-O bond cleavage occur at the same time.

It is still undecided whether the mechanism of phosphoryl transfer of the monoanion involves a transition state where a nucleophile (Nuc), e.g. water, is bound to the substrate (associative mechanism)

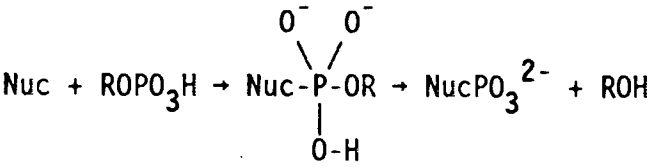

or whether the transition state involves the formation of a metaphosphate intermediate PO_3^- (dissociative mechanism)

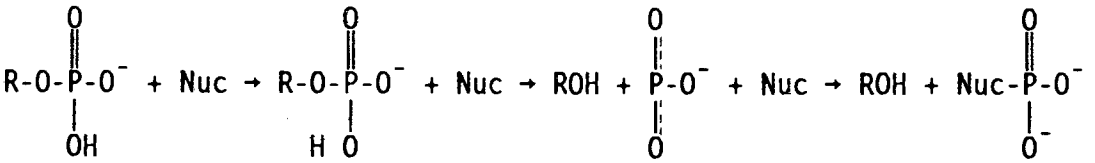

Ramsay and Cox [9] and Westheimer [10] have interpreted their own and literature data in favour of the dissociative mechanism. On the other hand, Bourne and Williams [11] and Skoog and Jencks [12] provided evidence that the reaction of pyridines with monoanions of phosphorylated pyridines and isoquinoline do not involve metaphosphate intermediates. Herschlag and Jencks [13] studied the formation of pyrophosphate from acetyl phosphate and orthophosphate and could not find any evidence for the existence of a metaphosphate intermediate. Obviously, a lot more work is needed to clarify the controversy about the structure of the transition state.

P-O bond fission must be accelerated by an electron withdrawing substituent in either of the two mechanisms. This has been confirmed in

several hydrolysis studies (e.g.[11,14,15]). Linear relationships have been found between the hydrolysis rates and the pK value of the ester, which reflects the nucleophilicity of the ester group [15]. This holds also for phosphate esters in which the substituent contains an additional binding site, e.g. a nitrogen atom or a hydroxide group.
Under normal conditions phosphoryl transfer reactions are slow. Their biological significance arises because these reactions are catalyzed by enzymes. For example, the enzyme phosphoglucomutase catalyzes the conversion of glucose-1-phosphate (G1P) to glucose-6-phosphate (G6P):

$$\text{G1P} + \text{G-1,6-diP} + \text{enzyme} \rightarrow \text{G6P} + \text{G-1,6-diP} + \text{enzyme}$$

(G-1,6-diP = glucose-1,6-diphosphate). This conversion is one of the steps involved in glycogen degradation. The reaction is sensitive to the presence of metal ions and is greatly stimulated by magnesium(II) ions [16]. Another enzyme, alkaline phosphatase, catalyzes the hydrolysis of phosphate monoesters. The action of alkaline phosphatase is dependent on the presence of zinc ions [17]. In fact, at least 30% of all enzymes have metal ions built into their structures, require metal ions for activity or are further activated by the presence of metal ions [18]. In order to gain some insight into the processes involved, the hydrolyses of several nucleotides (e.g.[19,20,21]) and of 8-quinolyl phosphate [22], pyridylmethyl phosphates [23,24], 2-(4(5)-imidazoyl) phenyl phosphate [25] and salicyl phosphate [26,27] have also been studied in the presence of divalent metal ions. Large rate enhancements have been observed in some cases. It has been suggested that the mechanism involves the formation of a chelate between the metal ion and the ligand. For example, Murakami and Sunamoto [22] found that the hydrolysis of 8-quinolyl phosphate is catalyzed by copper(II) ions, but not by nickel(II) ions. They postulate that the mechanism involves the formation of a chelate between copper(II) ions and 8-quinolyl phosphate (figure 1.1). This initial complexation step is then followed by an intramolecular rearrangement to form a transition state where the copper ion is bound by the nitrogen and the ester oxygen. Subsequently the phosphate-ester bond is cleaved and metaphosphate is released. The fact that nickel(II) ions were ineffective as catalyst was ascribed to the low affinity of nickel ions to the quinolyl nitrogen, which would not result in the formation of a chelate. The role of the copper ion in the

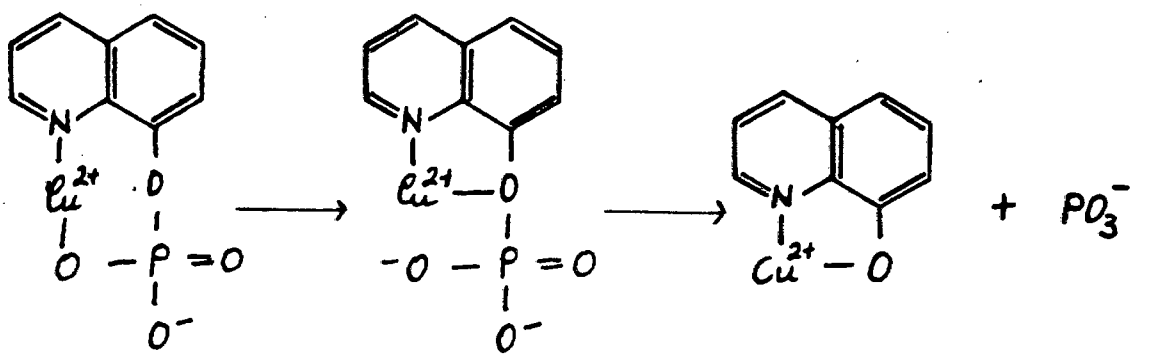

Figure 1.1: Mechanism of the copper(II) catalyzed hydrolysis of 8-quinolyl phosphate as suggested by Murakami and Sunamoto [22]

hydrolysis of 8-quinolyl phosphate is thus complexation of the leaving group, 8-hydroxyquinoline. This renders the leaving group more acidic and consequently, hydrolysis is facilitated because the P-O bond is weakened.

A different mechanism of metal ion involvement operates in the phosphoryl transfer from phosphoryl imidazol to pyridine-2-carbaldoxime, which was studied by Lloyd and Cooperman [151]. They showed that the reaction is dependent on the presence of zinc ions. The metal ion has two catalytic roles in this reaction (fig.1.2). The predominant role is shielding of the charge on the phosphate group so that the negatively charged pyridine-2-carbaldoxime anion can approach the phosphoryl imidazolium ion.

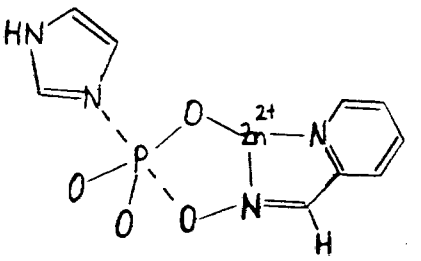

Figure 1.2: Transition state for the zinc(II) catalyzed phosphoryl transfer from phosphoryl imidazol to pyridine-2-carbaldoxime

Secondly, the zinc ion acts as a template. By coordinating to both phosphoryl imidazol and pyridine-2-carbaldoxime, the two reactants are favourably orientated towards each other so that the intramolecular rearrangement is facilitated. In addition, the reaction has been turned into a unimolecular reaction. Unimolecular reactions are generally faster than bimolecular reactions.

Another important possible role of metal ions that has been suggested is activation of the attacking nucleophile. The metal ion can increase the

nucleophilicity of a bound nucleophile by lowering its pK_a by for example converting a bound water molecule from the coordination sphere of the phosphate into a bound hydroxide. The hydroxide is then held in a favourable position to attack the ester bond. The mechanism of intramolecular nucleophilic attack by a coordinated hydroxide has been demonstrated for triphosphates. Hydrolysis studies of nucleotides [29, 31] showed that the reactive species is a metal-ligand-hydroxo complex with a metal to ligand ratio of 2:1. One of the metal ions is coordinated to the terminal γ-phosphate group whereas the second metal ion is bound to the α- and β-phosphate groups. The hydrolysis mechanism involves intramolecular nucleophilic attack at the γ-phosphorus via a bound hydroxide (fig. 1.3).

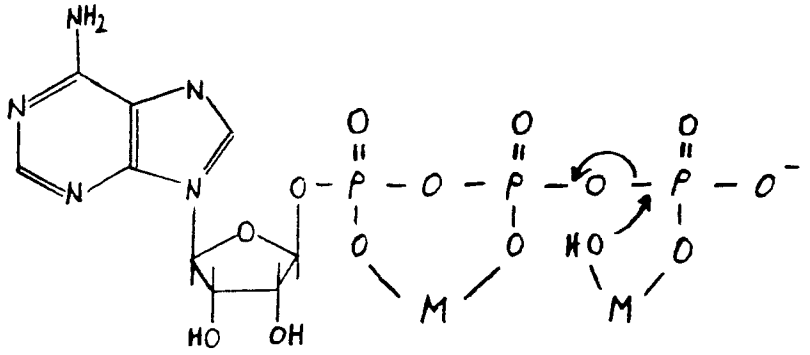

Figure 1.3: General scheme for the hydrolysis of triphosphates, illustrated for adenosine triphosphate

In a comparison of the catalytic effect of various metal ions on the hydrolysis of adenosine triphosphate and uracil triphosphate, Milburn et al. [31] confirmed that the hydrolysis rates increase with increasing tendency of the metal ion to form hydroxo complexes. The important role of hydroxo complex formation was also emphasized by Norman et al. [32], who studied the hydrolysis of triphosphate in the presence of cobalt(III) ions. They conclude that the relative nucleophilicity of the coordinated hydroxide and the γ-phosphate group determines whether or not hydrolysis occurs. If the nucleophilic character of the γ-phosphate is lower than that of the hydroxide hydrolysis will occur. If it is higher the phosphate group will act as the nucleophile and displace the hydroxide from the coordination sphere of the metal ion. Consequently, the metal ion will be chelated by the two terminal phosphate groups and little or no hydrolysis will result. The nucleophilicity of the coordinated hydroxide ion is believed not to change significantly from one system to another. It is thus the nucleophilicity of the phosphate group that determines whether hydrolysis or complexation is favoured. The

nucleophilicity of the phosphate group is ~~lowered~~ increased by electron-donating substituents and ~~increased~~ lowered by electron-withdrawing substituents.
Presently the mechanism of intramolecular attack by a coordinated hydroxide has not been demonstrated clearly for monophosphates, but there are strong indications supporting this hypothesis. Butzow and Eichhorn [20] studied the lead catalyzed hydrolysis of several nucleotides and found that hydroxylation of the metal ion was one of the important factors promoting hydrolysis. A hydrolysis study of some simple phosphate esters with trivalent cerium and lanthanum ions shows that hydrolysis rates increase with increasing tendency of the metal ion to coordinate to hydroxide ions [33,34]. Unfortunately, no attempt was made to identify the reactive species. There are also indications that the hydrolysis rate of p-nitrophenyl phosphate in the presence of calcium and magnesium ions increases drastically at high pH [13]. On the other hand, present evidence is not sufficient to support the suggestion that hydroxo complex formation plays a role in the hydrolysis of 8-quinolyl phosphate (see Appendix A).
As discussed above, there are several possibilities how metal ions can catalyze phosphoryl transfer and hydrolysis reactions. On the other hand there are some examples where metal ions have been reported to retard hydrolysis. The hydrolysis of phenyl phosphate and of glucose-1-phosphate at low pH is retarded by the presence of metal ions [24,28]. The hydrolysis of inorganic diphosphate and triphosphate has been studied in detail by Watanabe et al. [30]. At low pH the hydrolysis of uncomplexed polyphosphates is acid catalyzed. Watanabe et al. postulate the following hydrolysis mechanism (fig. 1.4):

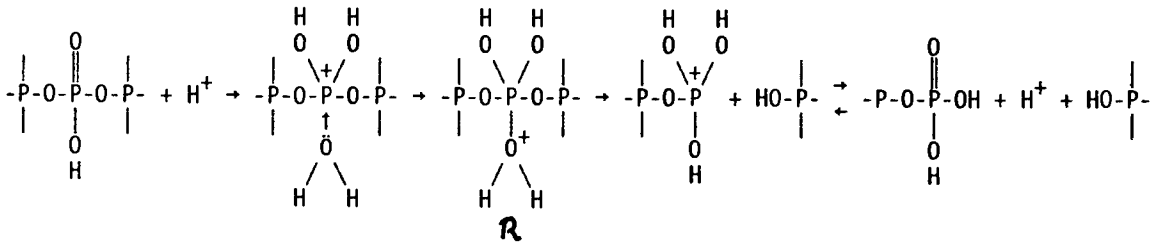

Figure 1.4: Mechanism of the acid catalyzed hydrolysis of polyphosphates, as proposed by Watanabe et al. [30].

They also studied the hydrolysis in the presence of metal ions and report that at low pH trivalent metal ions are better inhibitors than divalent and univalent metal ions. They conclude that the inhibition of the hydrolysis is due to a decrease of the amount of reactive species R (see fig. 1.4). Metal ions compete for the phosphate oxygen and displace

a proton. The resulting metal complex is less susceptible to attack by a water molecule than the protonated compund. The order of inhibition is explained by the increase in ion-exchange efficiency with increasing charge of the cation.

Several studies deal with the influence of metal ions on the rate of phosphoryl transfer reactions. Some typical examples have been presented above to illustrate different possibilities of metal ion involvement. Complex formation is a first, essential step in these reactions. It is therefore surprising how little is known about the metal complexes that form between phosphate esters and metal ions. Only few complexation equilibria of phosphates other than those of inorganic phosphates and the nucleotides have been studied in detail [35-37]. Complexation of the nucleotides with alkaline earth or transition metal ions has been found to involve mainly the phosphate moiety. Weak interactions with the potential binding sites of the ester group, such as e.g. the nitrogen of the purine base in adenosine monophosphate were found for some metal ions only [2b,38,39], e.g. for copper(II). Obviously a detailed knowledge of the complexes present should always be the prerequisite before any suggestions about reaction mechanisms can be attempted. On the other hand, it is not feasible to investigate metal-ligand equilibria for every single combination of ligands and metal ions. It therefore seemed worthwhile to investigate some metal ion-phosphoric acid ester equilibria in detail. This is the subject of this thesis. If the parameters that determine the strength of these complexes could be identified, predictions could be made of the equilibria of structurally related compounds. In addition, some of the most important factors that govern complex formation could be identified.

Apart from their key role in biological systems, organic phosphates are frequently being used as fertilizers and insecticides [40-42], but little is known about their effect on the equilibria in soil and the consequences for the bioavailability and uptake of trace metals and micronutrients by plants. In addition, the industrial applications of organic phosphates as detergents, plasticizers, stabilizers, additions to lubricating oils or as fire proofing agents is still increasing [43], and phosphate esters have even been used as metal ion extractors for trivalent metal ions [44]. A detailed knowledge of the complexes formed between organic phosphates and metal ions has thus a wide variety of applications not only to biochemical reactions, but also to numerous different environmental and industrial processes.

1.2 Objectives of the research

The initial aim of this work was to investigate the inductive effect of different substituents on the metal binding and hydrolysis rates of triphosphoric acid monoesters. It had been suggested [32] in an investigation of the cobalt(III) assisted hydrolysis of triphosphate that hydrolysis rates of triphosphates depend on both the nucleophilicity of the ester group and on the ability of the metal ion to coordinate to hydroxide ions, i.e. on the metal ion hydrolysis constant. It turned out, however, that the synthesis of triphosphoric acid esters was much more difficult than anticipated (see Appendix C). In addition, triphosphates are very complicated systems because they have three phosphate groups which can all act as binding sites. There are also several positions for bond fission during the hydrolysis. It has been demonstrated that metal ions do not only accelerate the dephosphorylation, but also the depyrophosphorylation [45,46]. In order to find out whether there exists a simple correlation beween the nucleophilicity of the ester group and the metal binding or hydrolysis properties, interest turned towards the study of monophosphoric acid esters, where different effects are more likely to be distinguished from one another. If a set of compounds were studied for which the only binding site is the phosphate group, it may be possible to see whether such a relation holds and maybe identify other parameters which play an important role. The following hypothesis was put up and investigated. The less nucleophilic, i.e. the more electron-withdrawing the substituent of the phosphate ester, the weaker will be the metal complex because negative charge is displaced from the phosphate oxygens towards the substituent. The phosphate oxygen is therefore rendered less negative and cannot attract positive cations as strongly as a more negative site. If, on the other hand, the ester group is electron-donating, the phosphate group will be polarized such that the charge density at the phosphate oxygens will increase. Cations will be bound more strongly.

If the inductive effect of the substituent as described above is the major factor that governs complex formation, the complex formation enthalpies should reflect this, too. If they do not follow the predicted trend, it may be possible to gain some insight as to which other factors affect the complex equilibria, e.g. whether or not solvation, size, or shape of the ligands play any detectable role.

Another point of interest is the possible correlation of the strength of the metal complexes with the particular properties of the metal ion. The

affinity of a metal ion for a negatively charged ligand can be measured by the strength of its hydroxo complex, M-OH. The stronger the metal-hydroxo complex, the weaker should be the metal ligand complex because the ligand and the hydroxide ions compete for the metal ion. It is also interesting to see which metal ions form metal-ligand-hydroxo complexes and to compare their stabilities with each other. The knowledge about metal-ligand-hydroxo complexes is of particular interest in connection with the hypothesis that coordinated hydroxide ions play an important role in phosphate ester hydrolysis (as discussed in section 1.1).

In this thesis I present an investigation of complex formation equilibria between simple phosphate esters and divalent copper, zinc and calcium ions. The objective of this research is to seek a correlation between the nucleophilicity of the ester group and the strength of the metal complexes of phosphoric acid esters. In addition, protonation and copper complex formation enthalpies have been determined in an attempt to identify other factors that influence the stability of the metal complexes. The possibility of similar correlations for triphosphates is also discussed.

2 CHOICE OF LIGANDS AND METAL IONS

2.1 Nucleophilicity scales

There are several applications where it is essential to know the stability of ligand-metal complexes. For example, a prediction of the sensitivity or specificity of a metal separation method must take into account not only the stability and specific properties of the complex, but also those of possible side reactions. In the computer modelling of biological fluids, e.g. plant nutrient solutions [47,48], seawater [49-51], sewage water [52], urine [53] or blood plasma [54], a data base of as many as possible stability constants of the complexes formed between all relevant metal ions and all relevant ligands is required. Not all these stability constants have been measured and it is therefore essential to develop methods in order to predict them. A lot of effort has been invested in the prediction of formation constants. Different approaches have been used, e.g. analogy with similar ligands, extrapolation or interpolation from existing data or linear free energy relationships [55,56]. Free energy relationships relate energy changes in equilibria or reactions as expressed through log β or a rate constant k with those of a chosen standard. Since Hammett [70] discovered that for substituted benzoic acids, a plot of pK against log k, the rate constant for the ester hydrolysis, is linear, similar relationships have been found for a variety of monodentate and polydentate ligands. The main types of relationships that have been considered are correlations of the magnitude of stability constants of a fixed ligand with the properties of different metal ions [57], correlations between stability constants of a series of related ligands with one particular metal ion [58-62] and correlations between the variation of stability and the composition of the solvent [63]. Numerous suggestions [57,63-69] have been made, both theoretical and semi-empirical, as to which general equation should be used to describe such relationships, and the conditions under which such relationships are valid have been discussed.

The two equations most commonly used are the Hammett equation [55] and the Taft equation [56]. Both correlate the pK or log k of a member of a certain class of ligands with a so called substituent constant σ^0 and σ^*, respectively. The Hammet equation relates pK_a (or the hydrolysis constant k) of substituted acids and bases to the pK_a (k) of the unsubstituted acid or base, pK_a^0 (k^0) by

$$pK_a = pK_a^0 - \rho \sum_i \sigma_i^0 \qquad (2.1)$$

σ_i^0 is called the substituent constant assigned to a particular substituent i and is set equal to zero for hydrogen. ρ is constant for a particular equilibrium and is called the reaction constant. It is being arbitrarily assigned the value 1 for benzoic acids.

To improve the fit of the Hammett equation to experimental data, and to extend its application range, σ^0 can be divided into different components, e.g. σ_I and σ_R, where σ_I describes the inductive effect of the substituent and σ_R the contribution due to resonance, e.g. π-electron delocalisation in benzoic acids. In addition it has been found that the position of the substituent influences the pK_a considerably, which lead to the distinction of σ values according to the position of the substituent [55].

The Taft equation is a special case of the Hammett equation; it is applicable to systems where resonance effects do not play any considerable role, e.g. to aliphatic ester hydrolysis. In the Taft equation

$$pK_a = pK_a^* - \rho^* \sum_i \sigma_i^* \qquad (2.2)$$

ρ^* and σ_i^* are again the reaction constant and the substituent constants, respectively. In contrast to the Hammett equation, σ^* equals zero for the methyl group rather than hydrogen.

Because of the numerous successful correlations of σ^0 or σ^* with pK_a values and hydrolysis constants, the substituent constants can be regarded as a general nucleophilicity scale. Because the correlation of σ^0 and σ^* was not always favourable for phosphorus compounds, however, it has been suggested [71] that a different set of substituent constants σ^ϕ should be used. The authors explain the need for the special set by the fact that although electronic effects of the substituents are most probably of the same nature as those at carbon atoms, there are specific differences in the resonance effects. Carbon binds substituents through its π-electrons whereas binding at phosphorus involves d-electrons. Unfortunately, none of the nucleophilicity scales σ^0, σ^* or σ^ϕ could be used in this thesis. Such constants were not available for all the ligands studied. Rather than trying to estimate substituent constants by some more or less accurate procedure, a different measure for the nucleophilicity of the ester group was looked for. The possibility of using the -O-H stretching frequencies of the substituent alcohols was discarded because apart from the fact that again not enough data were available, it has been demonstrated that -O-H stretching frequencies do not correlate with hydrolysis rate constants [15]. Nmr chemical shifts

are pH dependent and although they have been successfully applied as structural parameters [15,73] they are somewhat problematic. The pK value of the substituent alcohol pK_{ROH} had also been successfully used as a structural parameter to correlate hydrolysis constants of aryl phosphates with a property of the aryl moiety [11]. The pK value of the substituent alcohol, pK_{ROH}, was eventually chosen as the structural parameter to be used in this thesis to describe the nucleophilicity of the substituent R. The higher the pK_{ROH}, the higher the nucleophilicity. pK_{ROH} values of alcohols are normally measured by potentiometry or - especially if the pK is high as in the case of the simple alkyl alcohols- by spectrophotometric techniques. The alcohol itself is often used as the solvent rather than water. Therefore some caution must be applied when comparing the pK values. pK values measured in solvents less polar than water tend to be lower than those measured in water [74].

2.2 Choice of ligands

In order to ensure that metal binding occurs only at the phosphate moiety, the substituent R must be chosen so that it does not contain any binding sites. This is important as it is very difficult to account for the increase of stability due to chelation when comparing stability constants of different ligands.

The following set of monophosphates has been chosen for the present study: p-nitrophenyl phosphate, phenyl phosphate, 1-naphthyl phosphate, α-D-glucose-1'-phosphate, glycerol-2-phosphate and methyl phosphate.The pK values of the substituent alcohols are summarized in table 2.1.

The glycerol and glucose molecules (fig.2.1) contain more than one hydroxide group.

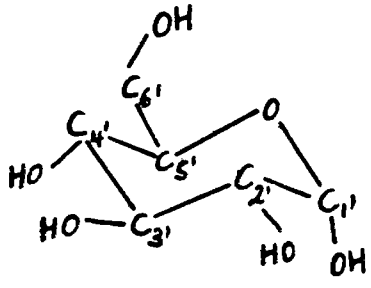

Figure 2.1a: α-D-Glucose

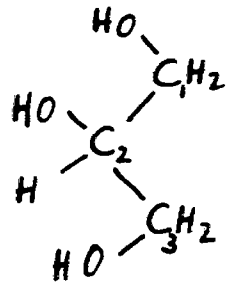

Figure 2.1b: Glycerol

The pK of all but one OH group are so high that they have not been determined. It is therefore justified to assume that these OH groups do not have any disturbing effect on the equilibria of the phosphate group. In order to predict the complexation of glycerol phosphate and glucose phosphate from pK_{ROH} the phosphate group must be attached to the "right" oxygen, i.e. the oxygen which pK_{ROH} refers to. In the case of glucose, pK_{ROH} has been assigned to the 1′ position [75] which means that glucose-1′-phosphate is a member of the series of compounds under investigation, whereas glucose-6′-phosphate is not. Assignment of the pK_{ROH} of glycerol to any of the three possible OH groups could not be found in the literature. I therefore attempted to assign the pK_{ROH} to either the central or a terminal OH group by carbon nmr of solutions containing 0.5 mol/l glycerol and varying amounts of NaOH (0-8 mol/l). The chemical shifts of both the central and the terminal -C-OH groups was found to increase with increasing hydroxide concentration by exactly the same amount. It is therefore impossible to assign the pK_{ROH} to one particular site. This indicates that the protons are being shared by the three OH groups and that these cannot be distinguished. Consequently it cannot be decided which of the two isomers, glycerol-1-phosphate or glycerol-2-phosphate belongs to the series of phosphate esters under investigation. As the pK=14.15 seems to be an average for all three protonation sites (see above), it seems most likely that neither of the two isomers fits into the series. It is still interesting, however, to study the complexation of glycerol phosphate in order to see whether a linear free energy relationship holds for all phosphate esters (not containing binding sites in their ester group), or whether such a relationship is restricted to certain types of phosphate esters.

It would have been desirable also to investigate the di- and triphosphate analogs in detail. Unfortunately, there are few published synthetic routes other than for the nucleotides, and often the amount of substance obtained is minute compared to the amounts of starting material used, so that these procedures cannot be applied if several grams of product are required. An attempt was made to synthesize methyltriphosphate, phenyltriphosphate and p-nitrophenyltriphosphate but the products obtained were not pure enough (see Appendix C). Instead, it was decided to investigate the complexation behavior of fluorotriphosphate. This is not a true analog as it is not a phosphate ester because the substituent F is bound directly to the phosphorus atom. The effect of the strongly electronegative F should be enlarged with the missing oxygen which would have acted as a type of buffer.

Table 2.1: Protonation constants of alcohols

alcohol	log β	I	T	solvent	reference
methanol	16.05	1.0 LiCl	20°C	methanol	[76]
	16.60	1.0 $[CH_3]_4NCl$	20°C	methanol	[76]
	15.89	1.0 Li tosylate	20°C	methanol	[76]
	16.68		25°C	methanol	[77]
glycerol	14.15				[78]
glucose	12.28	0	25°C	water	[79]
	12.46	0	25°C	water	[80]
1-naphthol	9.411	0.01	25°C	water	[81]
	9.416	0.02	25°C	water	[81]
	9.416	0.04	25°C	water	[81]
	9.36	0.063	25°C	water	[82]
phenol	9.996	0.02	25°C	water	[83]
	9.999	0.05	25°C	water	[83]
	10.003	0.1	25°C	water	[83]
	9.79	0.5 KNO_3	25°C	water	[84]
	9.85	0.027 $NaClO_4$	25°C	water	[84]
	9.80	0.1 $NaClO_4$	25°C	water	[85]
p-nitrophenol	6.89	0.1 $NaClO_4$	25°C	water	[85]
	6.96	0.5 KNO_3	25°C	water	[84]
	7.16	0.05	25°C	water	[82]
	7.152	0.02	25°C	water	[83]
	7.148	0.03	25°C	water	[83]
	7.140	0.04	25°C	water	[83]
	7.144	0.06	25°C	water	[83]
	7.138	0.08	25°C	water	[83]

2.3 Choice of metal ions

The tendency of a metal ion to form M-OH bonds is expressed by its hydrolysis constants

$$M^{z+} + H_2O \rightleftharpoons MOH^{(z-1)+} + H^+ \qquad \log \beta = \frac{[MOH^{(z-1)+}][H^+]}{[M^{z+}]} \qquad (2.3)$$

Divalent metal ions were used in this study because their hydrolysis constants cover a rather wide range (-3 to -14 [86]). Their behaviour in aqueous solution is well characterized and they themselves and their metal complexes can be studied at physiological pHs. Results can be directly applied to biochemical reactions where divalent metal ions are abundant and play an important role in several metabolic processes.

Initially, it was thought that the metal ions Ca^{2+}, Zn^{2+}, Cu^{2+}, and Hg^{2+} or Sn^{2+} would be a suitable set where Hg^{2+} or Sn^{2+} would serve as probe for a strongly hydrolyzing metal ion; Cu^{2+} and Zn^{2+} has intermediate and Ca^{2+} has low hydrolysis power.
The hydrolysis constants of these divalent metal ions are summarised in table 2.2

Table 2.2: Hydrolysis constants of divalent metal ions at T=25°C and I=0 [86]

metal ion	Ca^{2+}	Zn^{2+}	Cu^{2+}	Hg^{2+}	Sn^{2+}
hydrolysis constant	-12.85	-8.96	-8.00	-3.40	-3.40

However, preliminary experiments with the monophosphoric acid esters showed that with tin and mercury precipitates occurred over the whole pH region (as in the case of mercury and orthophosphate [87]), so that complexation with these two metal ions could not be studied.

3 EXPERIMENTAL APPROACH

3.1 Choice of method and experimental conditions

Several methods are applied to investigate metal complexes in solution; e.g calorimetry, solvent extraction, absorption spectroscopy, polarimetry, nuclear magnetic resonance spectroscopy (nmr), infrared spectroscopy and potentiometry [88,89]. Potentiometry is widely used as one of the most accurate and sensitive techniques to determine stability constants and has also been used in this investigation. During a potentiometric titration, the hydrogen ion concentration is measured as a function of the volume of titrant added to a solution containing ligand, metal ion and strong acid. In order to obtain the protonation constant, the hydrogen ion concentration can be compared to the expected hydrogen ion concentration if no ligand is present. The protonation constants are obtained by an optimization procedure by means of a computer program, e.g. ESTA [90] or MINIQUAD [91]. Similarly, metal complex formation constants are obtained by comparing the hydrogen ion concentration of a solution containing ligand and metal with that of a solution of the uncomplexed ligand. The sensitivity to pick up metal complexation can, in principle, be greatly enhanced by the use of metal ion sensitive electrodes. They can directly measure the concentration of uncomplexed metal ions rather than determining their concentration indirectly via the effect their complexation has on the release or uptake of hydrogen ions by the ligand, as measured by a glass electrode. Unfortunately, some of the presently available metal ion sensitive electrodes have slow response times or are sensitive to the presence of other ions which interfere with the electrode reaction. The precision that can be obtained is often lower than that of a glass electrode [93]. For some metal ions, e.g. zinc, such electrodes have not yet been developed. In the potentiometric investigations undertaken in this thesis, glass electrodes were used throughout.

There are two important methods used in the determination of reaction heats: calorimetry and potentiometry. In the potentiometric approach, the formation constant of the complex under investigation is measured at different temperatures. ΔH is calculated from the slope of a plot of ln K versus 1/T according to the van't Hoff equation

$$\frac{\partial \ln K}{\partial T} = \frac{\Delta H}{RT^2} \qquad (3.1)$$

Integration of the van't Hoff equation (eq. 3.1) leads to

$$\ln K_1 - \ln K_2 = \frac{\Delta H}{R} \left(\frac{1}{T_2} - \frac{1}{T_1}\right) \qquad (3.2)$$

In the derivation of equation 3.2, it has been assumed that both ΔS and ΔH do not vary with temperature. This assumption is not normally valid but in many cases the variation is negligible if the temperature range is not too large. Calorimetry is a more direct method to determine ΔH and no assumptions with respect to ΔH or ΔS have to be made if isothermal conditions are employed. Data obtained from calorimetric measurements are therefore believed to be more accurate. Hence in the present work the calorimetric approach was chosen to determine reaction heats of phosphoric acid esters.

Nuclear magnetic resonance spectroscopy was used to assign the various possible binding sites of a ligand.

Although the aim of this work is to study the influence of different substituents on the metal binding properties of phosphate esters, one might still want to apply the results obtained here to biochemical systems. Therefore the experimental conditions should resemble the biological environment as closely as possible. The ionic strength of most body fluids is around 0.15 mol/l, and sodium chloride is present in high concentrations, so that a 0.15 mol/l solution of sodium chloride constitutes a suitable background electrolyte and was employed in the studies of the monophosphates. Triphosphoric acid, however, complexes sodium ions to a non-negligible extent [35], so that the triphosphates were studied in tetramethylammonium chloride solution. Triphosphoric acid does not form complexes with the tetramethylammonium ion [93]. Competition between the metal ion under investigation and the ions of the background electrolyte is thus avoided. The ideal temperature for an application in biological systems would be 37°C. At 37°C it would have been necessary to ensure that the whole titration setup is kept insulated in order to avoid vapour condensation inside the titration assembly for the potentiometric titrations. Besides, most formation constants and enthalpies found in the literature were determined at 25°C. It was therefore decided to perform all experiments at 25°C, thus avoiding the insulation problem and having the advantage of being able to compare directly the results with literature values.

3.2 Potentiometry

3.2.1 Titration apparatus

The potentiometric titrations were performed in a titration vessel using a Metrohm automatic burette (Dosimat E635) controlled by a Metrohm automatic titration controller (Titroprocessor E636), which also recorded the experimental emf readings and the volume of titrant added. The emf was measured by a glass electrode (Metrohm 1047) with a calomel reference electrode (Metrohm 1028). The calomel electrode was filled with saturated sodium chloride solution in order to match the background electrolyte and to minimize the liquid junction potential. The titration vessel was thermostatted at 25±0.1°C with a Lauda thermostat. In order to exclude carbon dioxide and oxygen a nitrogen atmosphere was maintained in the vessel. Before being admitted to the titration vessel the high purity nitrogen was passed through a sequence of wash bottles for further purification. The five bottles contained:

1. 50% potassium hydroxide to remove carbon dioxide
2. Fieser's solution [94] to remove oxygen
3. distilled water
4. an empty bottle (trap) thermostatted at 25°C
5. a solution of the background electrolyte (0.15 mol/l sodium chloride or tetramethylammonium chloride solution thermostatted at 25°C

The nitrogen was released to the atmosphere via a trap containing the background electrolyte. This prevents back diffusion.
The schematic of the setup is shown in figure 3.1.

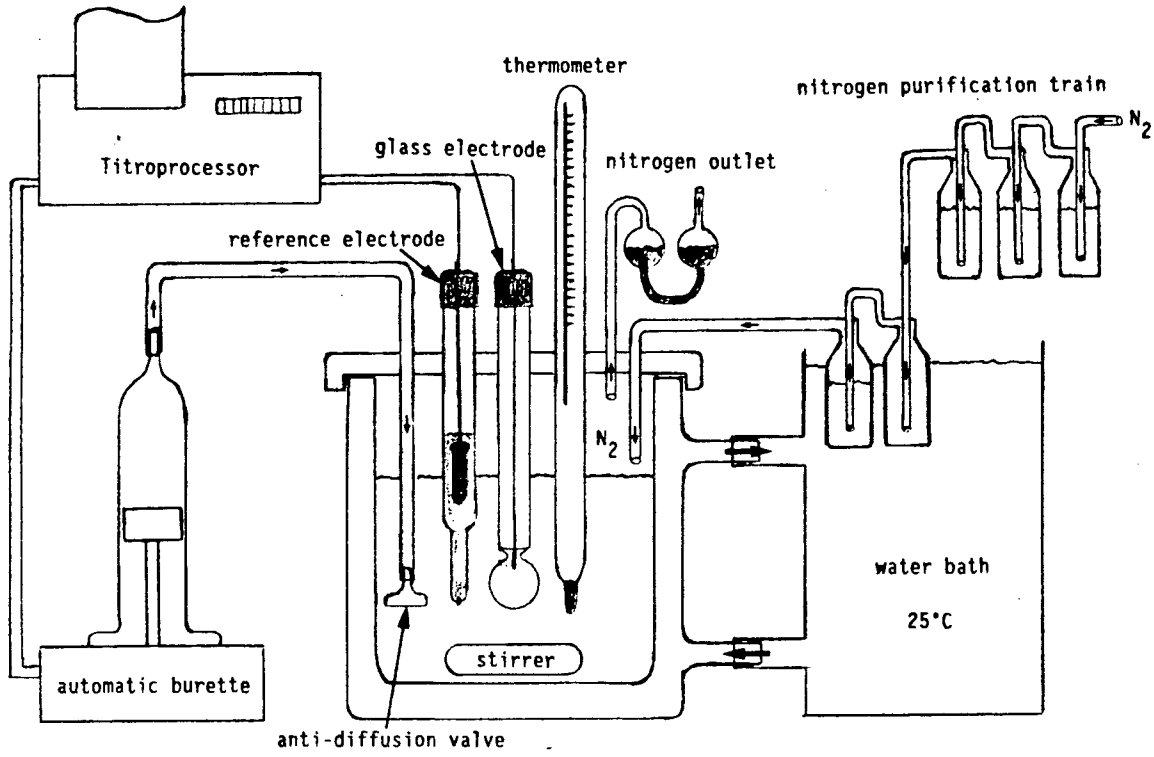

Figure 3.1: Schematic setup of the titration apparatus

3.2.2 Performance of the titrations

Two different approaches were used in the titrations:

1. Titration with hydroxide solution or hydrochloric acid solution (0.01-0.02 mol/l):

   Acidic solutions with ligand to metal ratios between 4:1 and 1:4 were titrated with hydroxide solutions (0.1-0.2 ml aliquots) until a precipitate formed. Protonation constants were determined from titrations without metal ions. Reversibility of protonation titrations was checked by titrating acidic solution with base and basic solution with hydrochloric acid.

2. Titration with metal chloride solution (0.02-0.05 mol/l):

   The ligand solution was brought to the desired pH by titration with hydroxide or hydrochloric acid solution. Metal chloride was then added (0.1 or 0.2 ml aliquots). Several titrations at different pHs were performed.

The first approach has the advantage that the entire pH range can be covered in one experiment. The second approach has the advantage that a considerably greater range of extent of complexation can be attained without interference by precipitate formation. This is especially useful in the study of weakly complexing ligands. Some of the ligands were studied by both methods.

Two different glass electrodes were used in turn. At 25°C their emf reading E is related to the pH of the solution by $E = E_0 - 59.16 \log [H]$. E_0 values shift with time and have to be determined frequently. Initially, the electrodes were calibrated by titration of ligand solution in the low pH region before metal solution was added, and E_0 calculated by ESTA. Later, however, they were calibrated weekly in acid-base titrations. Prior to each metal-ligand titration, the emf of a hydrochloric acid solution was compared with the reading the same hydrochloric acid solution gave prior to the initial acid-base calibration. E_0 values were adjusted accordingly. They were found to differ by less than 0.1 mV, i.e. within error from the E_0 found in the ligand titration, so the second approach was adopted.

3.2.3 Data Analysis

In any solution containing metal ion M, a strong acid H and a ligand L complexation can occur. The complexes can be characterized by their overall thermodynamic equilibrium constants $\bar{\beta}$:

$$pL + qM + rH \rightleftarrows L_pM_qH_r$$

$$\bar{\beta} = \frac{\{L_pM_qH_r\}}{\{L\}^p\{M\}^q\{H\}^r} \qquad (3.3)$$

Negative r refers to the removal of H and {x} is the activity of the species x.

Alternatively, complexes can be described by stepwise formation constants K. The corresponding reaction is the addition of one ligand molecule, one metal ion or one proton to an already existing complex. For example, the formation of the complex L_2MH can be regarded to occur in three complexation steps and can be described by the three stepwise formation constants K_1, K_2, and K_3:

$$L + H \rightleftarrows LH \qquad K_1 = \frac{\{LH\}}{\{L\}\ \{H\}}$$

$$LH + M \rightleftarrows LMH \qquad K_2 = \frac{\{LMH\}}{\{LH\}\ \{M\}}$$

$$LMH + L \rightleftarrows L_2MH \qquad K_3 = \frac{\{L_2MH\}}{\{LMH\}\ \{L\}} \tag{3.4}$$

The overall stability constant for the formation of L_2MH, β_{L_2MH}, is the product of all n stepwise stability constants K_n:

$$\beta_{L_pM_qH_r} = \prod_1^n K_n \tag{3.5}$$

There is only one way to define the overall stability constant, but there are various possibilities to define stepwise formation constants. In the above example one could have built the complex L_2MH by subsequently forming LM, L_2M, and then L_2MH. Although the use of stepwise formation constants can be employed to indicate the proposed mechanism of the complex formation during a titration, overall stability constants are unambiguous without having to state the particular reaction step they refer to.

Thermodynamic equilibrium constants are defined in terms of activities. In practice activities are very difficult to measure and are normally unknown. Therefore, one usually defines stability constants in terms of concentration:

$$\beta = \frac{[L_pM_qH_r]}{[L]^p[M]^q[H]^r} \tag{3.6}$$

All equilibrium constants reported in this thesis are defined according to equation 3.6.

With $\{x\} = \gamma_x[x]$, where γ_x is the activity coefficient of x we get:

$$\beta = \frac{\{L_pM_qH_r\}}{\{L\}^p\{M\}^q\{H\}^r} \cdot \frac{\gamma_{M_p}\ \gamma_{M_q}\ \gamma_{H_r}}{\gamma_{L_pM_qH_r}} = \tilde{\beta}\cdot\gamma \tag{3.7}$$

β will only be constant if γ is kept constant. Activity coefficients vary with varying ionic strength $I = \frac{1}{2}\sum_i z_i^2[x_i]$ (z_i is the charge of species i) i.e. $\gamma = f(I)$. In order to keep γ constant, the ionic strength must be kept constant. This can be achieved by carrying out the investigations in a large excess of inert background electrolyte. The

background electrolyte must not participate in any reactions and its concentration must be high compared to the concentrations of the reacting species M, L and H so that it is always the dominant contribution to the ionic strength I. Stability constants determined in this way are valid at the ionic strength and for the background electrolyte employed only. Strictly, they cannot be transferred to other systems. On the other hand, it is not practicable to determine stability constants at every single ionic strength. Therefore procedures have been developed to convert stability constants from one ionic strength I to another. For example, the Debye-Hückel theory relates the activity coefficient γ_i of the ion i to the ionic strength I:

$$- \ell n\ \gamma_i = \frac{z_i^2 A \sqrt{I}}{1 + a_i B \sqrt{I}} \qquad (3.8)$$

where z_i is the charge of the ion, A and B are constants, and a_i is an ionic size parameter.
The derivation of the Debye-Hückel equation is based on the following assumptions:

- complete dissociation of the electrolyte
- non-ideal behavior of the ions is caused by interionic attractions
- no interaction with the solvent
- the ions are spherically symmetrical
- the Boltzmann distribution function applies.

The Debye-Hückel theory is a good description in very dilute solutions. At high ionic strength, deviations become large. Therefore several attempts have been made to improve the theory by incorporating e.g.

- interactions between solute and solvent
- solvent orientation
- dielectric saturation
- different interaction potentials leading to different distribution functions
- overlap of hydration spheres (i.e. no longer hard spheres).

All the theories involve experimental parameters, e.g. an ionic size parameter which are normally refined from experimental data. The whole problem is thus not yet satisfactorily solved.
If only small changes in ionic strength occur, an extended form of the Debye-Hückel equation

$$\gamma_i(I) = \frac{z_i^2 A \sqrt{I}}{1 + a_i B \sqrt{I}} + c_i I, \quad \text{where } c_i \text{ is an additional constant} \qquad (3.9)$$

has been found useful [95]. Satisfactory results are obtained by this equation. This method was used if stability constants had to be transferred to a different ionic strength to be comparable with experimental results obtained in this thesis. It is also used in the computational analysis of experimental data (see below).

The data obtained from the titrations (ml titrant added, emf measured) were processed by the computer program library ESTA [90]. The data analysis is illustrated in Fig. 3.2. In the initial stage, the average number of protons released per metal ion

$$\bar{Q} = (T_H^* - T_H) / T_M \qquad (3.10)$$

is calculated by the program QBAR. T_H^* is the calculated total concentration of protons in the system, that would be necessary to give rise to the observed pH if no complexation took place, and T_H and T_M are the total concentrations of protons and metal ions, respectively. The average number of ligands bound per metal ion, $\bar{Z}$

$$\bar{Z} = (T_L - [L]) / T_M = (T_L - A\,(1+\Sigma_n \beta_{LH_n} [H]^n) / T_M \qquad (3.11)$$

$$\text{where } A = (T_H - [H] + [OH])/\Sigma_n \beta_{LH_n} [H]^n)$$

is calculated by the program ZBAR. T_L is the total ligand concentration.

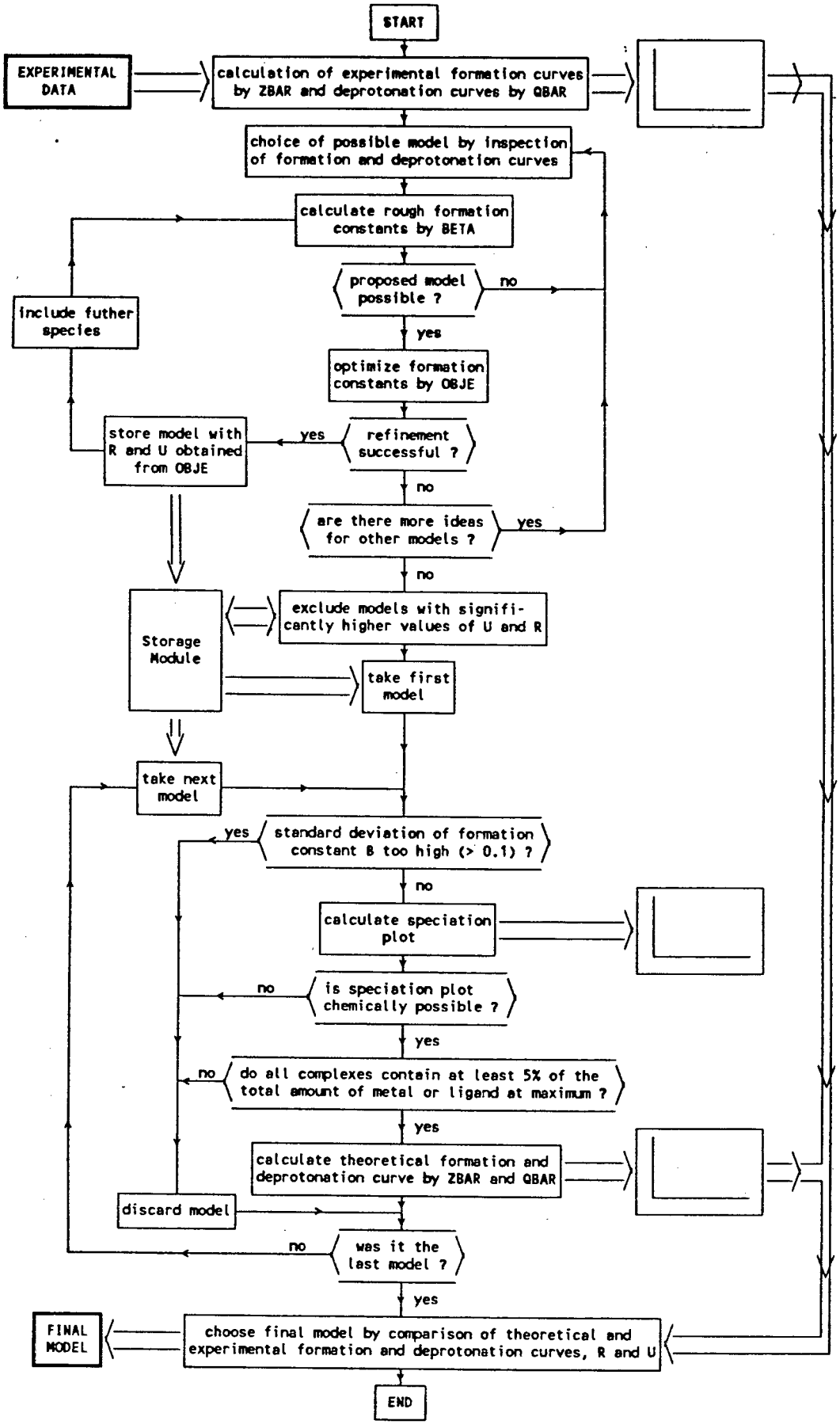

Figure 3.2: Flow diagram showing the data analysis procedure

Both $\bar{Q}$ and $\bar{Z}$ are calculated under the assumption that only mononuclear complexes of the type H_nL and L_nM occur. In this case, the formation curves for different ligand to metal ratios overlap. If the highest value of $\bar{Z}$ lies on a plateau and is equal to an integer p, then the highest mononuclear complex formed is L_pM. Often it is impossible to obtain a full formation curve, either because experimental conditions cannot be chosen as to cover the appropriate pA range because of e.g. precipitate formation, or because the complexation is too weak to convert all ligand molecules into the complex. The highest value of $\bar{Z}$ still gives an indication of the minimal number of ligand molecules bound per metal ion. If for example q=1.5 we can be sure that at least the two complexes LM and L_2M occur in the solution. The assumption of only mononuclear complexes is not valid for many systems, but a plot of $\bar{Q}$ versus pH and $\bar{Z}$ versus pA, i.e. -log[L], can still serve to give an indication which complexes might be present. From experience, we know that hydroxy complexes often cause a backfanning pattern of $\bar{Z}$ at low pA, and protonated species sometimes cause bumps at high pA as well as cross-over of titration curves of different ligand to metal ratios. If $\bar{Q}$ exceeds $\bar{n}$, the number of protons bound to the ligand with no metal present, this indicates species of the type L_2M, L_3M ... at low and intermediate pH and/or hydroxy species at higher pH. If, on the other hand, $\bar{n} = \bar{Q}$, we most probably have a LM species in our solution.
If no metal ions are present, the proton formation function $\bar{Z}_H$ is calculated instead of $\bar{Z}$ or $\bar{Q}$. $\bar{Z}_H$ is defined as:

$$\bar{Z}_H = \frac{T_H - [H] + [OH]}{T_L} \qquad (3.12)$$

$\bar{Z}_H$ is the average number of protons bound to each ligand molecule. Initially, $\bar{Z}_H$ was also calculated for systems containing metal ions, but because it was found to be difficult to interpret, it was only considered in some special cases.
Once a set of possible complexes had been selected, starting values for the refinement of these were obtained using the program BETA. This program calculates formation constants separately for each data point. It also gives an indication in which pH range proposed complexes occur and whether they have significant concentrations. If the chosen set of complexes seems reasonable, the formation constants can finally be optimised by a least squares procedure, using a weighted objective function U based on emf residuals using the program OBJE. OBJE simultaneously solves the three mass balance equations that can be set up for

the total concentrations of ligand, metal ion and hydrogen ion. At any point during the titration they can be calculated from the free concentration plus the concentrations of the various species:

$$T_L = [L] + [LM] + 2[L_2M] + \ldots.$$

$$= \sum_{r=-R}^{R} \sum_{q=0}^{Q} \sum_{p=0}^{P} p\, \beta_{L_pM_qH_r} [L]^p [M]^q [H]^r$$

$$T_M = \sum_{r=-R}^{R} \sum_{q=0}^{Q} \sum_{p=0}^{P} q\, \beta_{L_pM_qH_r} [L]^p [M]^q [H]^r$$

$$T_H = \sum_{r=-R}^{R} \sum_{q=0}^{Q} \sum_{p=0}^{P} r\, \beta_{L_pM_qH_r} [L]^p [M]^q [H]^r \qquad (3.13)$$

[H] has been measured by the glass electrode (as emf) and the total concentrations are analytically known. Thus, the parameters [M] and [L] have to be refined for each titration point and the formation constants $\beta_{L_pM_qH_r}$ for the whole set of data.

The objective function U used in the program OBJE is defined in terms of emf values:

$$U = (N - n_p)^{-1} \sum_{n=1}^{N} w_n (emf_n^{obs} - emf_n^{calc})^2 \qquad (3.14)$$

N is the total number of experimental points and n_p is the number of parameters that are optimized. The weights w_n are calculated at each titration point from the specified standard deviations σ according to:

$$w_n = \left(\sum_p \left(\frac{\partial}{\partial p} (emf_n^{obs} - emf_n^{calc}) \right)^2 \sigma_p^2 \right)^{-1} \qquad (3.15)$$

where the sum extends over all p parameters for which errors are specified. The goodness of fit is expressed by the R-factor

$$R = \left(U / \sum_{n=1}^{N} w_n (emf_n^{obs})^2 \right)^{\frac{1}{2}} \qquad (3.16)$$

Ideally, R should be equal to R_{lim},

$$R_{lim} = \left(N / \sum_{n=1}^{N} w_n (emf_n^{obs})^2 \right)^{\frac{1}{2}} \qquad (3.17)$$

if the model describes the system perfectly. Strictly, R_{lim} can only be applied if all errors are non-systematic. This assumption, however, is not true for the analysis of titration data. A random error in e.g. the electrode intercept acts as a systematic error on all titration points. It is nevertheless assumed that a comparison between R and R_{lim} is a reasonable measure of the goodness of the fit. Because the assumption of non-systematic errors is not satisfied, R can drop slightly below R_{lim} in some systems (see e.g. table 4.1 or table 4.6).

Often only the titre volume and the emf are weighted, as these are supposed to be causing the greatest statistical errors. In this work, however, I decided to introduce weighting for all experimental values. The following errors were specified: concentrations 0.1%; electrode intercept E_0 0.1mV; electrode slope 0.05mV/pH; titre volume 0.001ml; emf 0.1mV; initial volume 0.1%. The choice of the standard deviations leads to enormous differences of the objective function U. R decreases as the specified errors increase, but the obtained formation constants are not affected. To correct for the small changes of ionic strength during the titrations, corrections were applied using the D-HC block of ESTA, where an extended form of the Debye-Hückel equation (eq. 3.9) is used.

The procedure described above was repeated for different possible sets of complexes. For those sets which fitted the data well, speciation plots were obtained, i.e. the concentration of each complex was plotted against pH. Complexes in which less than 5% of the metal or the ligand is bound were regarded as artefacts and the models discarded unless these complexes occured on either end of the pH range studied. Models containing complexes with calculated standard deviations exeeding 0.1 were also discarded. Finally, theoretical $\bar{Z}$ and $\bar{Q}$ plots were obtained for the remaining models and compared to the experimental plots. Sometimes models seemed to fit equally well and they were distinguished by the Hamilton R ratio test [96]. It is expected that by using these four criteria, U, R, $\bar{Z}$ and $\bar{Q}$, the best models have been found.

In order to confirm the model, the stability constants were re-refined using the OBJT program of ESTA or MINIQUAD [91], where in contrast to the OBJE program, the objective function is based on the total hydrogen ion concentrations. No corrections for ionic strength can be applied here. It has been suggested [97] that once the final model is found, the stability constants can be further improved by refining the stability constants ß, the electrode intercept E_0, and the concentrations of acid and ligand in the vessel, $[H]_{vessel}$ and $[L]_{vessel}$ at the same time. This procedure is discussed in Appendix B.

3.3 Calorimetry

3.3.1 Titration apparatus

The calorimetric titrations were performed in an isothermal titration calorimeter, Tronac model 550 [98,99]. The schematic of the setup is shown in figure 3.3.

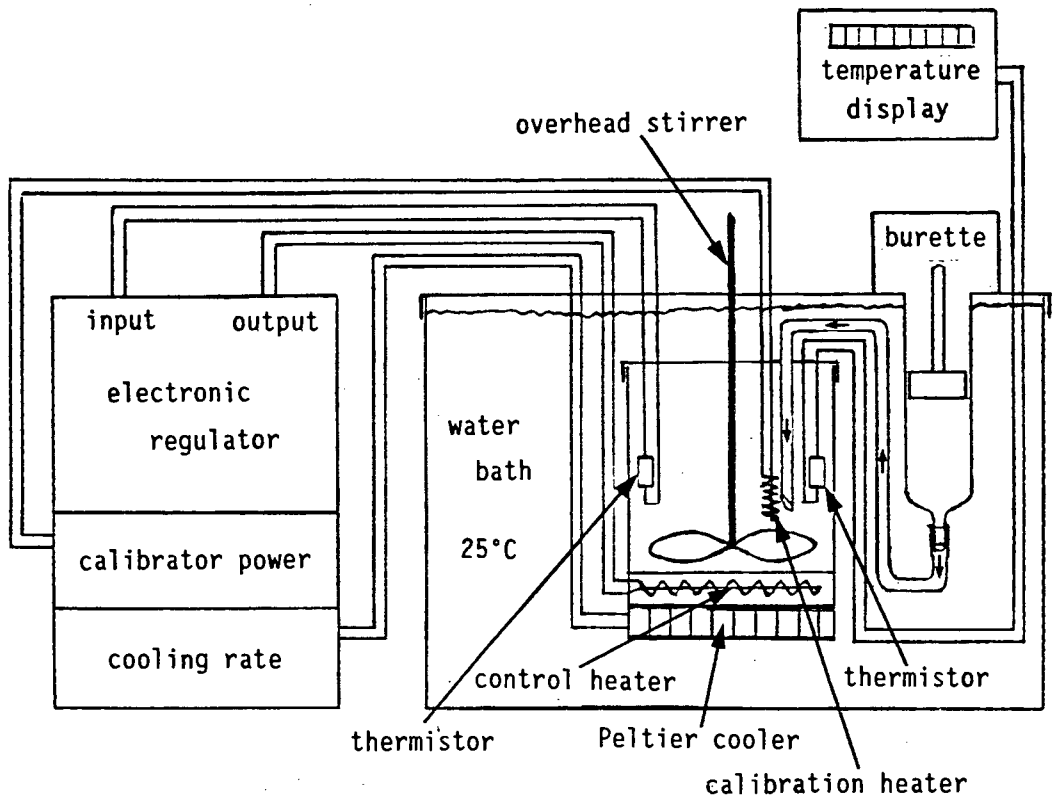

Figure 3.3: Schematic setup of the titration calorimeter

The reaction vessel is a small thermally insulated chamber that holds 30ml of solution. The inside wall is made of tantalum which is very reaction inert. In the vessel are a glass stirrer, a calibration heater and two thermistors. One monitors the temperature in the reaction vessel and the second one is part of the temperature regulation system. The reaction vessel is immersed in a 100 l water bath. The water temperature is regulated so that it does not vary by more than 0.002°C. The reaction vessel is maintained at the average bath temperature to $\pm 5 \cdot 10^{-5}$°C. This is achieved by applying a constant cooling rate through the Peltier cooler, which is balanced by an appropriate heating rate from the control heater. The heating rate is automatically adjusted by a regulation circuit which obtains its input signal from one of the thermistors. The reference signal i.e. the required constant temperature, was set to the average bath temperature.

The heat is admitted in the form of pulses of fixed energy. The amount of heat per pulse as well as the cooling rate are adjusted manually. During a titration the cooling rate is kept constant. Up to 2.5ml of titrant is added to the reaction vessel from a motorized Gilmont precision microburette. If the reaction is exothermic (endothermic) fewer (more) heat pulses per time interval are needed to keep the temperature at its initial value. The difference in the number of heat pulses in equal time intervals before and during a titration run is a measure of the heat of reaction released or absorbed during the interval.

3.3.2 Performance of the calorimetric titrations

Protonation enthalpies were determined by titrating 22ml ligand solution (0.05 mol/l) with hydrochloric acid solution (0.45 mol/l). It would have been desirable to perform the calorimetric titrations under exactly the same conditions as the potentiometric titrations. Unfortunately, this proved to be impossible because the reaction heats are rather small. In order to obtain a reasonably large signal the concentration of the acid in the burette had to be as large as 0.45 mol/l. The ligand concentration in the vessel was raised to 0.05 mol/l so that the whole content of the burette, 2.5ml, was needed to protonate fully 22ml of ligand solution. Ligand solutions were made up to a chloride concentration of 0.055 mol/l. If 0.15 mol/l had been used as in the potentiometric titrations, the initial ionic strength of the solution would have been as high as 0.3 mol/l. I decided that it would be preferable rather to keep the ionic strength near the chosen value of 0.15 mol/l than to keep the chloride concentration at 0.15 mol/l because all equilibria depend strongly on the ionic strength, but not on the individual ion concentrations. With 0.055 mol/l sodium chloride the initial ionic strength of the whole solution was adjusted to 0.19 mol/l. During a titration, it changed between 0.19 and 0.13 mol/l This change can be tolerated considering that in general ΔH does not vary significantly with varying ionic strength [100]. The acid was added at a rate between 0.125 ml/100sec and 1 ml/100sec depending on the heat of reaction.
Copper complexation enthalpies were determined such that a maximum change of the number of moles of the complex of interest, LM, occurred during the titration. 25ml of ligand solution (0.005 mol/l, 0.15 mol/l Cl^-) at various pHs were titrated against copper chloride solution (0.12 mol/l). The chloride concentration thus increases to 0.16 mol/l at the end of the titration.

The heat of dilution of hydrochloric acid was measured in separate experiments by titrating hydrochloric acid into 0.055 mol/l sodium chloride solution. The heat of dilution of copper chloride was measured by titrating the copper chloride solution into 0.15 mol/l sodium chloride solution.

3.3.3 Calculation of complex formation enthalpies

Before ΔH can be calculated the heat of dilution has to be subtracted. Baseline shifts due to the change of stirring heats and possible drift of the apparatus were assumed to be linear with time. The measured heats were corrected accordingly. From the corrected heats Q, the protonation enthapies ΔH_{LH} for the reaction $L + H \rightarrow LH$ were calculated according to

$$\Delta H_{LH} = \frac{Q}{\text{moles of LH formed}} \tag{3.18}$$

and the results for the different titrations were averaged. In order to obtain ΔH_i for the formation of the different copper complexes, the linear equation

$$\sum_i n_i \Delta H_i = Q \tag{3.19}$$

has to be solved (n_i is the number of moles of complex i generated and ΔH_i the enthalpy of formation of complex i). There are more equations (experiments) than there are unknowns (complexes). Therefore the program MINUIT (CERN program library D506) was used to calculate ΔH_i by minimizing

$$\sum_j \left(\frac{Q_{exp,j} - Q_{calc,j}}{Q_{exp,j}}\right)^2 = \sum_j \left(\frac{Q_{exp,j} - \sum_i n_{ij} \Delta H_i}{Q_{exp,j}}\right)^2 \tag{3.20}$$

The index i again refers to the different complexes and the index j to the different titrations.
The change in the number of moles of each compound present was calculated using the SPEC program of ESTA.

3.4 Nuclear magnetic resonance spectroscopy

^{31}P and ^{13}C nuclear magnetic resonance (nmr) spectra of the solutions were recorded on a Varian VXR 200 spectrometer.
Each solution was introduced to a nmr tube and into this a capillary tube containing deuterium oxide and trimethyl phosphate was inserted. Deuterium oxide provides the lock and trimethyl phosphate was used as internal reference both for phosphorus and carbon spectra.
Nmr "titrations" were performed by making up a series of solutions containing the ligand and the background electrolyte at specific pHs. In order to obtain evidence on the possible intramolecular stacking interactions of 8-quinolyl phosphate, a series of solutions at fixed pH, but with different ligand concentrations was prepared. Nuclear magnetic resonance spectroscopy was done at room temperature.

4. RESULTS

4.1 Potentiometric results and nmr results

4.1.1 General

In this chapter all potentiometric results will be reported and compared to literature values, if available. Results obtained by nuclear magnetic resonance spectroscopy will also be presented. After a short summary of some general observations, the particular problems that occurred with each of the ligands will be discussed, and the final results will be presented.
All experimental data were analyzed for the following complexes and combinations thereof: ML, ML_2, ML_3, MLH, MLH_{-1}, MLH_{-2}, M_2L. In the case of triphosphates the additional complexes M_3L, MLH_2 and MLH_3 were also considered. The protonation constants that had been determined from titrations without metal ion were fixed in the refinements. pK_w was adjusted to an ionic strength of 0.15 mol/l by extrapolation of literature data [35-37], and was fixed at 13.73. The final models of 1-naphthyl phosphate, 8-quinolyl phosphate and 8-quinolyl methyl phosphate were confirmed using MINIQUAD [91]. The models and stability constants of all other ligands were confirmed using the OBJT program of ESTA. Although MINIQUAD and OBJT do not allow for ionic strength corrections the agreement with the formation constants obtained by OBJE was

always found to be favourable. This confirms that ionic strength changes during the titrations are negligible.

Complexation of the monophosphates could only be studied in the lower pH range because precipitates occured in the alkaline pH region. None of the precipitates was analyzed. It is however likely that these precipitates are not ligand-metal complexes, but metal hydroxides, because they always occur at pHs where one can expect metal hydroxide precipitates. The only exceptions are the titrations with phenyl phosphate, where precipitation occurs at lower pHs. These precipitates are probably metal-phenyl phosphate complexes.

For complexation of copper and zinc the agreement between experimental and theoretical formation and deprotonation curves was generally good except where indicated (see the separate paragraphs on each ligand). The complexation with calcium is always very weak and the reproducibility of the experimental titration curves was not always favourable. Titrations which did not overlap with the majority within 0.03 $\bar{Z}$ units were excluded from the modelling.

All monophosphates form metal complexes of the composition LM. For some of the ligands the metal-ligand-hydroxo complexes LMH_{-1} and LMH_{-2} were also found. Hydroxo complexes are believed to be formed by the removal of a proton from one of the water molecules in the hydration sphere of the complex LM. All hydroxo complexes occurred at pH values not very far below the onset of precipitation. Therefore, the number of data points from which the respective stability constants were obtained is few. In addition, metal ion hydroxides start forming in the same pH region. Metal ion hydrolysis constants [86] were adjusted to an ionic strength of 0.15 mol/l according to the equations in [86] and included into all refinements to account for the effect metal-hydroxide formation has on the pH. Nevertheless, the stability constants obtained for metal-ligand-hydroxo complexes are probably not as precise as those for complexes in the low pH region.

A common problem encountered during the modelling is that often, it was possible to refine either of the complexes L_2M or LMH_{-1} in addition to LM, but not both. In most cases the fit including LMH_{-1} was significantly better than the fit including L_2M, or L_2M was a minor complex and the model was discarded. Apart from the fact that there is insufficient evidence to propose the existence of a complex L_2M, this species is also considered to be unlikely. The complex formation between the phosphate group of the ligands and metal ions is weak ($1.2<\log \beta_{LM}<2.8$) so that the addition of a second ligand molecule seems unrealistic.

Complexes of the type L_2M were not even found for 8-quinolyl phosphate, which binds metal ions much more strongly due to chelate formation.
Generally the overlap between experimental and theoretical formation and deprotonation curves seemed to improve with increasing strength of the complexes. It was found that the overlap between experimental and theoretical formation curves was usually better than the overlap between the respective deprotonation curves.
As it would be awkward to show all the experimental and theoretical $\bar{Z}$, $\bar{Q}$ and $\bar{Z}_H$ curves as well as all speciation plots I will only present the plots for the protonation and copper complexation of two of the ligands. Figure 4.1a - figure 4.1e show all experimental and theoretical plots for the protonation and copper complexation of α-D-glucose-1′-phosphate. Figure 4.2a - figure 4.2e show the plots for the protonation and copper complexation of phenyl phosphate. (In all plots every second data point has been omitted for clarity).
Fig. 4.1a and fig. 4.2a show protonation curves of α-D-glucose-1′-phosphate and phenyl phosphate, respectively. The protonation curves for different ligand concentrations overlap. $\bar{Z}_H$ does not rise above 1. This indicates that in the pH range studied the complex LH is the only protonated species. At pHs below 4, $\bar{Z}_H$ is equal to 1, i.e. the ligands are fully protonated. The rise of $\bar{Z}_H$ to above 1 in the case of phenyl phosphate (fig. 4.2a) is thought to be caused by experimental error (see section 4.1.4).
Between divalent copper ions and phenyl phosphate only one complex, LM, forms. Accordingly, the formation curves obtained from titrations with different ligand to metal ratios overlap (fig. 4.2b). The complexation of α-D-glucose-1′-phosphate with copper ions leads to the three complexes LM, LMH_{-1} and LMH_{-2}. The presence of hydroxo complexes is indicated by the strong backfanning pattern of the formation curves (fig. 4.1b). The higher the ligand to metal ratio, the lower is the pA at which fanning starts.
The deprotonation curves of the two ligands are quite similar (fig. 4.1c and fig. 4.2c). This reflects the fact that for both ligands, LM is the major species. Both deprotonation curves do not rise above 0.4, indicating that complexation is rather weak. The theoretical deprotonation curves of phenyl phosphate (fig. 4.2c) indicate a levelling off to the maximum possible degree of complexation. In contrast, the deprotonation curves of α-D-glucose-1′-phosphate (fig. 4.1c) start rising more steeply as pH increases. This rise is caused by the presence of the hydroxo

complexes, the presence of which is also indicated by the fact that $\bar{Q}$ exceeds $\bar{n}$ at high pH (the $\bar{n}$ curve is not shown on the plot).

Plots of $\bar{Z}_H$ against pH in the presence of copper ions are shown in fig. 4.1d and fig. 4.2d. A comparison of $\bar{Z}_H$ plots with the protonation curves obtained in the absence of metal ions (fig. 4.1a and fig. 4.2a) shows at which pH metal complexes start forming. The metal complexation reaction is a displacement of hydrogen ions by metal ions. Consequently, at fixed pH, $\bar{Z}_H$ is smaller in the presence of metal ions (fig. 4.1d and fig. 4.2d) than in the absence of metal ions (fig. 4.1a and fig. 4.2a). The information contained in the $\bar{Z}_H$ plots is also contained in the formation and deprotonation curves where interpretation in terms of possible metal complexes is more obvious. $\bar{Z}_H$ plots were thus not used in the search for possible species.

The speciation plots for the two copper systems (fig. 4.1e and fig. 4.2e) show that complexation is rather weak, as is already indicated by the low values of $\bar{Q}$. Not more than about 35% of the ligand is present as a metal complex at any pH. In both systems, LM is the major complex in the pH range studied. Hydroxo complexes of α-D-glucose-1'-phosphate only occur in small concentrations at pHs just below the onset of precipitation.

For triphosphates there exists a large variety of possible complexes because these ligands have several possible coordination sites. The complexes formed are discussed separately for each ligand.

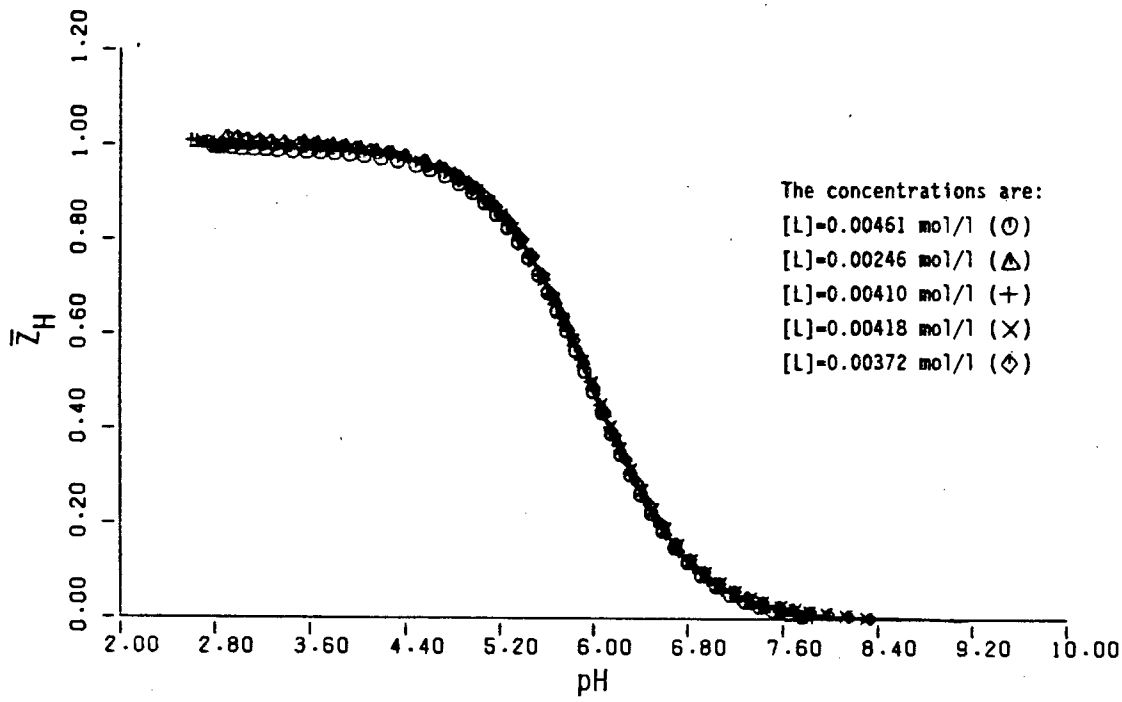

Figure 4.1a: Experimental (symbols) and theoretical (lines) protonation curves for the protonation of α-D-glucose-1'-phosphate.

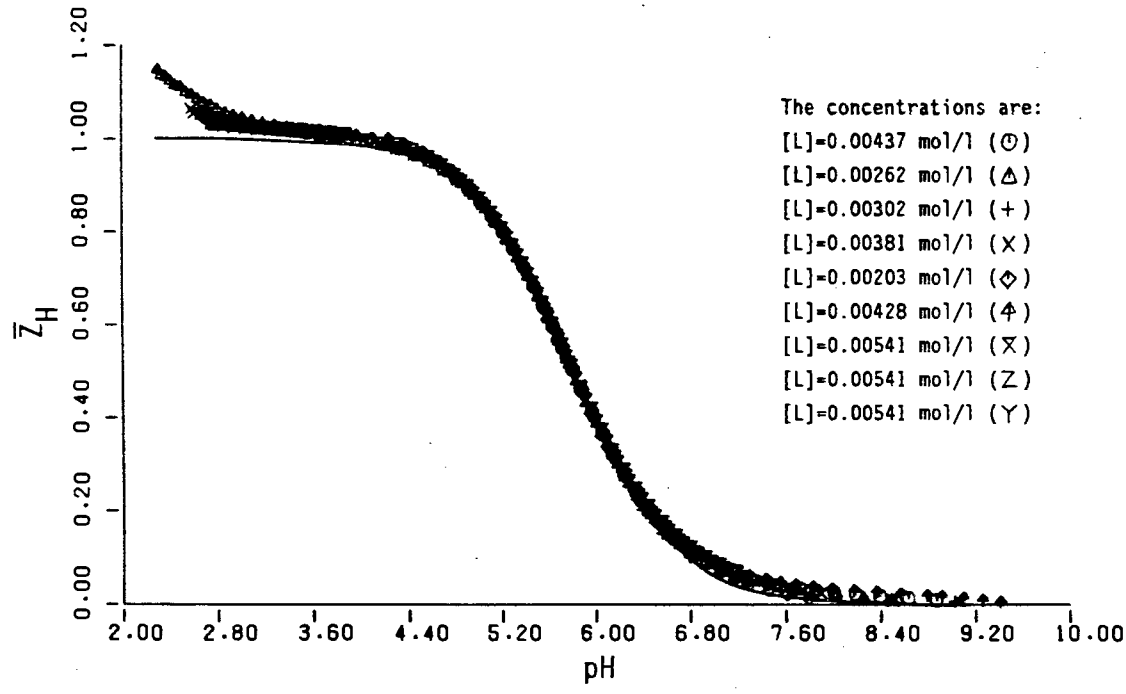

Figure 4.2a: Experimental (symbols) and theoretical (line) protonation curves for the protonation of phenyl phosphate.

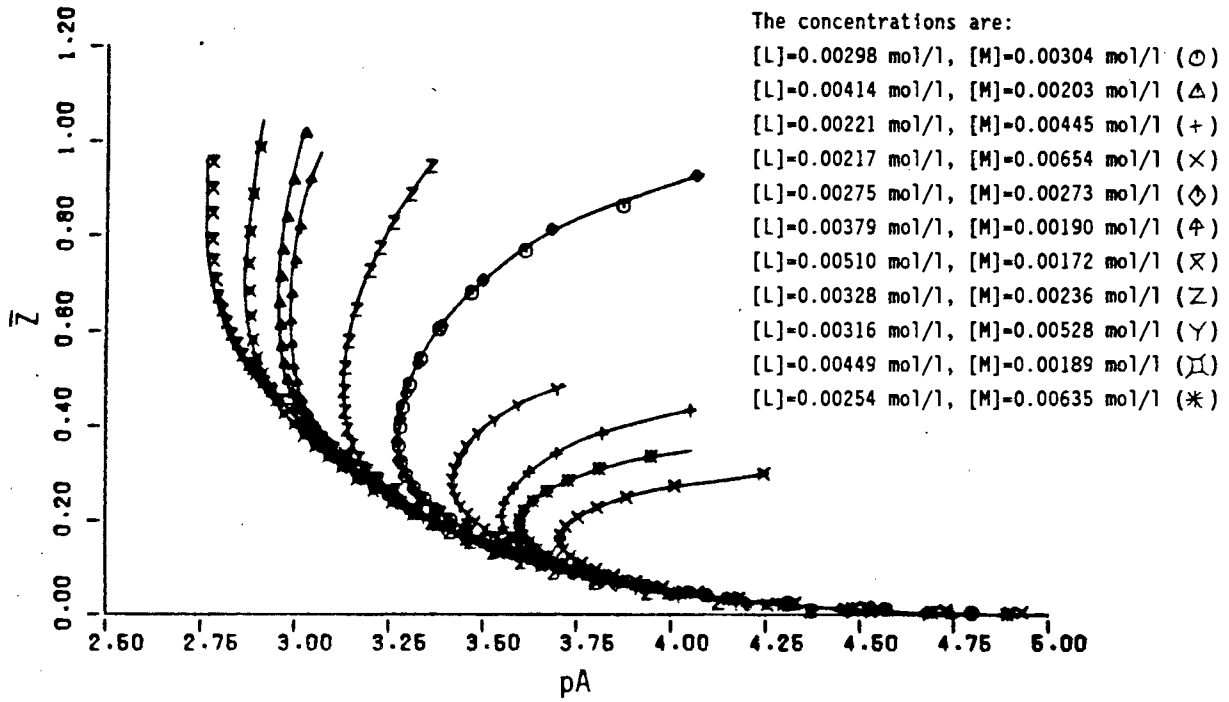

Figure 4.1b: Experimental (symbols) and theoretical (lines) formation curves for the complexation of α-D-glucose-1′-phosphate with copper ions.

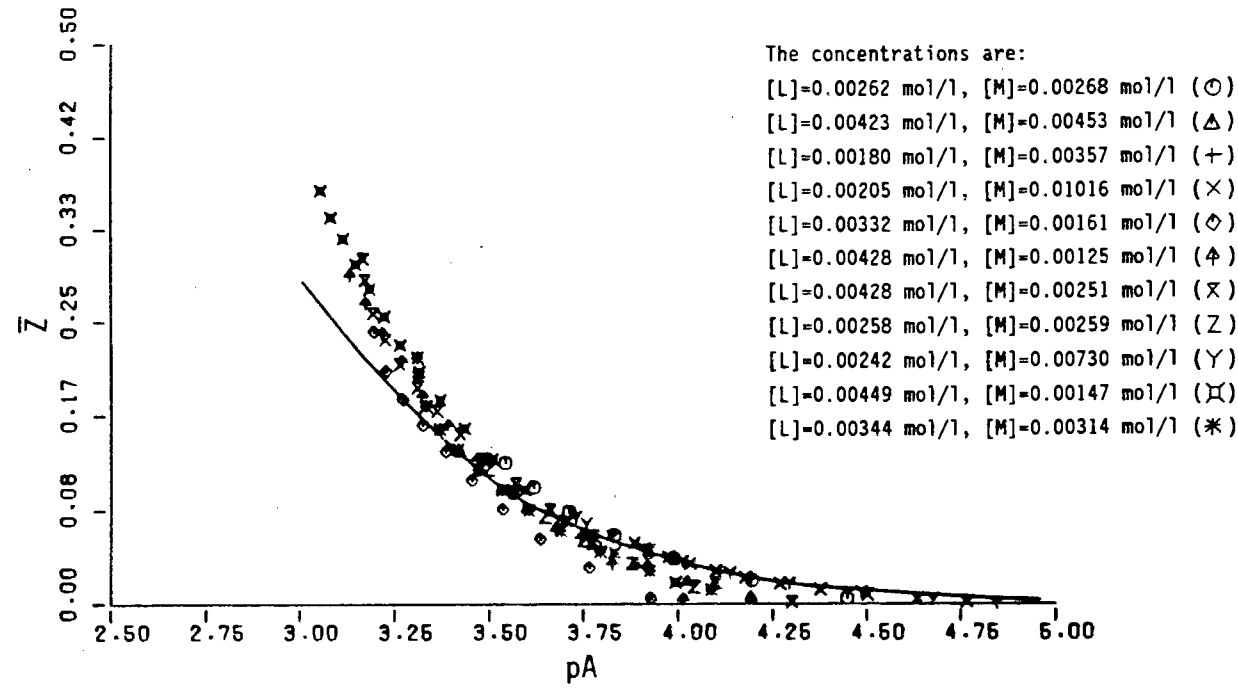

Figure 4.2b: Experimental (symbols) and theoretical (lines) formation curves for the complexation of phenyl phosphate with copper ions.

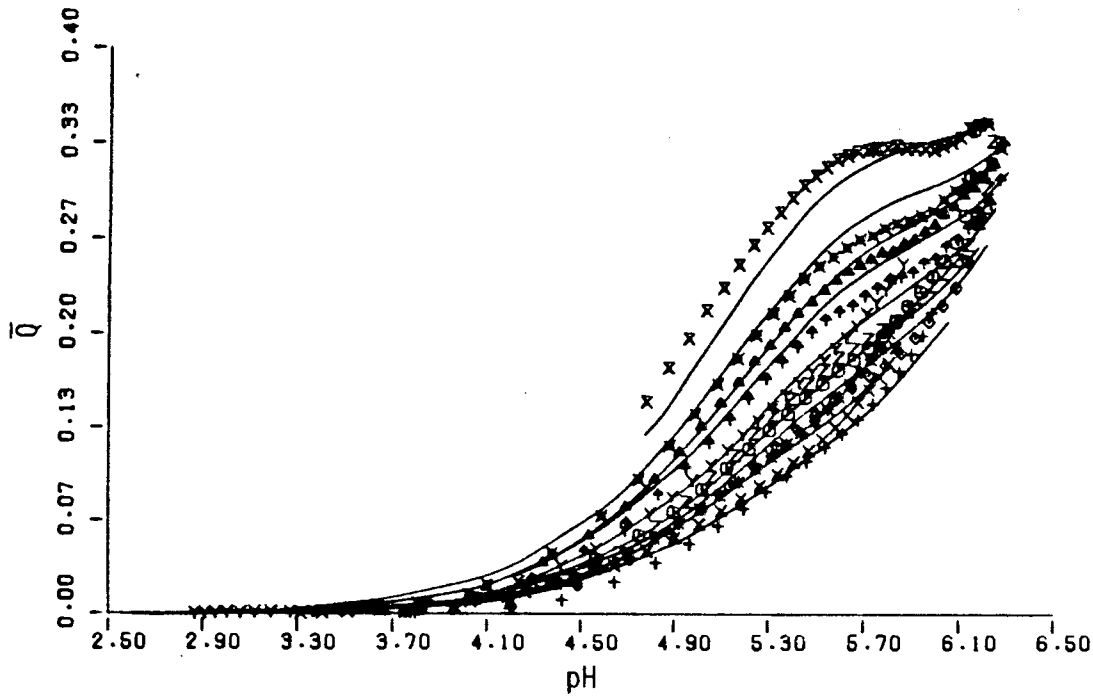

Figure 4.1c: Experimental (symbols, as in figure 4.1b) and theoretical (lines) deprotonation curves for the complexation of α-D-glucose-1'-phosphate with copper ions

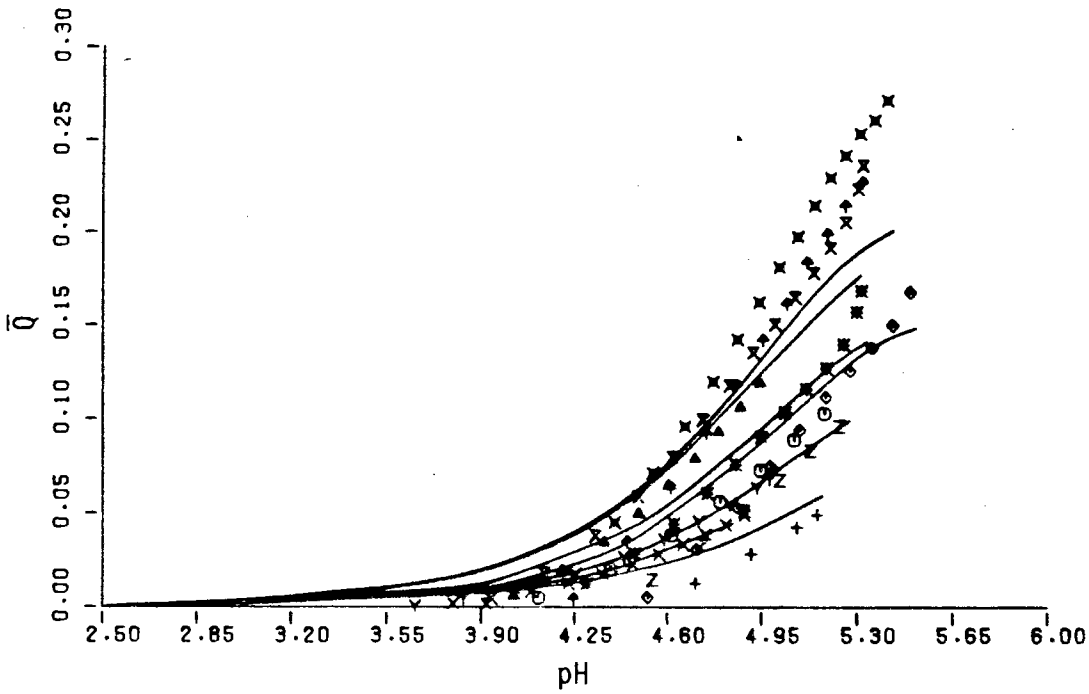

Figure 4.2c: Experimental (symbols as in figure 4.2b) and theoretical (lines) deprotonation curves for the complexation of phenyl phosphate with copper ions

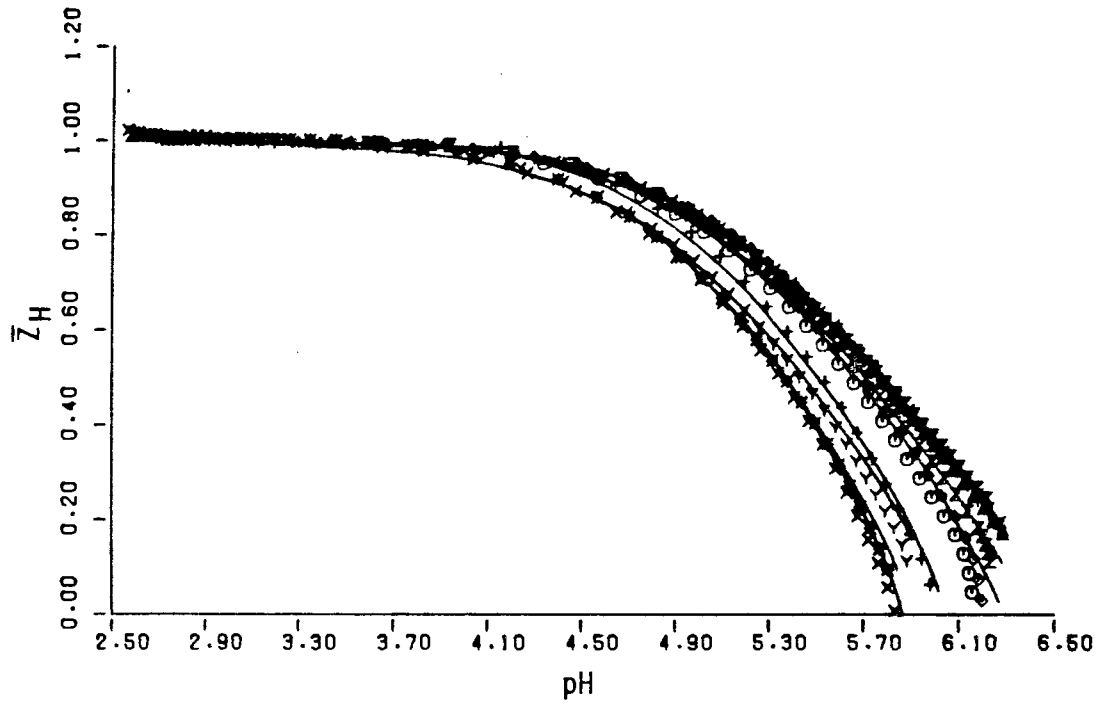

Figure 4.1d: Experimental (symbols as in figure 4.1b) and theoretical (lines) protonation curves for the complexation of α-D-glucose-1'-phosphate with copper ions

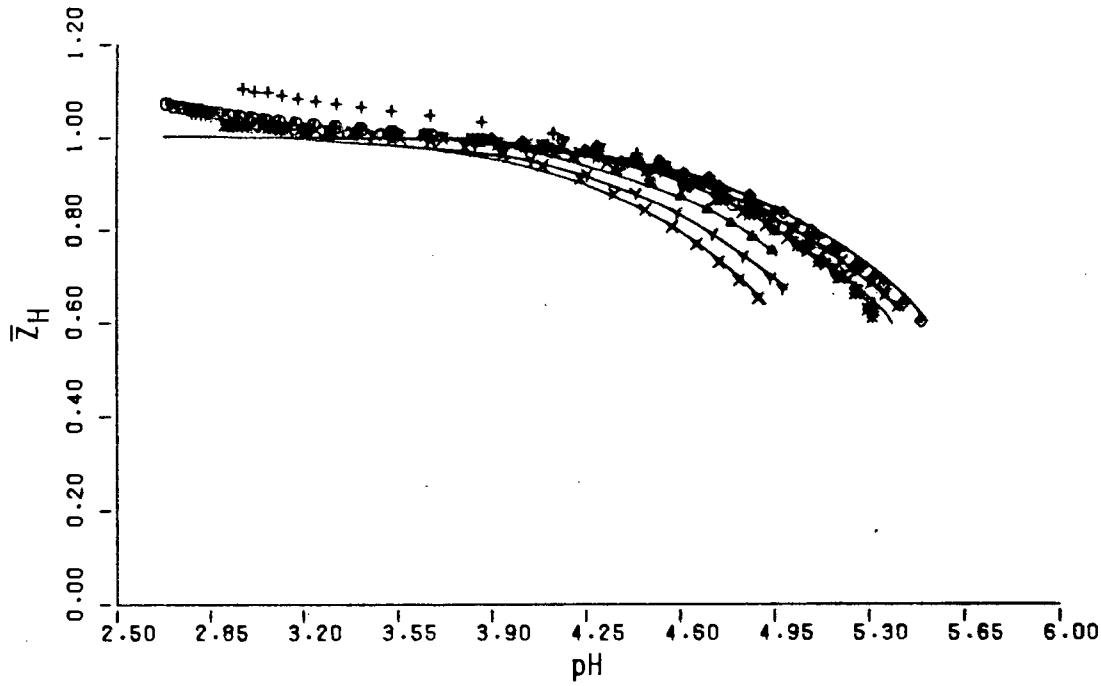

Figure 4.2d: Experimental (symbols as in figure 4.2b) and theoretical (lines) protonation curves for the complexation of phenyl phosphate with copper ions

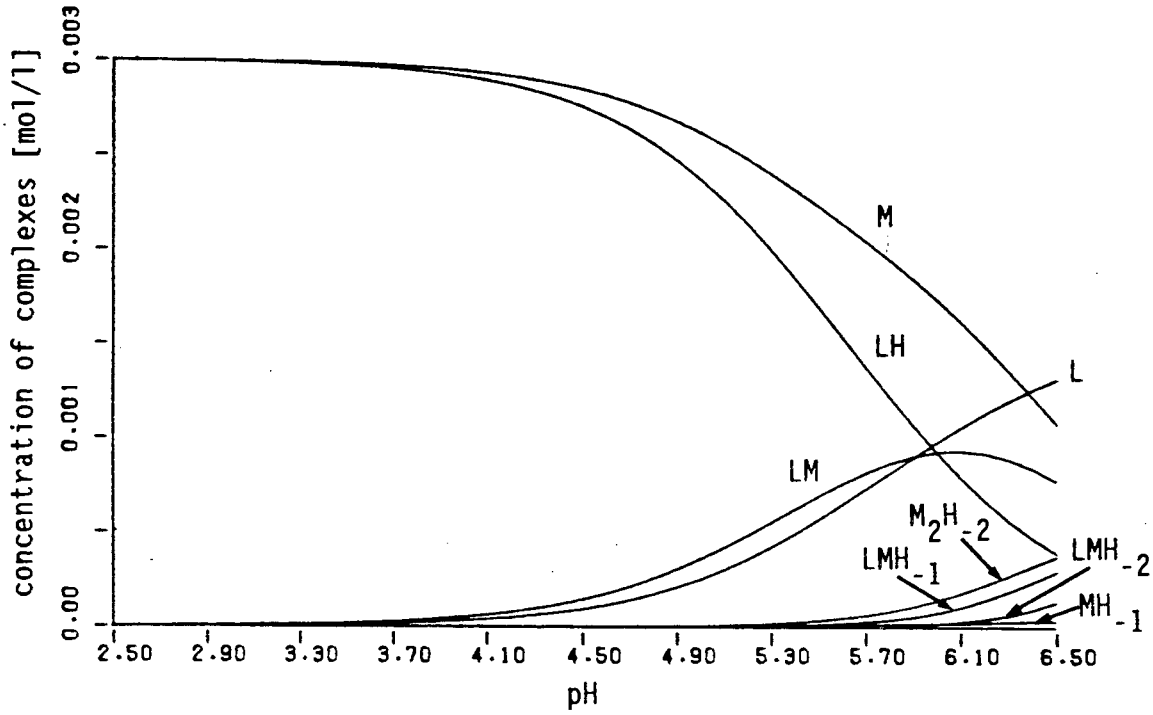

Figure 4.1e: Speciation plot of the copper-α-D-glucose-1'-phosphate system for a copper ion and ligand concentration of 0.003 mol/l

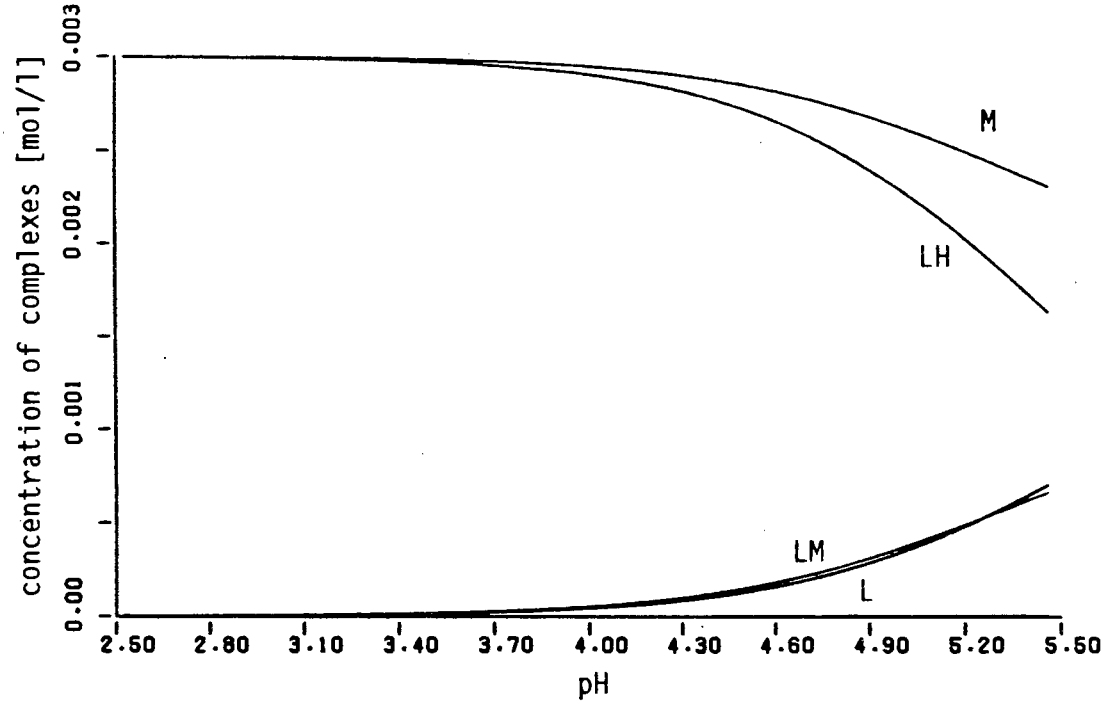

Figure 4.2e: Speciation plot of the phenyl phosphate system, for a copper ion and ligand concentration of 0.003 mol/l

4.1.2 p-Nitrophenyl phosphate

No major problems were encountered during the experimental work to determine protonation and copper complexation constants. The reproducibility of titrations of the zinc-p-nitrophenyl phosphate system was poor. It was confirmed by orthophosphate analysis [101] that the reason is not an accelerated hydrolysis of the ligand in the presence of zinc. Not all the data collected were therefore used in the computations. In the case of copper, some problems arose during the modelling. Like with zinc, no fanning was observed, and LM is the major complex. Addition of the complex L_2M improved the fit considerably. Application of the Hamilton R-factor test [96] showed the model including L_2M to be significantly better at the 95% confidence level. On the other hand a complex of the type L_2M has not been found for any of the other ligands studied here and is thus thought to be very unlikely to occur for the weakest member of the series. This is also indicated by the fact that $\bar{Q}$ never exeeds 0.1. Therefore, although a better fit is obtained for the two complexes LM and L_2M, I believe that LM is the only complex present.

The stability constants obtained for the complexation of the ligand with protons, copper and zinc are summarized in table 4.1. A protonation constant of 4.96 (T=25°C, I=1 mol/l KCl) has been reported in the literature [11] and agrees favourably with the value obtained here.

No attempt was made to study the complexation with calcium because it is known to be too weak (log β = 0.88 [102]) to obtain reliable data by potentiometry.

Table 4.1: Equilibrium constants of p-nitrophenyl phosphate at T=25°C and I=0.15 mol/l (NaCl)

cation	cplx	log β	std. dev.	n_t	n_p	R R_{lim}	pH	initial concentration	K
H^+	LH	4.987	0.001	5	275	0.0054 0.0091	2.2-8.5	L:0.002-0.006	B
Cu^{2+}	ML	2.148	0.004	9	509	0.0150 0.0042	2.6-6.3	L:0.002-0.007 M:0.002-0.005	B
Zn^{2+}	ML	1.758	0.004	6	233	0.0055 0.0143	2.4-5.8	L:0.003-0.007 M:0.002-0.009	B

4.1.3 1-Naphthyl phosphate

Performing the titrations to obtain the stability constants of the proton, copper, zinc, nickel, cobalt and calcium complexes of 1-naphthyl phosphate did not give any unforseen complications. The zinc-1-naphthyl phosphate system was used to check for the agreement between titrations with hydroxide in the burette and titrations in which metal ion was added. Good agreement was found for both the formation and the deprotonation curves obtained by the different approaches. The stability constants calculated from the titration data from the titrations with hydroxide solution agree with those calculated from the metal ion titrations within error. When titrating with metal ion solution it is difficult to obtain data points in the pH region where hydroxo complexes form. This is due to the formation of precipitates. i.e. it is not easy to aim at the right pH to start the titration.

The formation curves obtained for the complexation with zinc and copper ions show a backfanning pattern and in both instances the inclusion of the hydroxo complex LMH_{-1} improved the fit to the experimental data considerably. No backfanning is found for the complexation with nickel ions and cobalt ions. It is impossible to decide here whether no hydroxo complexes form or whether they have not been picked up. In all titrations with nickel ions and cobalt ions, metal ion solution was added from the burette. If hydroxo complexes only occur in a very narrow pH region just below the pH at which precipitates start forming, they may be easily missed.

The complexation of calcium with 1-naphthyl phosphate is very weak. Nevertheless reasonable looking formation curves were obtained which show a systematic fanning pattern. Unfortunately the data cannot satisfactorily be fitted by any model. Results depend strongly on the number of data points used in the refinements. Therefore only data points with with $\bar{Z} \leq 0.06$ were used to calculate β_{LM}. This constant was then fixed. Further refinements were performed to obtain a value for the suspected hydroxo complex LMH_{-1} using different numbers of data points. From the formation constant obtained as well as from the R value and objective function it is impossible to decide whether this complex really exists or whether its introduction into the model only absorbs experimental error. The complex LMH_{-1} can thus only be suspected to exist. All attempts to introduce complexes other than the hydroxo complex were unsuccessful.

The results obtained for the protonation and complex formation of 1-naphthyl phosphate are summarized in table 4.2. Agreement with literature values is good (table 4.3).

Table 4.2: Equilibrium constants of 1-naphthyl phosphate at T=25°C and I=0.15 mol/l (NaCl)

cation	cplx	log β	std. dev.	n_t	n_p	R / R_{lim}	pH	initial concentration	K
H^+	LH	5.740	0.005	4	301	0.0020	2.0-8.0	L:0.002-0.011	A,B
Cu^{2+}	ML	2.635	0.006	6	207	0.0026	2.0-6.0	L:0.002-0.004	B
	MLH_{-1}	-3.840	0.021			0.0026		M:0.002-0.004	
Zn^{2+}	ML	2.014	0.011	14	400	0.0049	2.0-6.0	L:0.003-0.011	B,M
	MLH_{-1}	-4.730	0.025			0.0020		M:0.002-0.015	
Ca^{2+}	ML	1.223	0.006	7	203	0.0302	5.2-6.8	L:0.003-0.004	M
	MLH_{-1}	-6.1to-6.8 suspected				0.0457			
Ni^{2+}	ML	1.568	0.006	7	84	0.0244	4.0-6.0	L:0.005-0.015	M
						0.0072			
Co^{2+}	ML	1.681	0.002	5	139	0.0104	4.5-6.0	L:0.005-0.012	M
						0.0075			

Table 4.3: Equilibrium constants of 1-naphthyl phosphate Comparison with literature values

cation	complex	log β	I	T	reference
H^+	LH	5.827	0.15 NaCl	25°C	this study
		5.85	0.1 KCl	26°C	[103]
		5.85	0.1	25°	[72]
	LH_2	6.82	0.1 KCl	26°C	[103]

4.1.4 Phenyl phosphate

Protonation curves indicated the beginning of the second protonation step and consequently both protonation constants of phenyl phosphate could be determined. There remains however some uncertainty about the reliability of the second protonation constant (log $\beta_{LH_2} = 7.32 \pm 0.02$) as only few data points were collected in the low pH region. It seems surprising that it should be possible to determine log β_{LH_2} for phenyl phosphate, but not for any other of the stronger ligands (stronger in the sense that log β_{LH} of these ligands and the respective pK_{ROH} is higher) unless one can propose a special mechanism which operates for phenyl phosphate only.

Reproducibility of metal complex formation curves was poor for calcium. This is reflected in the calculated standard deviations obtained in the refinements. In all three metal-ligand systems only one complex LM could be detected. Hydroxo complexes did not form as indicated by the fact that no fanning was observed, and by the early onset of precipitation. The search for a complex LMH was unsuccessful for all three metal ions. To insure that the presence of the somewhat uncertain stability constant of LH_2 did not cause any artefacts, refinements were carried out with and without inclusion of the complex. The same models were obtained and formation constants agreed within the calculated standard deviations.

The final results are displayed in table 4.4. Table 4.5 contains a comparison with literature values.

Table 4.4: Equilibrium constants of phenyl phosphate at T=25°C and I=0.15 mol/l (NaCl)

cation	cplx	log β	std. dev.	n_t	n_p	R R_{lim}	pH	initial concentration	K
H^+	LH	5.827	0.002	9	394	0.0118 0.0062	2.2-10.0	L:0.002-0.006	A,B
Cu^{2+}	ML	2.611	0.005	11	414	0.0104 0.0022	2.8-5.4	L:0.002-0.005 M:0.001-0.008	B
Zn^{2+}	ML	2.146	0.004	9	191	0.0142 0.0066	2.3-6.2	L:0.003-0.006 M:0.002-0.009	B
Ca^{2+}	ML	1.442	0.025	9	161	0.0327 0.0069	3.0-6.0	L:0.003-0.008 M:0.002-0.007	B

Table 4.5: Equilibrium constants of phenyl phosphate Comparison with literature values

cation	complex	log β	I	T	reference
H^+	LH	5.827	0.15 NaCl	25°C	this study
		5.88	0.1 KCl	26°C	[103]
		5.70	1 KCl	25°C	[11]
		5.823	0.11	25°C	[105]
		5.719	0.26	25°C	[105]
		5.786	0.15	25°C	extrapolated from the 8 values reported in [105]
	LH_2	7.315	0.15 NaCl	25°C	this study
		6.88	0.1 KCl	26°C	[103]

4.1.5 α-D-Glucose-1'-phosphate

No experimental problems were experienced during the potentiometric study of this ligand. Reproducibility of the titrations was always excellent.

As with the other phosphate esters only the first protonation constant could be determined. The complexes LM and LMH_{-1} were found for the complexation of α-D-glucose-1'-phosphate with zinc and copper. In addition, $CuLH_{-2}$ forms just before the onset of precipitation. With calcium some problems occurred during the modelling. Although the experimental formation curves show a strong systematic fanning pattern no reasonable model could be found that reproduces the fanning. These data points were eventually discarded in order to obtain a more reliable formation constant for the complex LM which would otherwise have been overestimated. Maybe the fanning was caused by the formation of invisible precipitates, or, more likely, by small experimental errors in the analytical concentrations of ligand, metal ion and hydrogen ion. Formation curves are particularly sensitive to small errors of the hydrogen ion concentrations at high pH [149,150].

A complex CaLH could be refined if the high pH data were kept, but not on low pH data only. This complex is therefore regarded as a "computer complex". Thus only one formation constant for the (presumably) only calcium complex LM was successfully determined.

Table 4.6 summarizes the results obtained here. A comparison with literature data is shown in table 4.7. The stability constants for the protonation and the ZnL complex are in good agreement but a considerably higher constant has been reported for the calcium complex (see table 4.7). It cannot be decided here whether the different ionic strength could have such a large effect on the value of the stability constant.

Table 4.6: Equilibrium constants of α-D-glucose-1'-phosphate at T=25°C and I=0.15 mol/l (NaCl)

cation	cplx	log β	std. dev.	n_t	n_p	R / R_{lim}	pH	initial concentration	K
H^+	LH	5.9767	0.0003	5	245	0.0012 0.0095	2.5-8.6	L:0.002-0.005	A,B
Cu^{2+}	ML	2.736	0.003	11	726	0.0110	2.5-6.5	L:0.002-0.006	B
	MLH_{-1}	-4.080	0.018			0.0036		M:0.001-0.008	
	MLH_{-2}	-11.028	0.049						
Zn^{2+}	ML	2.118	0.003	9	521	0.0028	2.5-7.5	L:0.002-0.007	B
	MLH_{-1}	-5.818	0.009			0.0026		M:0.002-0.009	
Ca^{2+}	ML	1.773	0.007	10	429	0.0030 0.0046	2.4-8.0	L:0.002-0.007 M:0.002-0.008	B

Table 4.7: Equilibrium constants of α-D-glucose-1'-phosphate Comparison with literature values

cation	complex	log β	I	T	reference
H^+	LH	5.977	0.15 NaCl	25°C	this study
		6.04	0.145 NaCl	30°C	[106]
		6.51	→ 0	30°C	[107]
		6.13	I>0.3	30°C	[108]
	LH_2	1.11	I>0.3	30°C	[108]
Zn^{2+}	LM	2.181	0.15 NaCl	25°C	this study
		2.34	0.1 KNO_3	25°C	[109]
		2.37	0.1 KNO_3	25°C	[109]
Ca^{2+}	LM	1.773	0.15 NaCl	25°C	this study
		2.495	→ 0	25°C	[110]

4.1.6. Glycerol-2-phosphate

As with most of the other phosphate esters only one protonation constant could be determined in the pH region 2-11.

For copper and zinc the metal complex formation curves showed a fanning pattern and indeed, stability constants for the hydroxo complex MLH_{-1} in addition to ML could be obtained. Furthermore it is possible to refine a formation constant for a second copper hydroxo complex, $CuLH_{-2}$. A speciation plot shows that this complex only appears at the very end of the titrations at pH>6.3. Although the R values and objective functions of the two models, $LM + LMH_{-1}$ and $LM + LMH_{-1} + LMH_{-2}$ are not significantly different and any statistical criterion like e.g. the Hamilton test [96] will always eliminate the second model, I nevertheless believe that the complex LMH_{-2} must not be discarded. The fact that the two models are not significantly different from the statistical point of view only reflects that there are few data points in the pH region where the additional complex occurs. The number of points represents a kind of weighting and consequently complexes which only just occur on either side of the pH range studied will be eliminated.

Surprisingly no complexation of glycerol-2-phosphate with calcium could be detected. Experiments both with hydroxide or metal ion in the burette were performed. Both methods yielded formation curves with $\bar{Z}=0$ at high pA. Below pA=3.0 a very steep, non-systematic increase in $\bar{Z}$ occurs. This increase cannot be ascribed to the formation of a very fine precipitate because no precipitates could be detected in the titration vessel or after the solutions had been kept for 48 hours. The sudden rise is probably a manifestation of small experimental error. I nevertheless attempted to process the data with the program OBJE and surprisingly, it is possible to calculate a formation constant for the complex ML ($\log \beta_{ML} = 1.528 \pm 0.008$) but the experimental $\bar{Z}$ values differ by up to 0.3 units from the theoretical values. Being able to calculate a constant at all seems to be a statistical artefact and one cannot have any confidence in the calculated formation constant. The conclusion is that no detectable complexation occurs between calcium and glycerol-2-phosphate. The experimental results are listed in table 4.8. A protonation constant of $\log \beta_{LH} = 6.673$ (T=25°C, I=0.11 NaCl [111]) has been reported and does not agree with the value obtained here. The value obtained here seems more reliable (see section 5.1.1)

Table 4.8: Equilibrium constants of glycerol-2-phosphate at T=25°C and I=0.15 mol/l (NaCl)

cation	cplx	log β	std. dev.	n_t	n_p	R R_{lim}	pH	initial concentration	K
H^+	LH	6.1054	0.0005	7	366	0.0010 0.0034	2.0-11.0	L:0.002-0.007	A,B
Cu^{2+}	ML	2.808	0.008	8	357	0.0150	2.4-6.5	L:0.002-0.006	B
	MLH_{-1}	-3.728	0.037			0.0029		M:0.002-0.007	
	MLH_{-2}	-10.312	0.070						
Zn^{2+}	ML	2.137	0.007	9	737	0.0058	2.2-7.3	L:0.003-0.005	B
	MLH_{-1}	-5.628	0.019			0.0019		M:0.002-0.006	
Ca	no complexation								

4.1.7. Methyl phosphate

The experimental work to determine protonation constants and stability constants for zinc and calcium complexes did not pose any major problems. The determination of stability constants for the copper-methyl phosphate system, however, turned out to be quite difficult due to the formation of precipitates. The initial ligand concentration had to be kept below 0.002 mol/l and titrations had to be carried out by adding copper ions from a burette to ligand solutions at pH<6 to obtain non zero formation curves. Once reliable data had been collected a suitable model was easily established. The exceptionally high R-value reflects the experimental difficulty rather than indicating a missing species. Like for the complexation of copper and zinc ions with methyl phosphate, the experimental formation curves for the calcium-methyl phosphate system show a strong systematic fanning pattern and suggest the formation of hydroxo species. Although a formation constant for $CaLH_{-1}$ could be obtained in addition to CaL it should be regarded as a good estimate rather than a reliable value as it fails to reproduce the experimental fanning of the formation curves. The value obtained for CaL is unaffected by the absence or presence of $CaLH_{-1}$ in the refinements and does not change significantly if the high pH data (fanning) are deleted. It is therefore considered reliable.

Table 4.9 lists the protonation and metal complex formation constants of methyl phosphate. In table 4.10 they are compared to values available in the literature. Good agreement is generally found.

Table 4.9: Equilibrium constants of methyl phosphate at T=25°C and I=0.15 mol/l (NaCl)

cation	cplx	log β	std. dev.	n_t	n_p	R R_{lim}	pH	initial concentration	K
H^+	LH	6.251	0.001	5	261	0.0182 0.0094	2.5-9.5	L:0.002-0.007	A,B
Cu^{2+}	ML	2.819	0.007	6	391	0.0593	4.0-6.0	L:0.001-0.002	M
	MLH_{-1}	-3.427	0.020			0.0239		pH<6	
Zn^{2+}	ML	2.175	0.008	8	189	0.0240	2.7-7.3	L:0.003-0.007	B
	MLH_{-1}	-5.124	0.013			0.0311		M:0.002-0.007	
Ca^{2+}	ML	1.394	0.009	7	435	0.0369	3.0-8.0	L:0.003-0.006	B,M
	MLH_{-1}	-7.093	0.016			0.0146		M:0.003-0.008	

Table 4.10: Equilibrium constants of methyl phosphate Comparison with literature values

cation	complex	log β	I	T	reference
H^+	LH	6.251	0.15 NaCl	25°C	this study
		6.58		22.5°C	[112]
	LH_2	1.52		22°C	[112]
Zn^{2+}	LM	2.175	0.15 NaCl	25°C	this study
		2.16	0.1 Cl	20°C	[113]
Ca^{2+}	LM	1.394	0.15 NaCl	25°C	this study
		1.49	0.1 Cl	20°C	[113]

4.1.8 Hydrogen phosphate

In the pH region 2 to 9 two protonation constants were determined. The third proton is released at pH>9 and is treated as a hydroxo complex due to our definition of the ligand. As only few data points were collected in the pH region 9-11 these data were initially excluded when the two protonation constants in the acidic region were refined. They were then fixed and a value for the stability constant of the hydroxo complex obtained by using the complete set of data. The protonation constants obtained here are shown in table 4.11. They are in very good agreement with literature values as seen in figure 4.3. Figure 4.3 also illustrates the need for ionic strength corrections.

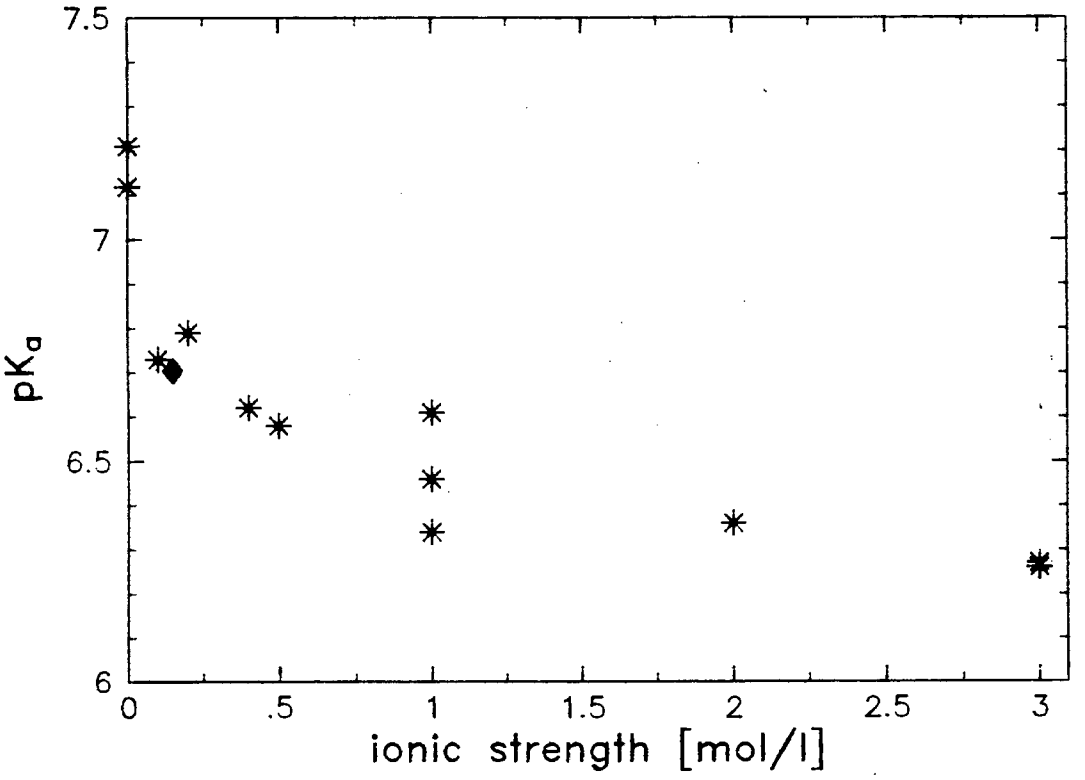

Figure 4.3: Protonation constants of hydrogen phosphate at 25°C as a function of ionic strength. * denotes literature values [35-37], and ◆ the value obtained here

The stability constants for the complexation of copper, zinc and calcium that have been reported in the literature are listed in table 4.12. In order to obtain stability constants for these metal-ligand systems under the same experimental conditions as used for the other ligands considered here, a lot of effort was put into the determination of stability constants with copper and zinc. The pH range had to be kept

below pH=4.2 for copper and below pH=4.7 for zinc. At higher pH very fine precipitates occured. The formation curves obtained by using hydroxide solution in the burette gave $\bar{Z}$ = 0±0.02 over the whole titration for different ligand to metal ratios and for different concentrations (partly similar to those used in [114,115]). Therefore it was attempted to titrate with metal solution instead of hydroxide solution, but again $\bar{Z}$ was found never to rise above zero.

After these discouraging experiments theoretical formation curves for the experimental conditions used here and in [114,115] (assuming the same precipitation limits as found here) were calculated using the literature formation constants. $\bar{Z}$ was indeed found to vary between 0 and 0.02 and speciation plots showed that LM only just occurs before the onset of precipitation. It therefore seems impossible to obtain a reliable value for the complex of interest, LM and it was decided not to try and optimize experimental conditions. It may be necessary to study the complexation not only by potentiometric titration but to investigate a liquid-solid system including all the insoluble complexes (precipitates). Another option might be the use of a competing ligand which could reduce the free metal concentration and prevent precipitation. Both alternatives are very labour-intensive and will not necessarily be successful.

Table 4.11: Protonation constants of hydrogen phosphate at T=25°C and I=0.15 mol/l (NaCl)

cation	cplx	log β	std. dev.	n_t	n_p	R / R_{lim}	pH	initial concentration	K
H^+	LH_2	8.708	0.006	4	345	0.0065	1.5-11.0	L:0.002-0.005	A,B
	LH	6.704	0.003			0.0051			
	LH_{-1}	-11.553	0.011						

Table 4.12: Equilibrium constants of hydrogen phosphate literature values

cation	complex	log β	I	T	reference
Cu^{2+}	LM_2H	13.4	0.15 KNO_3	37°C	[114]
	LMH	8.0	0.15 KNO_3	37°C	[114]
	L_2M_2	9.2	0.15 KNO_3	37°C	[114]
	LM	3.3	0.15 KNO_3	37°C	[114]
		3.2	0.1 $NaClO_4$	25°C	[115]
Zn^{2+}	LM_2H	11.9	0.15 KNO_3	37°C	[114]
	LMH	7.9	0.15 KNO_3	37°C	[114]
	L_2M_2	8.4	0.15 KNO_3	37°C	[114]
	LM	2.4	0.15 KNO_3	37°C	[114]
		2.4	0.1 $NaClO_4$	25°C	[115]
Ca^{2+}	LM_2H	10.4	0.15 KNO_3	37°C	[114]
	LMH	7.3	0.15 KNO_3	37°C	[114]
	L_2M_2	6.3	0.15 KNO_3	37°C	[114]
	LM	1.3	0.15 KNO_3	37°C	[114]

4.1.9 8-Quinolyl phosphate

The determination of formation constants of 8-quinolyl phosphate with protons and divalent copper, zinc, nickel, cobalt and manganese ions was straightforward and no problems were experienced. The formation curves with copper, zinc and nickel ions show backfanning pattern and the hydroxo complex LMH_{-1} was found in addition to LM. No backfanning was observed with cobalt ions and with manganese ions. The stability constants are summarized in table 4.13. Unlike all other monophosphoric acid esters studied, this ligand has two potential binding sites, the quinolyl nitrogen and one of the non-ester oxygens. In order to assign the two protonation constants to the two binding sites a nmr titration was performed. The plot of the chemical shift of the phosphorus atom against the pH of the solution is shown in figure 4.4.

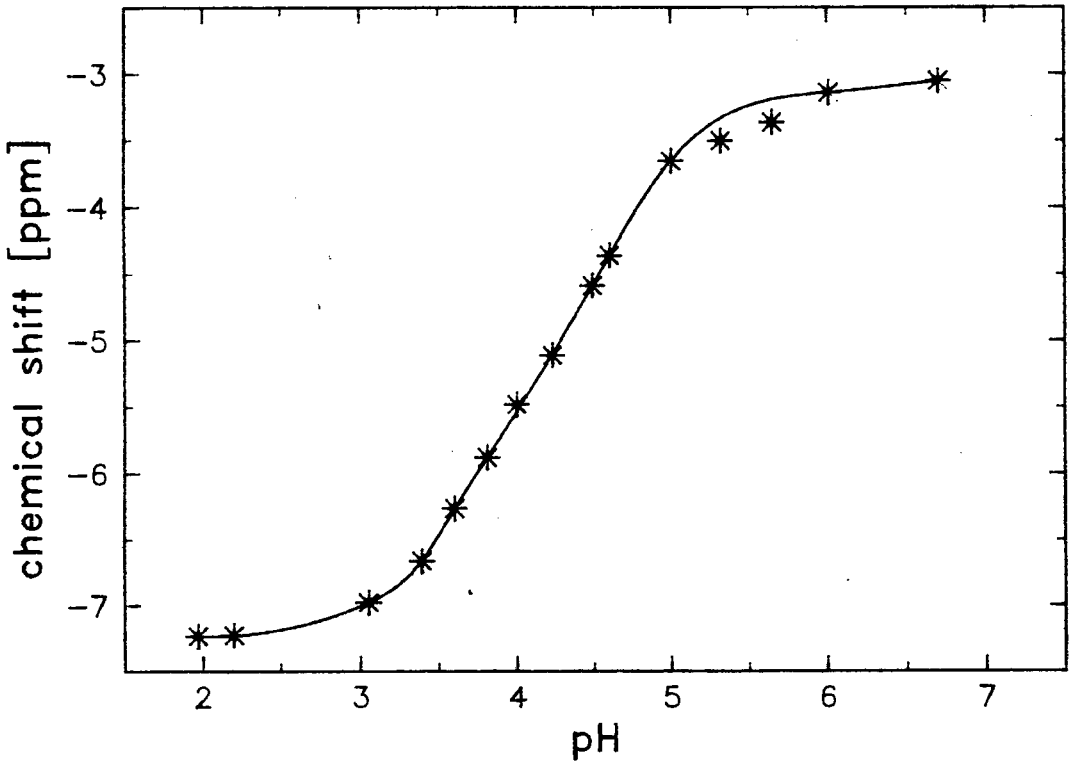

Figure 4.4: Plot of the ^{31}P-nmr chemical shift of the phosphorus atom of 8-quinolyl phosphate as a function of pH

The greatest rate of change of chemical shift occurs at a pH of about 4.2. This implies that the potentiometrically measured pK value of pK=4.13 corresponds to the phosphate group. This assignment is in direct contrast with the result of a comparison of the pK values of 8-quinolyl phosphate with those of the related ligands, 1-naphthyl phosphate and

8-quinolyl methyl phosphate (see sections 4.1.3 and 4.1.10, respectively). The pK of 4.13 is much closer to the pK=4.72 of 8-quinolyl methyl phosphate than to the pK=5.74 of 1-naphthyl phosphate. Although the pK of the phosphate group of 8-quinolyl phosphate is very likely to be lowered in comparison to the pK of 1-naphthyl phosphate due to the strong electron-withdrawing character of the quinolyl moiety, it seems unlikely that the lowering should be as large as 1.61. It is more likely to assume that the first proton to be bound is shared beween the two binding sites, and that this is probably accompanied by some hydrogen bonding. Any interference due to intramolecular stacking was ruled out. At pH=6.2, where stacking interactions are likely to be favoured, the chemical shift of the phosphorus peak of 8-quinolyl phosphate was found to be independent of concentration within the range 0.016-0.002 mol/l. Concentrations used in the potentiometric titrations and nmr titrations fall within these limits.

A comparison of the stability constants of 8-quinolyl phosphate with those of the two related ligands, 1-naphthyl phosphate (section 4.1.3) and 8-quinolyl methyl phosphate (section 4.1.10) shows that the complexes formed between 8-quinolyl phosphate and copper, zinc and nickel ions are considerably stronger. This indicates that these metal ions are complexed by the quinolyl nitrogen and one of the phosphate oxygens at the same time, i.e. chelates are formed between 8-quinolyl phosphate and copper, zinc and nickel ions.

In table 4.14 the stability constants obtained here are compared with literature values. Good agreement is found. The existence of a protonated copper complex CuLH reported in [22] could not be confirmed. It was in fact possible to refine a stability constant for this complex, but speciation plots showed that it occured in negligible concentrations, so that this complex was removed from the model.

Table 4.13: Equilibrium constants of 8-quinolyl phosphate at 25°C and I=0.15 mol/l (NaCl)

cation	cplx	log β	std. dev.	n_t	n_p	R / R_{lim}	pH	initial concentration	K
H^+	LH	6.333	0.001	4	265	0.0008	2.0-9.0	L:0.002-0.005	A,B
	LH_2	10.462	0.002			0.0019			
Cu^{2+}	LM	5.114	0.005	10	318	0.0103	2.2-6.0	L:0.002-0.005	B
	LMH_{-1}	-0.910	0.012			0.0021		M:0.002-0.003	
Zn^{2+}	LMH	9.695	0.014	7	263	0.0215	2.2-6.5	L:0.003-0.006	B
	LM	4.870	0.012			0.0025		M:0.002-0.005	
	LMH_{-1}	-1.697	0.036						
Ni^{2+}	LM	2.345	0.010	6	269	0.0204	3.0-7.5	L:0.003-0.004	B
	LMH_{-1}	-5.469	0.027			0.0038		M:0.002-0.006	
Co^{2+}	LM	1.781	0.024	6	294	0.0111	2.3-7.0	L:0.003-0.004	B
						0.0022		M:0.002-0.007	
Mn^{2+}	LM	1.909	0.015	7	245	0.0133	3.5-8.0	L:0.003-0.004	B
						0.0033		M:0.002-0.007	

Table 4.14: Equilibrium constants of 8-quinolyl phosphate Comparison with literature values

cation	complex	log β	I	T	reference
H^+	LH	6.333	0.15 NaCl	25°C	this study
		6.42	0.1 KNO_3	25°C	[22]
	LH_2	10.462	0.15 NaCl	25°C	this study
		10.59	0.1 KNO_3	25°C	[22]
	LH_3	11.59	0.1 KNO_3	25°C	[22]
Cu^{2+}	LM	5.114	0.15 NaCl	25°C	this study
		5.29	0.1 KNO_3	25°C	[22]
	LMH	8.85	0.1 KNO_3	25°C	[22]

4.1.10 8-Quinolyl methyl phosphate

8-Quinolyl methyl phosphate differs from the other monophosphoric acid esters studied. It is a diester and thus cannot bind through the phosphate oxygen, because again the pK of the first oxygen is so low that it will always be deprotonated within the pH range accessible to glass electrodes. The only relevant binding site is thus the quinolyl nitrogen.

During the experimental work it turned out to be favourable to determine the formation constants of the complexes of 8-quinolyl methyl phosphate with zinc, nickel and cobalt ions by titrations where metal ion solution was added from the burette. The formation constants of 8-quinolyl methyl phosphate with protons and metal ions are listed in table 4.15. The protonation and copper complexation constants are very similar to those of quinoline (log β_{LH}=4.97, log β_{LM}=2.65, T=25°C, I=0.1 mol/l KNO_3 [116]). This similarity shows that the phosphate group has a very small effect on the quinolyl moiety of 8-quinolyl methyl phosphate.

Table 4.15: Equilibrium constants of 8-quinolyl methyl phosphate at 25°C and I=0.15 mol/l (NaCl)

cation	cplx	log β	std. dev.	n_t	n_p	R / R_{lim}	pH	initial concentration	K
H^+	LH	4.275	0.001	6	246	0.0017 0.0020	2.0-8.0	L:0.002-0.006	A,B
Cu^{2+}	LM	2.523	0.004	8	277	0.0048	2.2-6.2	L:0.003-0.006	B
	LMH_{-1}	-4.062	0.020			0.0020		M:0.001-0.007	
Zn^{2+}	LM	1.187	0.021	6	215	0.0059	2.0-6.5	L:0.004-0.008	B,M
	LMH_{-1}	-5.531	0.041			0.0023		M:0.002-0.009	
Ni^{2+}	LM	1.724	0.015	5	174	0.0243	2.6-6.2	L:0.005-0.007	B,M
	LMH_{-1}	-5.083	0.038			0.0027		M:0.007-0.010	
Co^{2+}	LM	1.237	0.016	7	187	0.0186	3.2-6.3	L:0.006-0.008	B,M
	LMH_{-1}	-5.263	0.026			0.0038		M:0.008-0.010	

4.1.11 Triphosphate

The formation constants of triphosphate complexes with protons, copper, zinc and calcium ions are summarized in table 4.17. The first three protonation constants were determined. It is impossible to assign them to the different phosphate groups. A phosphorus nmr titration curve shows a large amount of sharing of the protons between the terminal and the central phosphate group [117].
The formation curve for the calcium-triphosphate system levels out at $\bar{Z}$=1 and LM is indeed the major complex. The metal complex formation curves of copper and zinc indicate a step at $\bar{Z}$=1 (fig. 4.5), and again LM is the major complex for these systems at intermediate pH.

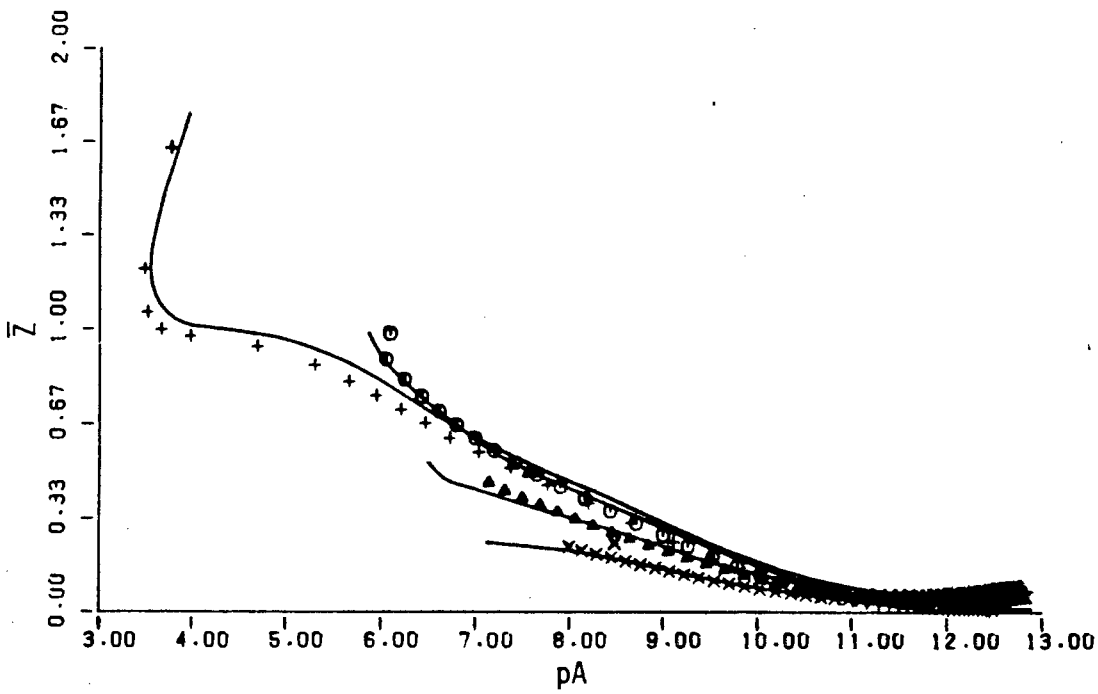

Figure 4.5: Selected experimental (symbols) and theoretical (lines) formation curves obtained for the complexation of zinc ions with triphosphate. The ligand concentration was kept fixed at 0.0015 mol/l and the metal concentrations were 0.0008 mol/l (+), 0.0015 mol/l (○), 0.0031 mol/l (△), and 0.0062 mol/l (×).

It cannot be decided whether the metal is bound to one, two or all three phosphate groups but there seems to be a general agreement that at least two phosphate groups participate [118,119]. This is in analogy to the proton complexation and is further supported by the fact that the metal

complexation constants of triphosphate are considerably higher than those of orthophosphate [35-37]. The rise to $\bar{Z}>1$ at low pA could be accounted for by introducing the hydroxo complexes LMH_{-1} into the models. For all three metal ions studied here, LMH is the dominant species at low pH. In addition to the complexes already discussed above two interesting minor complexes occur. The complex LM_2 is consistent with my experimental data for copper and zinc as well as calcium. Although LCu_2 has been suspected to exist long ago [119] no stability constants have so far been reported. In order to establish its existence some of the titrations were carried out in which the ligand concentration was kept fixed, but the metal concentration was varied. The result is shown in figure 4.5.

At fixed pA, $\bar{Z}$ decreases with increasing metal concentration, thus indicating the presence of species where more than one metal ion is bound to the ligand (The fact that $\bar{Z}$ of the [L]:[M]=1:1 titration is above $\bar{Z}$ for the 2:1 titration at low pA is due to the hydroxo complex). I propose the following structure for the complex LM_2 (figure 4.6)

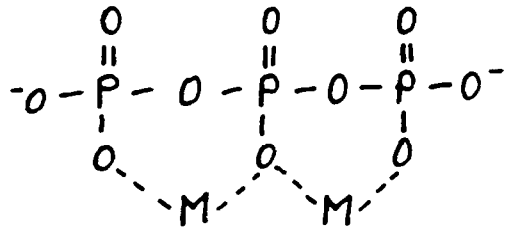

Figure 4.6: Proposed structure of the complex LM_2

Knowing that protons are being shared by the central and terminal phosphate group it seems likely that the same occurs when a metal ion is bound to the phosphate chain. There is no reason why the second metal ion should be bound to the ligand in a fashion different from the first because the ligand is symmetrical. Therefore I expect an arrangement in which both metals are equivalent, as suggested above.

A complex of the composition LMH_2 has been reported for the complexation of calcium with triphosphate ion [120]. The existence of this complex could be confirmed. In addition an equivalent complex has been found for zinc, but not for copper. Because copper has a stronger tendency to coordinate to the ligand than the two other metal ions, it is capable of displacing a proton from the complex LH_2 and coordinating to two phosphate groups at the same time. Zinc and calcium cannot displace protons so easily and therefore perhaps bind to only one phosphate group in this pH region. The complex LMH_2 results.

The fact that several new complexes were found partly explains why some of the formation constants found here are significantly, i.e. up to 0.5 log units lower than the corresponding literature values (table 4.18) Other possible reasons, e.g. different temperature, ionic strength or background electrolyte could be ruled out by adjusting the literature values to the conditions used here, using the van't Hoff equation (eq.3.2) to account for temperature changes if ΔH is known, and an extended form of the Debye-Hückel equation (eq.3.9) to account for ionic strength changes. The two most commonly used background electrolytes are chlorides and nitrates. Complexation of chloride and nitrate with copper, zinc and calcium is very similar under my experimental conditions (table 4.16) and cannot account for any large differences.

Table 4.16: Formation constants of complexes of divalent copper, zinc and calcium ions with chloride and nitrate at T=25°C and I=0.15 mol/l (as calculated by LOGK [95] from literature values [35])

cation	chloride $\log \beta_{LM}$	nitrate $\log \beta_{LM}$
Cu^{2+}	-0.03±0.13	0.12±0.13
Zn^{2+}	-0.04±0.13	-0.05±0.13
Ca^{2+}	0.55±0.29	0.24±0.13

As I put a lot of effort into eliminating possible errors, I have confidence in the values obtained here although they do not always agree favourably with literature values obtained quite a long time ago when titration and computation techniques were not as sophisticated as they are now.

Table 4.17: Equilibrium constants of triphosphate at T=25°C and I=0.15 mol/l (NaCl)

cation	cplx	log β	std. dev.	n_t	n_p	R / R_{lim}	pH	initial concentration	K
H^+	LH	8.649	0.003	6	315	0.0069	1.8-11.0	L:0.001-0.005	A,B
	LH_2	14.437	0.005			0.0180			
	LH_3	16.219	0.019						
Cu^{2+}	LMH	14.008	0.010	8	294	0.0081	2.2-9.0	L:0.001-0.003	B
	LM	8.624	0.017			0.0057		M:0.001-0.004	
	LM_2	12.322	0.036						
	LMH_{-1}	-0.391	0.041						
Zn^{2+}	LMH_2	16.691	0.079	9	245	0.0077	2.0-9.0	L:0.001-0.003	B
	LMH	13.575	0.030			0.0027		M:0.001-0.009	
	LM	8.114	0.033						
	LM_2	11.394	0.038						
	LMH_{-1}	-1.597	0.174						
Ca^{2+}	LMH_2	16.392	0.040	9	393	0.0031	1.9-9.5	L:0.001-0.005	B
	LMH	12.291	0.010			0.0035		M:0.001-0.006	
	LM	5.755	0.010						
	LM_2	8.344	0.026						

Table 4.18: Equilibrium constants of triphosphate Comparison with literature values

cation	com-plex	I [mol/l]	T [°C]	reaction	log β or log K	refe-rence	T→25°C	I→0.15mol/l	I→0.15mol/l T→25°C
H^+	LH	0.15 TMACl	25		log β=8.65	+			8.65
		0.1 TMACl	25		log β=8.73	[104]	8.61±0.5	8.61	
		1.0 TMACl	25	L+H=LH	log β=8.81	[104]			
		→0 TMACl	25		log β=8.90	[104]			
		→0	25		log β=9.52	[121]		8.65*	8.65*
		0.1 $TMA(NO_3)$	20		log β=8.82	[118]	8.82	8.74*	8.74*
H^+	LH_2	0.15 TMACl	25	L+2H=LH_2	log β=14.44	+			
					log K=5.79	+			5.79
		0.1 TMACl	25		log K=6.00	[104]		5.87±0.5	
		1.0 TMACl	25	LH+H=LH_2	log K=5.83	[104]			5.87
		→0 TMACl	25		log K=6.26	[104]			
		0.1 $TMA(NO_3)$	20		log K=5.93	[118]		5.86*	
H^+	LH_3	0.15 TMACl	25	L+3H=LH_3	log β=16.22	+			
					log K=1.78	+			1.78
		0.1 TMACl	25		log K=2.15	[104]		2.03±0.5	
		1.0 TMACl	25	LH_2+H=LH_3	log K=2.11	[104]			2.03
		→0 TMACl	25		log K=2.30	[104]			
		0.1 $TMA(NO_3)$	20		log K=2.2	[118]		2.13*	
Cu^{2+}	LM	0.15 TMACl	25		log β=8.62	+			8.62
		0.1 $TMA(NO_3)$	20	L+M=LM	log β=9.3	[118]	9.44	9.27*	9.27*
Cu^{2+}	LMH	0.15 TMACl	25	L+M+H=LMH	log β=14.01	+			
				LH+M=LMH	log K=5.36	+			5.36
		0.1 $TMA(NO_3)$	20		log K=6.1	[118]		5.94*	
Cu^{2+}	LM_2	0.15 TMACl	25	L+2M=LM_2	log β=12.32	+			12.32
Cu^{2+}	LMH_{-1}	0.15 TMACl	25	L+M-H=LMH_{-1}	log β=-0.39	+			-0.39
Zn^{2+}	LM	0.15 TMACl	25		log β=8.11	+			8.11
		0.1 $TMA(NO_3)$	20	L+M=LM	log β=8.35	[118]	8.53	8.36	8.36*
		→0	25		log β=9.7±0.5	[121]		7.89*	7.89*
Zn^{2+}	LMH	0.15 TMACl	25	L+M+H=LMH	log β=13.57	+			
				LH+M=LMH	log K=4.93	+			4.93
		0.1 $TMA(NO_3)$	20		log K=5.13	[118]		4.97*	
Zn^{2+}	LM_2	0.15 TMACl	25	L+2M=LM_2	log β=11.39	+			11.39
Zn^{2+}	LMH_{-1}	0.15 TMACl	25		log β=-1.5966	+			-1.5966
		→0	25	L+M-H=LMH_{-1}	log β=-1.0	[121]		-3.7[5d4]	-3.7
								-3.01*	-3.01*
Zn^{2+}	LMH_2	0.15 TMACl	25	L+2H+M=LH_2M	log β=16.69	+			16.69
Ca^{2+}	LM	0.15 TMACl	25		log β=5.75	+			5.75
		0.10 TMABr	25		log β=6.41±0.04	[120]		6.23±0.07	
		1.0 TMABr	25	L+M=LM	log β=5.36±0.02	[120]			6.23
		0.10 $TMA(NO_3)$	20		log β=6.31	[118]	6.41	6.24*	6.24*
		→0	25		log β=8.1±0.3	[121]		6.29*	6.29*
Ca^{2+}	LMH	0.15 TMACl	25	L+M+H=LMH	log β=12.29	+			
					log K=3.64	+			3.64
		0.10 TMABr	25	LH+M=LMH	log K=3.78±0.06	[120]		3.63±0.08	
		1.0 TMABr	25		log K=3.30±0.16	[120]			3.63
		0.1 $TMA(NO_3)$	20		log K=4.02	[118]		3.86*	
Ca^{2+}	LMH_2	0.15 TMACl	25	L+M+2H=LMH_2	log β=16.39	+			
				LH_2+M=LMH_2	log K=1.95	+			1.95
		1.0 TMABr	25		log K=2.77±0.4	[120]		3.39*	3.39*
Ca^{2+}	LM_2	0.15 TMACl	25	L+2M=LM_2	log β=8.34	+			
				M+ML=M_2L	log K=2.59	+			2.59
			25		log K=3.0	[122]			

\+ : denotes results obtained in this thesis
* : c has been set to c=0 (eq.3.9)
TMA: Tetramethylammonium

4.1.12 Fluorotriphosphate

In the pH region 1.5 to 12,two protonation constants could be determined which correspond to the first and second proton being bound to the fully deprotonated ligand $FP_3O_9^{4-}$. In order to identify the binding sites a phosphorus-nmr titration of the ligand was carried out. The chemical shifts δ measured for the different phosphate groups were plotted against pH (figure 4.7)

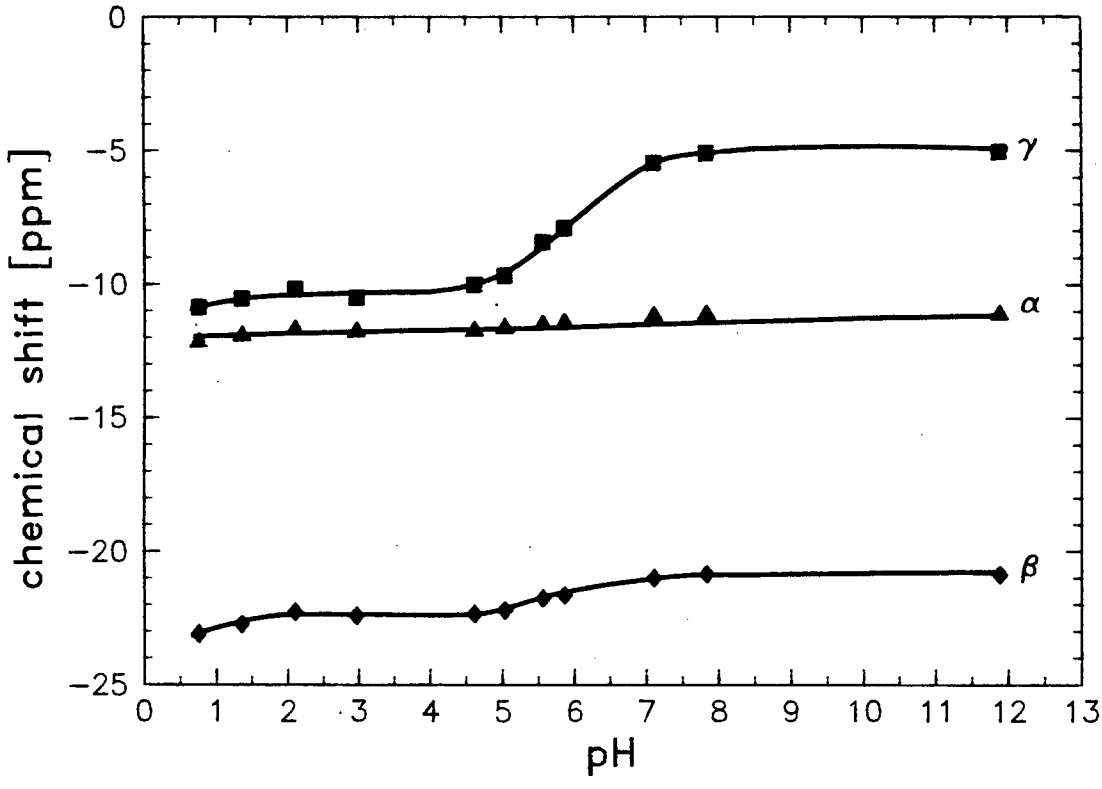

Figure 4.7: Plot of the ^{31}P-nmr chemical shift δ of the different phosphate groups of fluorotriphosphate against pH

From the plot it is clear that the first proton is bound to the γ-phosphate group because the rate of change of δ_γ has a maximum at pH≈6.0. The pK=6.648 is thus assigned to the γ-phosphate group. The β-phosphate group is affected to a small extent only indicating a small amount of sharing of the proton between the γ and the β phosphate group. The second proton is probably attached to the β phosphate group as δ_β seems to drop slightly at low pH. The α-phosphate group is unaffected by any pH change. This confirms that the strongly electronegative fluorine atom is electron-pulling and decreases the nucleophilic character of the adjacent α-phosphate group. The α-phosphate group is thus a very acidic site and does not participate in proton binding in the pH range studied.

No problems arose during the potentiometric work to determine metal complexation constants. The formation curves obtained for copper and zinc are of similar shape. In both cases, $\bar{Z}$ shows a step near $\bar{Z}$=1 (figure 4.8) and LM is indeed the major complex for these systems.

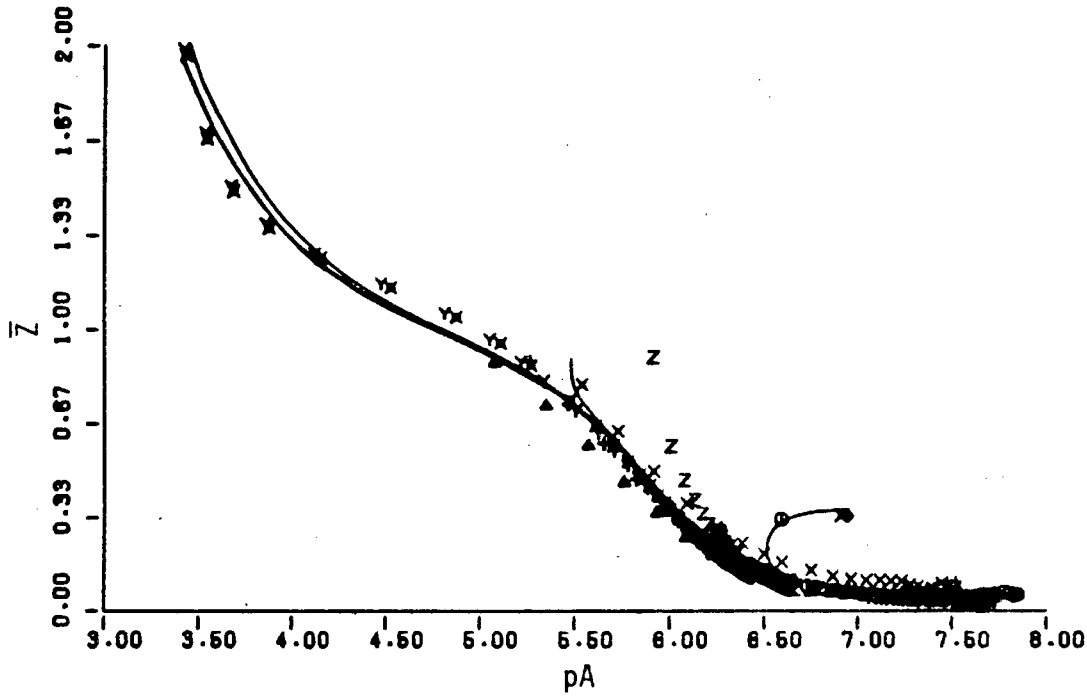

Figure 4.8: Experimental (symbols) and theoretical (line) formation curves obtained for the complexation between copper ions and fluorotriphosphate. The concentrations are:

[L]=0.00117 mol/l, [M]=0.00349 mol/l (○);
[L]=0.00159 mol/l, [M]=0.00158 mol/l (△),(+);
[L]=0.00138 mol/l, [M]=0.00134 mol/l (×);
[L]=0.00138 mol/l, [M]=0.00402 mol/l (◇);
[L]=0.00138 mol/l, [M]=0.00669 mol/l (☆);
[L]=0.00138 mol/l, [M]=0.00402 mol/l (☒);
[L]=0.00178 mol/l, metal titration (Z);
[L]=0.00170 mol/l, metal titration (Y);
[L]=0.00159 mol/l, metal titration (▯).

The rise to $\bar{Z}$>1 and the weak fanning pattern were accounted for by introducing the hydroxo species LMH_{-1} for copper and LM_2H_{-1} for zinc into the models. The zinc complex LM_2H_{-1} may initially seem somewhat unlikely. In a solution containing zinc and hydroxide, however, the complex Zn_2H_{-1} is inter alia formed at pH=8 [86], the pH at which LM_2H_{-1} also occurs. It is therefore not unlikely that a ligand can be attached to a Zn_2H_{-1} molecule. A species LMH is found for the interaction of the ligand with copper and accounts for the "fanning" of the formation curves at high pA. No such fanning was observed for zinc complexation

and no stability constant for a protonated zinc complex could be refined.

In contrast to the complexation of copper and zinc no step and no distinct fanning pattern is observed in the formation curves obtained for the calcium-fluorotriphosphate system. Also no precipitates occurred. After a lot of computing the final model consisting of the complexes LM, L_2M and L_2MH_{-1} was established. It is very surprising that a complex L_2M is found for calcium and not for the stronger zinc and copper systems. Maybe the bigger calcium ion is bound to the γ-phosphate group only whereas the copper or zinc ion is bound to γ and β phosphate groups at the same time. A densely packed complex is formed which makes it impossible for a second ligand molecule to coordinate to this cluster.

The potentiometric results are summarized in table 4.19. The high standard deviations of the hydroxo complexes reflect the fact that only few data points could be collected in the corresponding pH region due to the formation of precipitates.

A rough estimate of the first protonation constant, log β_{LH}=6.20 has been reported in the literature [123] and is in reasonable agreement with the more precise value obtained here.

Table 4.19: Equilibrium constants of fluorotriphosphate at T=25°C and I=0.15 mol/l (NaCl)

cation	cplx	log β	std. dev.	n_t	n_p	R / R_{lim}	pH	initial concentration	K
H^+	LH	6.648	0.006	4	209	0.0010	1.5-9.0	L:0.001-0.004	A,B
	LH_2	7.874	0.015			0.0025			
Cu^{2+}	LMH	9.081	0.036	10	515	0.0044	1.8-7.0	L:0.001-0.003	B,M
	LM	5.971	0.014			0.0018		M:0.001-0.007	
	LMH_{-1}	-0.264	0.028						
Zn^{2+}	LM	4.635	0.008	9	238	0.0195	2.0-7.5	L:0.001-0.004	B,M
	LM_2H_{-1}	1.810	0.031			0.0089		M:0.001-0.003	
Ca^{2+}	LM	3.734	0.006	7	571	0.0044	2.0-8.0	L:0.001-0.003	B,M
	L_2M	6.980	0.012			0.0034		M:0.002-0.005	
	L_2MH_{-1}	1.810	0.031						

4.2 Calorimetric results

4.2.1 Heats of dilution

The heat of dilution is the heat that is generated when the titrant distributes in the titration vessel. The heat of dilution of hydrochloric acid is rather large and its contribution to the total heat measured during the protonation of glycerol-2-phosphate and to α-D-glucose-1'-phosphate amounts to almost 50%. The contribution of the heat of dilution of copper chloride to the total heat measured during copper complexation amounted to about 5% except in the case of methyl phosphate, where it was about 10%. Both the dilution of hydrochloric acid and of copper chloride is exothermic.

4.2.2 Protonation enthalpies

A typical titration curve is shown in figure 4.9.

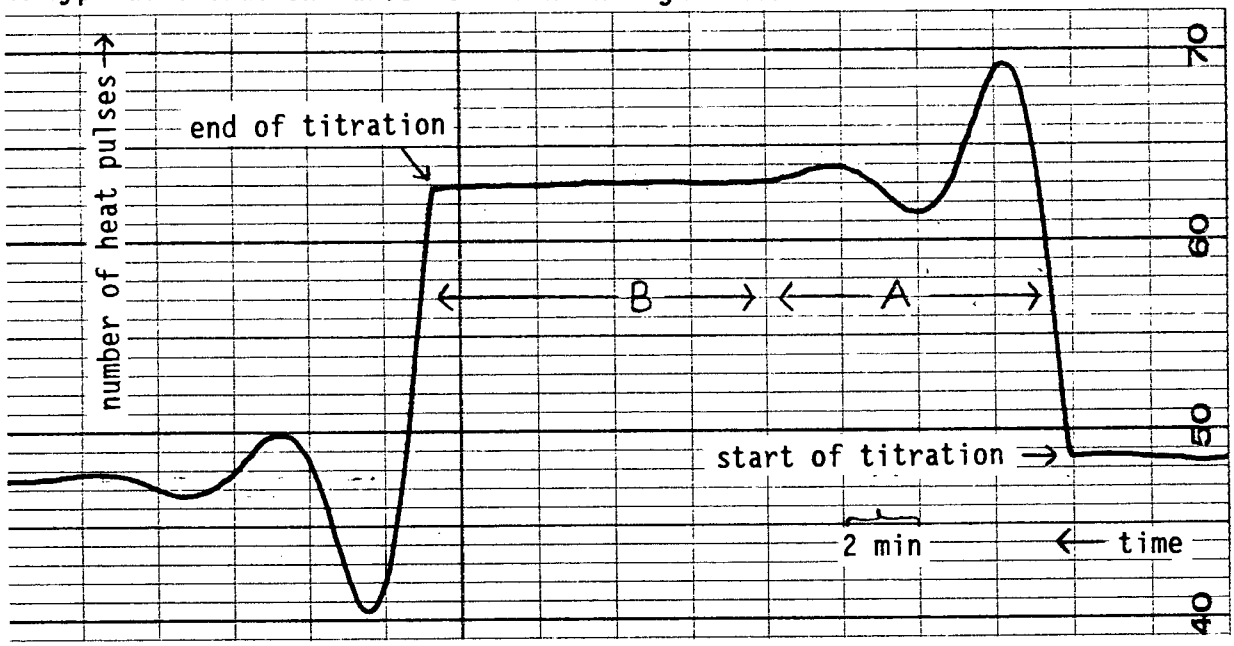

Figure 4.9: Titration curve for the titration of a solution of p-nitrophenyl phosphate with hydrochloric acid

In the initial part of the titration, the temperature change caused by the reaction is unavoidably overcompensated by the regulating system before a stable response is obtained. Unfortunately the time needed to reach the new equilibrium was rather long. Because the reaction heat of glycerol-2-phosphate and α-D-glucose-1'-phosphate is small, it was necessary to add the acid at the fastest possible speed (1ml/100sec) in order to obtain a significant change in the number of heat pulses. The

total amount of acid was added before the system reached the new equilibrium, i.e. the heat compensation never reached stage B. In order to calculate the protonation enthalpy ΔH_{LH} from these data the response of the regulating system was compared to the initial response obtained in the calibration experiments, i.e. the two overshoots were compared to each other. This calculation procedure gives results which differ up to 0.1% from results one obtains from data in region B. This was verified by applying both calculation methods to the data obtained for p-nitrophenyl phosphate. The reproducibility of identical titrations was found to be 1% for all ligands.

After about 95% of the glycerol-2-phosphate and α-D-glucose-1'-phosphate are protonated an additional endothermic reaction sets in, which is not observed for the other phosphate esters studied here. Data points collected in this region were not used in the calculation of ΔH_{LH}.

The results obtained for the heat of the first protonation of the ligands are summarized in table 4.20.

Table 4.20: Protonation enthalpies of phosphoric acid esters

Ligand	ΔH_{LH} [kJ/mol]	standard deviation [kJ/mol]	number of titrations	literature value [kJ/mol]		ref
p-Nitrophenyl phosphate	7.39	0.09	4	7.65	C	[124]
Phenyl phosphate	3.68	0.46	5			
1-Naphthyl phosphate	4.50	0.04	4			
α-D-Glucose-1'-phosphate	1.52	0.03	3	1.803	T	[107]
Glycerol-2-phosphate	0.94	0.05	3	1.209	T	[111]
Methyl phosphate	2.82	0.03	3			
Hydrogen phosphate	-5.10	0.23	3	-2.510 to -5.021		[100]

C = calorimetric T = by temperature change

Some standard deviations seem rather high. However, a deviation of 0.4 kJ/mol corresponds to a change of the protonation constant of 0.005 if the temperature is lowered from 25°C to 5°C, as calculated from the van't Hoff equation (eq.3.2). Standard deviations of protonation constants are in the order of 0.002. It is therefore doubtful whether a more accurate value could have been obtained by measuring protonation

constants at different temperatures and by then calculating ΔH_{LH} according to eq.3.2. In addition, our titration setup used for the potentiometric titrations (see section 3.3.1) is not suitable for temperatures far from room temperature.

4.2.3 Copper complexation enthalpies

In all cases the reaction was over 90% complete while the heat compensation was still not at equilibrium. There is no way to avoid this problem because at high pH precipitation occurs if the concentrations are raised. At low pH the amount of complex formed is so small that the reaction heat is too small to be reliably measured even if copper solution is added at a very fast rate. In contrast to the titrations to determine the heat of protonation, the heat generated during the addition of copper solution is not constant, but drops. This is illustrated in figure 4.10a for a titration of 25ml 0.0056 mol/l 1-naphthyl phosphate solution at an initial pH of 5.6. In figure 4.10b, the percentage of ligand bound in the two complexes LM and LMH_{-1} is plotted against the metal to ligand ratio.

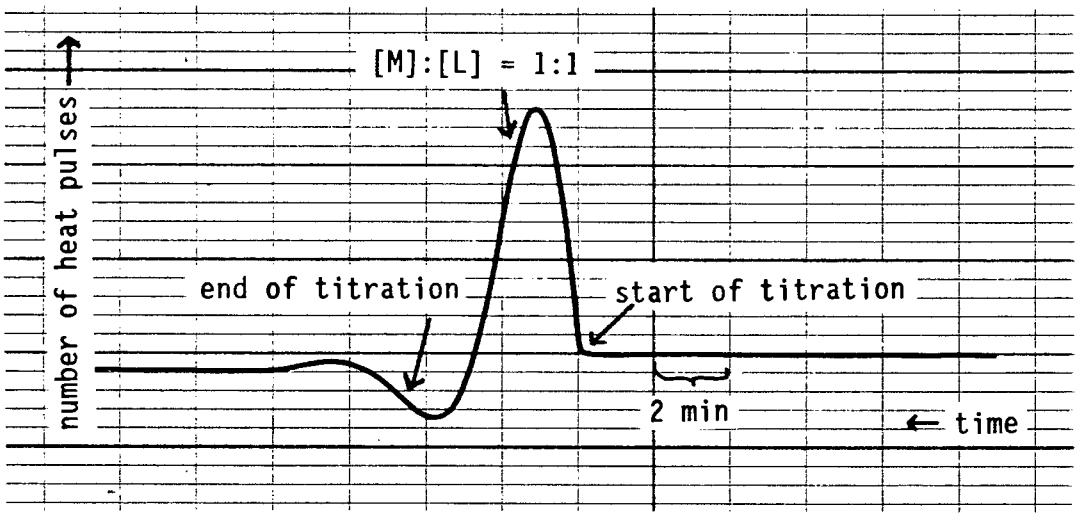

Figure 4.10a: Titration curve of the titration of 0.0056 mol/l 1-naphthyl phosphate solution with 0.012 mol/l copper(II) solution

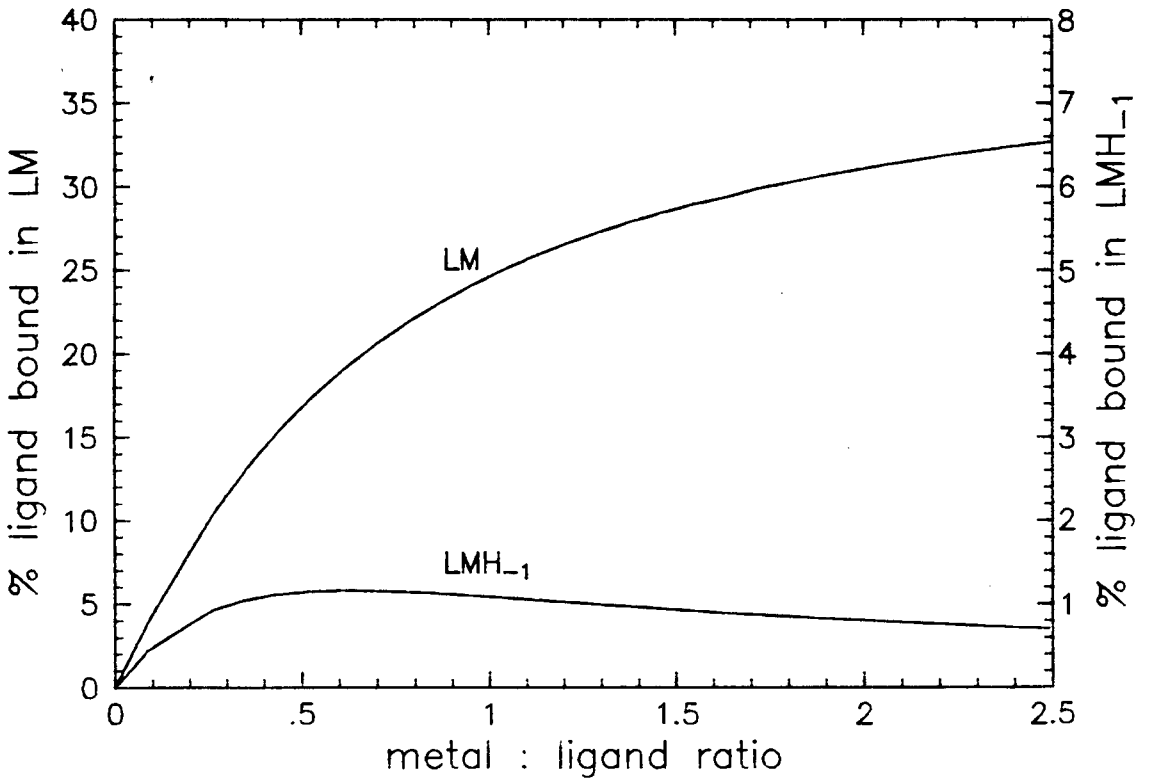

Figure 4.10b: Percentage of ligand bound in the two complexes LM and LMH_{-1} formed between copper ions and 1-naphthyl phosphate, plotted as a function of the metal to ligand ratio

In the initial stage of the titration the increase in the amount of complexes formed is high and a lot of heat is generated. As more copper solution is added the increase becomes increasingly smaller and less heat is generated. (The amount of hydroxo complex present drops because the pH of the solution drops upon complex formation). A situation where the amount of heat generated decreases as the reaction proceeds cannot be simulated by a calibration experiment. I nevertheless assume that one can still compare the overshoot of the calibration experiment with that of the actual titration. A big problem is the decision up to which point data points should be included into the calculation. Obviously (see fig.4.10b) all data must not be included because towards the end of the titration hardly any more complexes form. Consequently the heat effect is very tiny or zero. The heat compensation by the regulating system cannot keep up with the rapid changes and at the end of the titration, the heat is undercompensated due to the overshoot (fig. 10a). Data points in this region cannot be compared with the calibration experiment. Therefore I decided to use all data up to a ligand to metal

ratio of 1:1. In all titrations this ratio was reached just after the overshoot had reached its maximal value. (The choice of the ligand to metal ratio of 1:1 can be motivated as follows. If for any particular titration one evaluates ΔH_{LM} by taking the calorimetric data from the beginning of the titration up to different ligand to metal ratios above 1:1 one finds that these values differ by ±5% from each other. They tend to increase slightly until the maximum heating rate is reached and then drop again. The 5% variation of the values is within the experimental error and therefore the ligand to metal ratio of 1:1 seems to be a reasonable limit. For lower ligand to metal ratios ΔH_{LM} values drop significantly and even change sign.)

Eq.3.20 was used to calculate the complexation heats of the different complexes. The contributions to the measured heats due to the formation of LH, CuH_{-1} and Cu_2H_{-2} were calculated from the measured protonation heats and literature values ($\Delta H_{MH_{-1}}$ = -20.92 kJ/mol, $\Delta H_{M_2H_{-2}}$ = -35.56 kJ/mol [35]) and subtracted before the minimization. These three complexes together only contribute to up to 2% to the total heat. Unfortunately it turned out that the ΔH_i were correlated. This means that the equations are not independent of each other. The sum of squares of residuals did not rise significantly when only ΔH_{LM} instead of ΔH_{LM} plus $\Delta H_{LMH_{-1}}$ or ΔH_{LM} plus $\Delta H_{LMH_{-1}}$ plus $\Delta H_{LMH_{-2}}$ was refined. This indicates that the contributions due to the complexes LMH_{-1} and LMH_{-2} are negligible and that the ΔH values calculated for these complexes are arbitrary numbers, probably because the amount of hydroxo complexes are at least by a factor of 30 smaller than the amount of the complex LM. The relative proportion of hydroxo complexes cannot be raised because if pH is increased, precipitates occur. $\Delta H_{LMH_{-1}}$ and $\Delta H_{LMH_{-2}}$ can only be determined if the high experimental error can be lowered so that the contributions of the complexes LMH_{-1} and LMH_{-2} exceed the uncertainty of the measured heat.

As described above it is impossible to calculate reliable ΔH values for all the ligand-metal complexes present from the calorimetric data that have been obtained. In view of the fact that the number of moles of LMH_{-1} and LMH_{-2} are small compared to the number of moles of LM, I decided to assume that LM is the only species and calculated ΔH_{LM} for each experiment by simply dividing the corrected experimental heat by the number of moles of LM formed during the experiment. The averages of the results such obtained are listed in table 4.21.

Table 4.21: Copper complex formation enthalpies

Ligand	ΔH_{LM} [kJ/mol]	standard deviation [kJ/mol]	number of titrations
p-Nitrophenyl phosphate	20.4	0.8	5
Phenyl phosphate	21.6	1.6	4
1-Naphthyl phosphate	19.4	0.9	4
α-D-Glucose-1'-phosphate	21.8	1.3	5
Glycerol-2-phosphate	37.6	3.6	3
Methyl phosphate	29.9	2.3	4

The high standard deviations reflect the uncertainty in the calculation of the heat by comparing with the calibration experiments as well as the simplifying assumption that the contributions of LMH_{-1} and LMH_{-2} are zero. In contrast to the protonation enthalpies one could probably improve the complex formation enthalpies considerably by using a different experimental technique, e.g. by using a non-isothermal calorimetric approach or by measuring formation constants at various temperatures.

5. DISCUSSION

The aim of this research is to find a correlation between the strength of the proton and metal complexes of phosphate esters and the electron-donating or electron withdrawing potential of the ester group R. The electron donating potential is characterized by the protonation constant of the substituent alcohol, K_{ROH}. Formation constants β for the complexation of six phosphate esters and phosphoric acid with protons, copper, zinc and calcium have been determined. From these the free enthalpy ΔG can be calculated:

$$\Delta G = -RT \ln \beta \qquad (5.1)$$

ΔG is a measure of the driving force of a reaction. It is the sum of two contributions:

$$\Delta G = \Delta H - T\Delta S \qquad (5.2)$$

ΔH is the heat of reaction. If $\Delta H<0$ a reaction is energetically favoured. ΔS is the entropy of the system and represents the degrees of freedom of a system, as determined by e.g. the number of entities in solution as well as their possible modes of vibration or rotation, and their orientation towards each other. The protonation and copper complex formation heats have been determined by calorimetry. From ΔG and ΔH, ΔS can be calculated for these reactions.
I will now discuss in detail correlations between ΔG, ΔH and ΔS and pK_{ROH} for the protonation and copper complexation of phosphoric acid esters before finally, some speculations about similar effects in polyphosphate complexation will be considered.

5.1 Monophosphoric acid esters

The thermodynamic data on which the following discussion is based are summarized in table 5.1 and 5.2.

Table 5.1: Summary of formation constants

cation	ligand	log β_{LM}	log $\beta_{LMH_{-1}}$	log $\beta_{LMH_{-2}}$
H^+	p-nitrophenyl phosphate	4.987		
	1-naphthyl phosphate	5.740		
	phenyl phosphate	5.827		
	α-D-glucose-1'-phosphate	5.977		
	glycerol-2-phosphate	6.105		
	methyl phosphate	6.251		
	hydrogen phosphate	6.704		
Cu^{2+}	p-nitrophenyl phosphate	2.148		
	1-naphthyl phosphate	2.635	-3.840	
	phenyl phosphate	2.611		
	α-D-glucose-1'-phosphate	2.736	-4.080	-11.028
	glycerol-2-phosphate	2.808	-3.728	-10.312
	methyl phosphate	2.819	-3.427	
	hydrogen phosphate	3.2 [114]		
Zn^{2+}	p-nitrophenyl phosphate	1.758		
	1-naphthyl phosphate	2.014	-4.730	
	phenyl phosphate	2.146		
	α-D-glucose-1'-phosphate	2.118	-5.818	
	glycerol-2-phosphate	2.137	-5.628	
	methyl phosphate	2.175	-5.124	
	hydrogen phosphate	2.4 [114]		
Ca^{2+}	p-nitrophenyl phosphate	not studied		
	1-naphthyl phosphate	1.223		
	phenyl phosphate	1.442		
	α-D-glucose-1'-phosphate	1.712		
	glycerol-2-phosphate	no complexation		
	methyl phosphate	1.394		
	hydrogen phosphate	1.3 [115]		

Table 5.2: Calorimetric data

cation	ligand	ΔG [kJ/mol]	ΔH [kJ/mol]	TΔS [kJ/mol]
H^+	p-nitrophenyl phosphate	-28.47	7.39	35.86
	1-naphthyl phosphate	-32.77	4.50	37.27
	phenyl phosphate	-33.27	3.68	36.95
	α-D-glucose-1'-phosphate	-34.12	1.52	35.64
	glycerol-2-phosphate	-34.85	0.94	35.79
	methyl phosphate	-35.69	2.82	38.51
	hydrogen phosphate	-38.27	-5.10	33.17
Cu^{2+}	p-nitrophenyl phosphate	-12.3	20.4	32.7
	1-naphthyl phosphate	-15.0	19.4	34.4
	phenyl phosphate	-14.9	21.6	36.5
	α-D-glucose-1'-phosphate	-15.6	21.8	37.4
	glycerol-2-phosphate	-16.0	37.6	53.6
	methyl phosphate	-16.1	29.9	46.0

5.1.1 The relationship between the nucleophilicity of the ester group and the protonation constants of phosphate esters

Figure 5.1 shows a plot of pK_{LH} versus pK_{ROH}. The higher pK_{ROH}, i.e. the more electrondonating the substituent, the higher is the pK_{LH} of the phosphate ester, as predicted. The correlation is not linear.

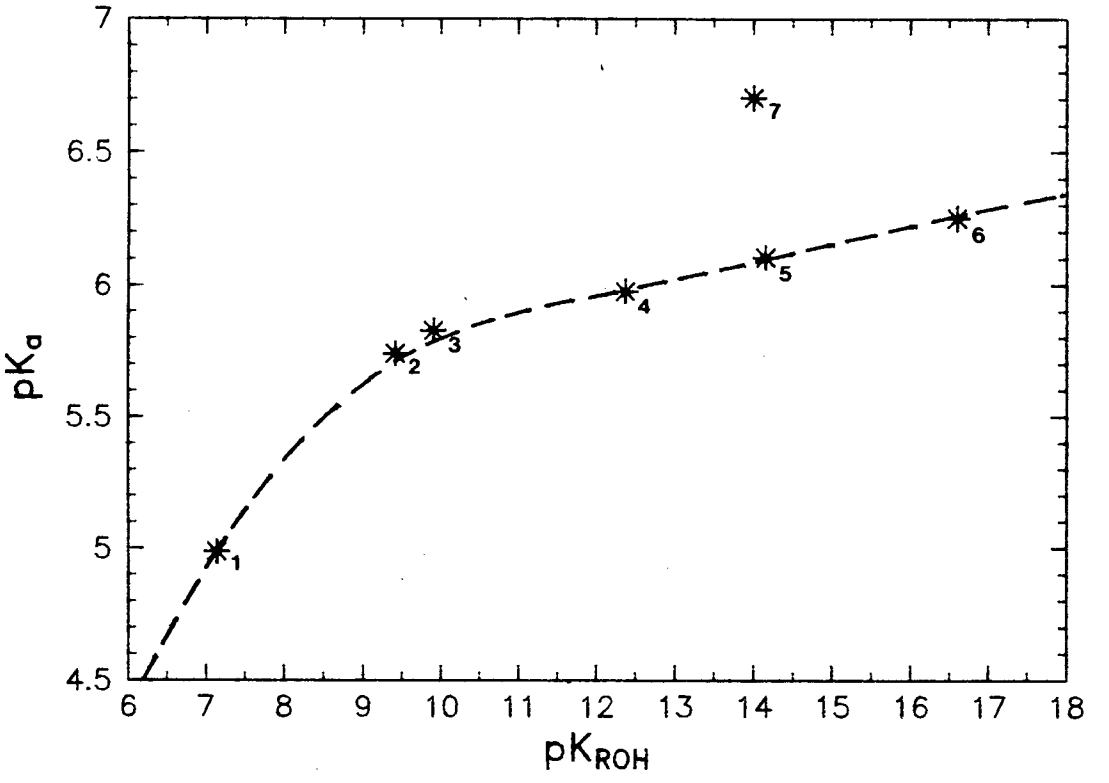

Figure 5.1: Plot of the pKs of monophosphoric acid esters against the pK_{ROH} of the ester alcohol. The ligands are: 1=p-nitrophenyl phosphate, 2=1-naphthyl phosphate, 3=phenyl phosphate, 4=α-D-glucose-1'-phosphate, 5=glycerol-2-phosphate, 6=methyl phosphate, 7=hydrogen phosphate.

As pK_{ROH} increases, the increase of pK_{LH} becomes smaller and smaller and seems to converge towards a limiting pK_{LH}. This is caused by ~~three~~ two effects. Firstly there is the non-linear charge transfer from the substituent through the phosphate group to the binding site. Both the P=O and all P-O bonds are influenced by the substituent and only a fraction of the total effect is seen by the binding site. This is also the reason why the range of pK_{LH} values is decreased considerably in comparison to the range of pK_{ROH} values. ~~Secondly, pK_{LH} reflects the strength of the L-H bond which manifests itself in e.g. the bond length. The larger pK_{LH}, the shorter one expects the bond to be. However, the proton can only approach the phosphate group to a certain minimal distance~~. The ~~third~~ second reason is that the negatively charged phosphate group cannot be infinitely polarized by an electrondonating substituent and eventually, saturation will be reached.

If it had been possible to plot pK_{LH} against e.g. σ^{ϕ} (see section 2.1) I would probably have obtained a straight line because the substituent constants already account for many non-linear effects. Unfortunately, no complete set of substituent constants for the compounds investigated here is available, as discussed in section 2.1.

The pK_{LH} of hydrogen phosphate does not fall on the line defined by the phosphate esters (figure 5.1). There are two reasons for that. Firstly, it is not clear whether water can be regarded as the corresponding substituent alcohol. The pK_{ROH} of all other alcohols refers to a C-O-H bond whereas water has a H-O-H bond. Secondly, if I assume that I can indeed use water as reference, it is still an open question whether one can compare the covalent -C-O-P bond with the more ionic H-O-P bond. There is certainly some sharing of the proton by the three phosphate oxygens. The difference between the phosphate esters and hydrogen phosphate is also obvious from the protonation heats. The protonation of the phosphate esters is endothermic whereas the protonation of hydrogen phosphate is exothermic (table 5.2).

5.1.2 The correlation between protonation constants and complex formation constants with copper, zinc and calcium ions

Figure 5.2 shows plots of log β_{LM} for copper, zinc and calcium ions against pK_{LH}. For copper and zinc ions a linear relation is followed.

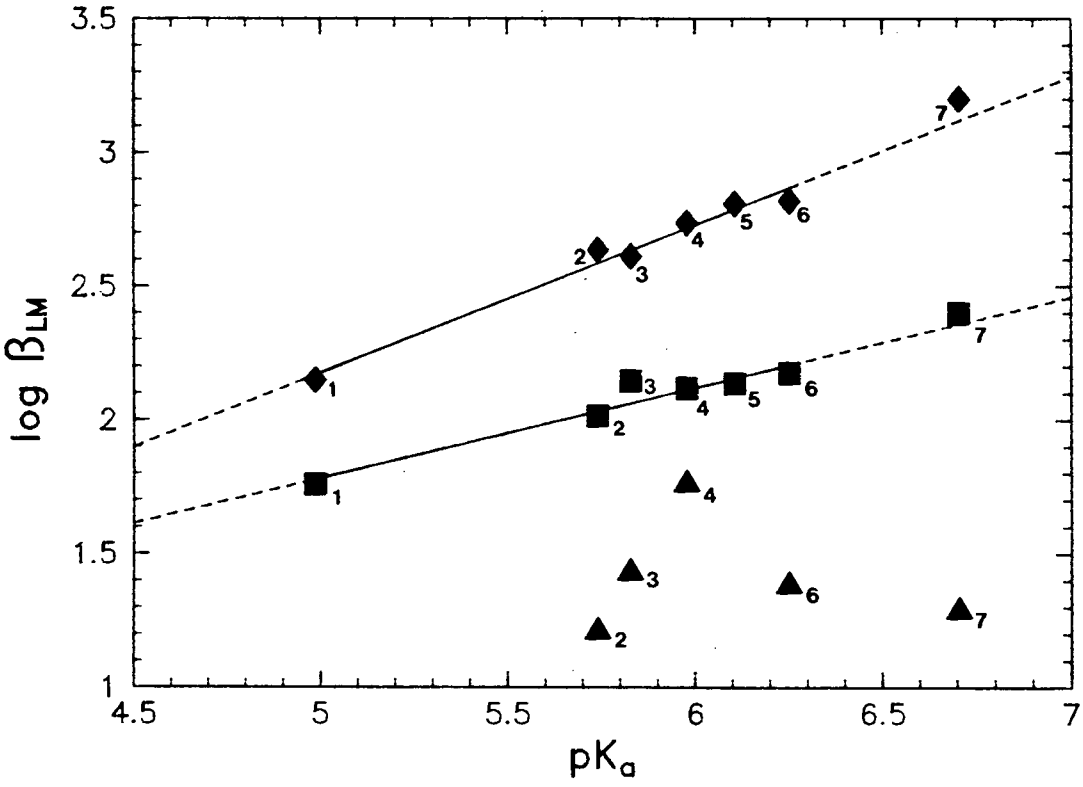

Figure 5.2: Plot of logβ_{LM} against pK_{LH} for copper (◆), zinc (■), and calcium (▲) ions. The ligands are: 1=p-nitrophenyl phosphate, 2=1-naphthyl phosphate, 3=phenyl phosphate, 4=α-D-glucose-1'-phosphate, 5=glycerol-2-phosphate, 6=methyl phosphate, 7=hydrogen phosphate.

In contrast to the plot of pK_{LH} against pK_{ROH}, the electronic transmission and saturation effects caused by the substituent are the same for both complexes LH and LM, and both proton and metal binding occur at the same binding site. Therefore the plot was expected to be linear. The range of log β_{LM} values of copper is, however, much smaller than the range of pK_{LH} values, and the range of log β_{LM} values for the complexation of zinc is even smaller than that of copper.

The formation constant of the complex between 1-naphthyl phosphate and copper ions deviates from the linear relationship. Although the protonation constant of 1-naphthyl phosphate is smaller than that of phenyl phosphate, its copper complex formation constant is slightly larger. It cannot be decided whether this is due to some chemical reason. It may

just be a manifestation of experimental error because the two formation constants are expected to be very similar.
It is interesting to note that log β_{LM} for the complexation of hydrogen phosphate with copper and zinc ions does fall on the line defined by the esters although this ligand is not part of the ester series.
The data points for the complexation of copper and zinc ions (excluding hydrogen phosphate) have been fitted to a linear equation

$$\log \beta_{LM} = a\ pK_{LH} + b \qquad (5.3)$$

where a and b are constants. a can be interpreted as a measure of the relative strength of the metal complex with respect to the protonated complex. It depends on the particular properties of the ligands as well as the metal ion considered. b can be regarded as a kind of barrier which has to be overcome before any complexation between the ligand and the metal can take place. b depends on the spacial structure of metal ion and ligand, i.e. on how well they fit to each other.
A determination of a and b by linear regression yields the following results:

cation	a	b	correlation coefficient
Cu^{2+}	0.55	-0.60	0.99
Zn^{2+}	0.34	+0.09	0.96

The smaller range of coordination strength of the metal ions as compared to the protonation is reflected in the fact that a is less than 1, and a is smaller for complexation with zinc than for complexation with copper.
A relationship of the form of eq.5.3 has also been derived from theoretical considerations [125]. a has been correlated with e.g. the ionization potential of the metal, the ionic radius, charge to size ratio or electronegativity [57,60,62]. Other researchers [58,61] found a correlation of a with the extent of π-bonding in the complexes.
Although there are numerous possibilities to try and correlate a with any of the above mentioned properties, this cannot be done here because I obtained linear relationships for two metal ions only.
The plot of log β_{LM} against pK_{LH} for calcium does not permit the conclusion that a linear relationship exists, although this might be indicated because one can indeed draw a straight line through the points of 1-naphthyl phosphate, phenyl phosphate and α-D-glucose-1'-phosphate.

More data is needed to confirm whether the calcium complexes of methyl phosphate, glycerol-2-phosphate and hydrogen phosphate are exceptions that do not follow a general trend, or whether the linear correlation does not exist. It is interesting to note that although the calcium complexes are very weak, the range of log β_{LM} values is larger than expected compared to the range of the copper and zinc complex formation constants, and even the protonation constants.
Although there is a linear relationship for the formation constants of copper and zinc with the pK_{LH} values of the ligands, no such correlation exists for the formation constants of the hydroxo complexes. There seems to be a trend that the higher pK_{LH}, the more hydroxo complexes are found. For example, two hydroxo complexes have been found for α-D-glucose-1'-phosphate and glycerol-2-phosphate. 1-Naphthyl phosphate only has one hydroxo complex, and for phenyl phosphate, no hydroxo complex could be detected at all. It cannot be decided whether hydroxo complexes do not exist with some of the ligands, or whether they have not been picked up in the titrations. They might be so weak that they occur in too small concentrations or at pH values which have not been covered by the titrations.

5.1.3 Interpretation of the calorimetric results

5.1.3.1 General discussion of the size and sign of the measured enthalpies

Both the protonation and copper complex formation heats are positive (see table 5.2). This means that energy is consumed when the protonated complex or the metal complex forms. The ~~heat~~ energy gain by bond formation is outweighed by the ~~heat consuming~~ energy consumed in desolvation of the cation and of the ligand. The complex will be solvated to a much lesser extent than the free ligand because of its smaller charge. The complex formation is therefore accompanied by an increase of the number of independent entities in solution, i.e. by an increase of ΔS. ΔS is expected to be larger for the copper complexation reaction than for the protonation reaction. Because the complex LM is neutral it has a much smaller ordering effect on the solvent than has the protonated ligand, LH. In addition the dehydration of the copper ion is more endothermic and more entropy is generated than in the dehydration of the proton (see table 5.3).

Table 5.3: Hydration enthalpies and entropies of protons and divalent copper ions at 25°C [126]

cation	ΔH [kJ/mol]	ΔS [kJ/mol°K]
H^+	-1.129	-0.131
Cu^{2+}	-2.174	-0.309

In contrast to the above prediction ΔS is found to be very similar for the protonation and copper complexation of the phosphate esters (table 5.2). The reason is probably that the equilibrium constant for the protonation is much larger than that for the copper complexation. The copper ion will be situated further away from the ligand than the proton. Although it carries two positive charges it will affect the solvation of the ligand to a moderate extent only. In addition, the copper ion itself might not be desolvated to the same extent as the proton. It therefore seems possible that the effect of the tightly bound proton on ΔS is of the same order of magnitude as the effect of the weakly bound copper ion.
The reason why the copper complexation enthalpy ΔH_{LM} is larger than the protonation enthalpy ΔH_{LH} is again the strength of bond formation. Less energy is gained in the formation of a weak ligand-metal bond than in the formation of a strong proton-ligand bond. If ΔS is similar for the two processes as in the case of the phosphate esters, ΔH must be larger for the weaker complex, i.e. for the copper complexation reaction.

5.1.3.2 The correlation between the nucleophilicity of the ester group and the protonation enthalpies

I will now turn to discuss relationships between pK_{ROH} and ΔH and ΔS, respectively. The good correlation between pK_{LH} and pK_{ROH} (figure 5.1) suggests that the substituent exhibits mainly an electronic effect. Thus I assume for the moment that protonation of the phosphate moiety is not disturbed by any effects originating from the particular structure of the substituent, and consequently ΔS should be constant throughout the ligand series. An increase of pK_{LH} with increasing pK_{ROH} must therefore lead to a similar decrease of ΔH.
The entropies determined for the protonation of the ligands are indeed very similar. One could thus conclude that the desolvation involves

mainly the phosphate moiety, which is the centre of the protonation reaction. The solvation of the particular substituent does not seem to be altered to a large extent and only constitutes a small contribution to $T\Delta S$. The plot of ΔH_{LH} versus pK_{ROH} (figure 5.3) does, however, reveal that ΔH_{LH} does not entirely follow the predicted trend.

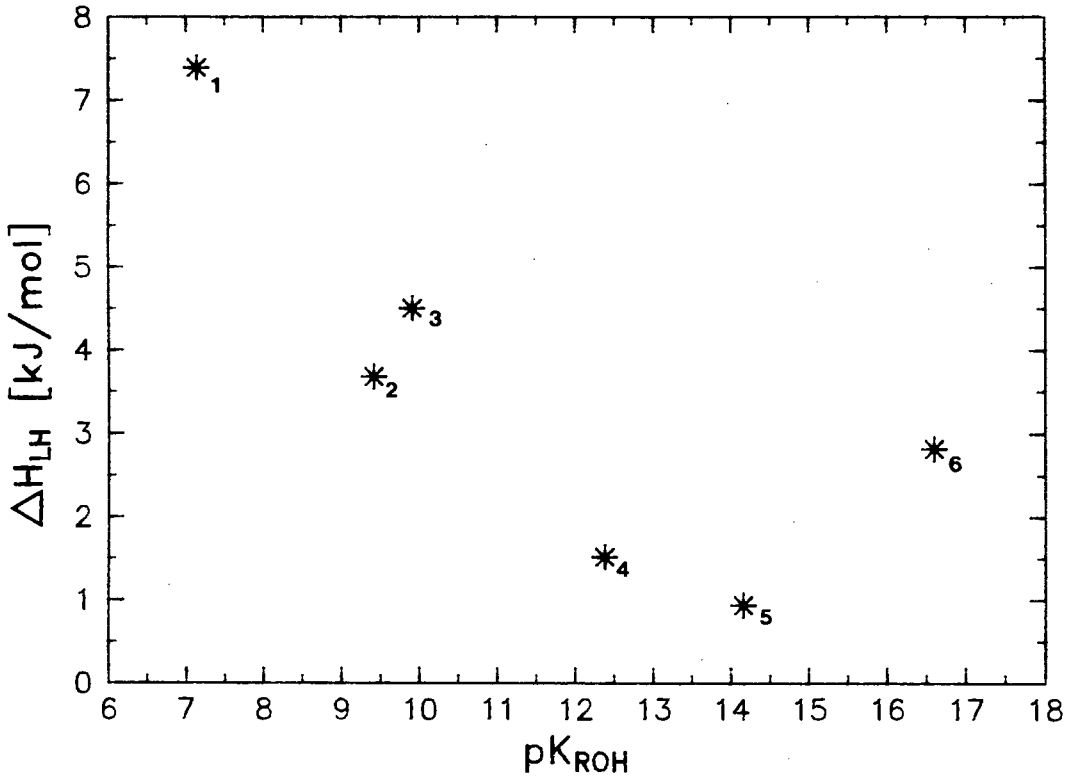

Figure 5.3: Plot of the protonation enthalpies ΔH_{LH} against pK_{ROH}. The ligands are: 1=p-nitrophenyl phosphate, 2=1-naphthyl phosphate, 3=phenyl phosphate, 4=α-D-glucose-1'-phosphate, 5=glycerol-2-phosphate, 6=methyl phosphate

As expected, ΔH_{LH} drops when going from p-nitrophenyl phosphate to phenyl phosphate. ΔH_{LH} of α-D-glucose-1'-phosphate and glycerol-2-phosphate are again smaller, but ΔH_{LH} of methyl phosphate is larger than the protonation heats of α-D-glucose-1'-phosphate or glycerol-2- phosphate, but smaller than that of phenyl phosphate. There are two possible explanations for this unexpected behaviour depending on whether one regards methyl phosphate as the exception, or α-D-glucose-1'-phosphate and glycerol-2-phosphate as being anomalous.

First, I will assume that the protonation enthalpies ΔH_{LH} of α-D-glucose-1'-phosphate and glycerol-2-phosphate are anomalously low. In contrast to the other ligands, both α-D-glucose-1'-phosphate and

glycerol-2-phosphate contain OH groups in their ester moiety. Consequently, there are several possibilities that hydrogen bonds can be formed. Some possible structures, both for the free ligand and the protonated ligand, are shown in figure 5.4.

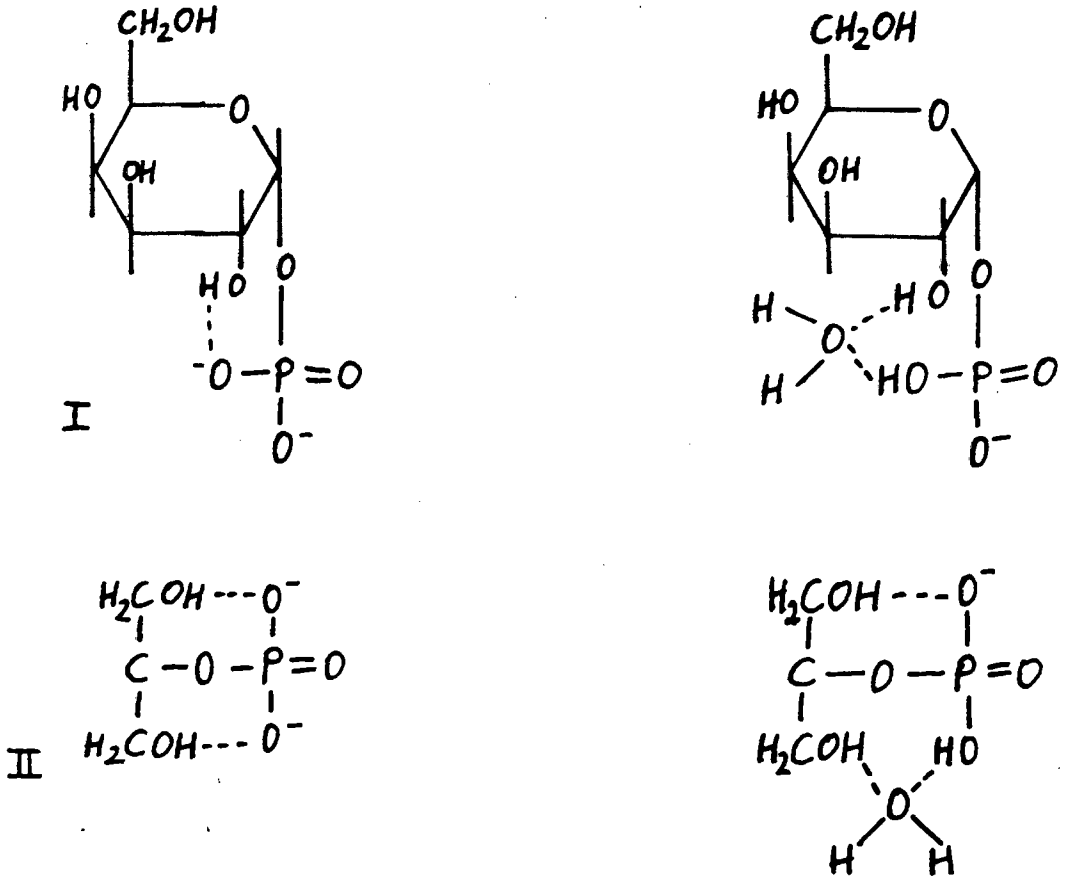

Figure 5.4: Possible hydrogen bonding in α-D-glucose-1'-phosphate and in glycerol-2-phosphate

The hydrogen bonds formed by the protonated ligand are extramolecular whereas the most likely structures of the free ligands involve intramolecular hydrogen bonds only. When the free ligand becomes protonated hydrogen bonds are broken and new hydrogen bonds are formed (in addition to the desolvation effect discussed above). It is also possible that while one hydrogen bond is broken, another hydrogen bond is strengthened at the same time. In order to explain the observed low values for the protonation enthalpies one must postulate that upon protonation the reorganisation of the hydrogen bonding is exothermic. In other words, the energy of the hydrogen bonds in the protonated ligands must be smaller than in the free ligands. This, however, seems somewhat unlikely because one would generally expect intramolecular bonds to be stronger than extramolecular bonds. In addition, structures like I and II (figure 5.4) have some similarity to the structure of solid ice and

are therefore expected to be energetically favoured. Unless the protonation and hydrogen bond destruction is accompanied by a considerable increase in hydrogen bonding at another site of the molecule, it seems unlikely that the protonation enthalpies of α-D-glucose-1'-phosphate and glycerol-2-phosphate should be anomalously low.

The other possibility is that the protonation enthalpy of methyl phosphate is raised. This can be explained by some steric considerations. All ligands considered contain non-polar ester groups. In contrast to the other ligands with bulkier substituents the substituent of methyl phosphate, the methyl group, is small. Methyl phosphate can therefore be solvated more easily because it does not disturb the structure of the solvent as much as the bulkier ligands. The solvation is generally favoured if the ligands are charged. Thus the free ligands will be stabilized. The higher the degree of stabilization the more energy is needed to break the structure of the solvation sphere in order that a proton can coordinate. Consequently the energy needed to desolvate methyl phosphate during the protonation is higher than for any other ligand, and consequently the protonation enthalpy ΔH_{LH} is higher than initially predicted. This view is supported by the observation that the protonation entropy of methyl phosphate is slightly higher than that of any of the other ligands (table 5.2).

There is, however, another aspect that has to be considered, namely the possible hydrogen bond formation of the glycerol and glucose moieties. These substituents exhibit two effects. The one is the unfavourable non-polar character leading to a destruction of the solvent structure as discussed above. This effect is opposed by the energetically favourable possibility of hydrogen bonding which leads to a stabilization of the solvated ligand. The explanation above is only valid if I assume that the two opposing effects cancel, or that the unfavourable solvation due to the bulky moieties dominates over the hydrogen bonding.

5.1.3.3 The correlation between the protonation enthalpies and the copper complex formation enthalpies

Figure 5.5 shows a plot of ΔH_{LM} against ΔH_{LH}. In contrast to the protonation heats the electrondonating capacity of the substituents is not reflected in the copper complex formation heats.

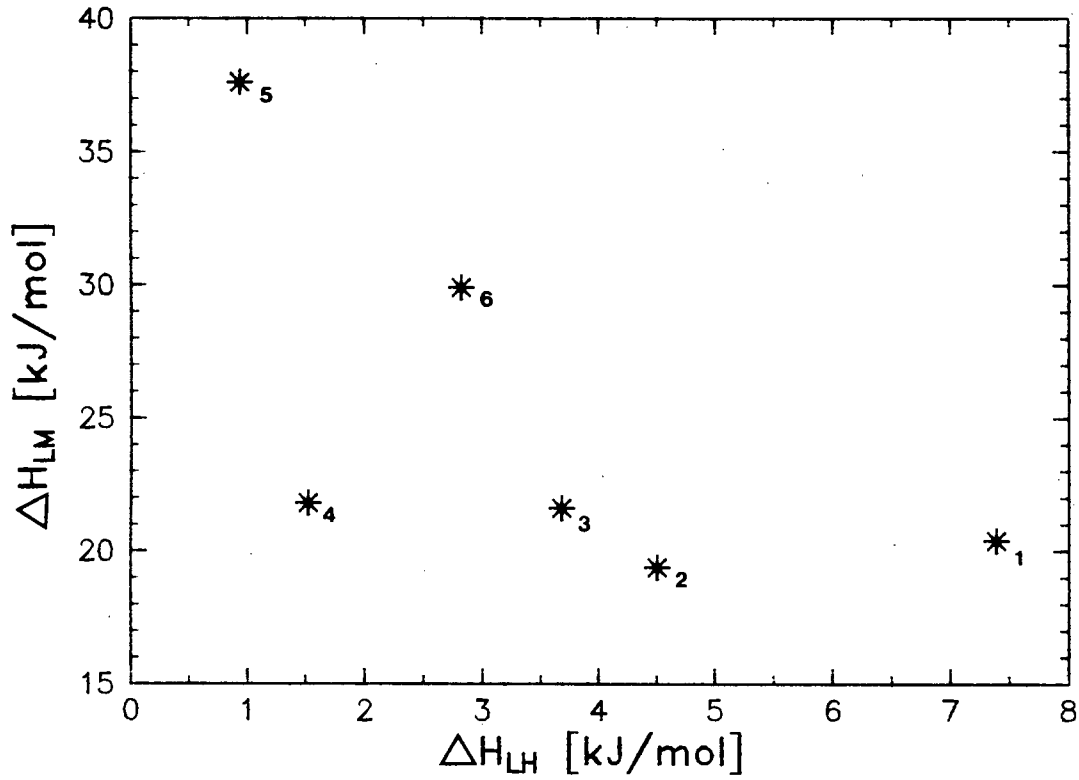

Figure 5.5: Plot of the copper complex formation enthalpies ΔH_{LM} against the protonation enthalpies ΔH_{LH}. The ligands are:
1=p-nitrophenyl phosphate, 2=1-naphthyl phosphate, 3=phenyl phosphate, 4=α-D-glucose-1'-phosphate, 5=glycerol-2-phosphate, 6=methyl phosphate

α-D-Glucose-1'-phosphate, phenyl phosphate, 1-naphthyl phosphate and p-nitrophenyl phosphate have ΔH_{LM} values which are the same within experimental error. This indicates that the different stabilities of the copper complexes, as reflected by β_{LM}, might not be due to any significant difference of the strength of the P-O-Cu bond as initially predicted. Solvation effects as reflected in the ΔS_{LM} values are just as important. The structures of p-nitrophenyl phosphate, 1-naphthyl phosphate, phenyl phosphate and α-D-glucose-1'-phosphate are quite similar in that the substituents of these four ligands are all non-polar rings. Accordingly, the complexation entropies ΔS_{LM} of these ligands are very similar (the same has been observed for ΔS_{LH}, see above).

The copper complex formation of methyl phosphate is more endothermic than that of p-nitrophenyl phosphate, phenyl phosphate, 1-naphthyl phosphate and α-D-glucose-1'-phosphate. As for the protonation, this can be explained by assuming that in solution the small methyl phosphate dianion is stabilized by solvation to a much larger extent than any of the other ligands carrying bulky substituents. Again, this is supported by the high entropy of the copper-methyl phosphate complex.
It remains unclear why the copper complex formation heat and entropy of glycerol-2-phosphate are much higher than those of any other ligand. Because structures originating from hydrogen bonding are believed to be very similar for both α-D-glucose-1'-phosphate and glycerol-2-phosphate (as discussed above), one would have expected similar copper complexation heats.

5.2 Triphosphates

5.2.1 The influence of the substituent on the metal complexation of triphosphates

Very little information is available about the metal complexation of triphosphates other than the nucleotides. Therefore no definitive relationships can be derived. I will however try to discuss some interesting observations which may be worth a detailed investigation.
Protonation constants and metal complexation constants of triphosphates with copper, zinc and calcium ions are summarized in table 5.5 (note that apart from the stability constants for the nucleotides and their derivatives, these are all the stability constants for the three metals considered that could be extracted from the literature after an extensive search of Chemical Abstracts).

Table 5.5: Equilibrium constants of triphosphates

cation / ligand	H^+	Cu^{2+}	Zn^{2+}	Ca^{2+}	I[mol/l]	T[°C]	reference
$P_3O_{10}H^{4-}$	5.79	5.36	4.93	3.64	0.15	25	*
$FP_3O_9^{4-}$	6.65	5.97	4.64	3.73	0.15	25	*
$CH_3OP_3O_9^{4-}$	6.45	6.17			0.10	20	[127]
ATP	6.51	6.13	4.85	3.77	0.10	25	[35]
$C_6H_5OP_3O_9^{4-}$	6.32						[128]
γ-phenylpropyl triphosphate	7.17				0.10	25	[129]
$H_2NP_3O_9^{4-}$	5.8						[130]

ATP: adenosine triphosphate *this thesis

Not all the compounds listed in table 5.5 are triphosphoric acid esters. The $-NH_2$ group of amidotriphosphate and the fluorine atom of fluorotriphosphate are directly bound to a phosphorus atom. Therefore the influence of these groups should be larger than the effect of an ester group because these substituents are directly bound to the phosphate chain without being separated by an ester oxygen. Although adenosine triphosphate (and all other nucleotides) is a phosphate ester, it strictly cannot be compared to the other compounds listed because it contains additional binding sites in the adenosine moiety. These have been demonstrated to participate the binding of at least some metal ions [38,39,131,132,2b]. Triphosphoric acid differs from the other compounds in that its substituent is a proton. The position of this proton is not fixed at one particular phosphate group, it can move around and is probably attached to more than one phosphate group at the same time. Therefore comparison with triphosphoric acid is also problematic.

A comparison of the range of the first protonation constant of triphosphates and monophosphates (table 5.5 and table 5.1) shows that the variation is smaller for the triphosphates. This can be explained by assuming that the major binding sites are the γ and β phosphate group.

These two phosphate groups are far from the substituent and will therefore only be affected to a small extent. Even the strongly electronegative fluorine atom of fluorotriphosphate does not affect the β phosphate to a considerable extent. This is confirmed by the observation that the fluorine atom splits the phosphorus nmr doublet of the adjacent α phosphate group due to strong F-P coupling, but not the triplet of the β phosphate group (see fig. A.5).

From the few available data it cannot be derived that an electron-withdrawing substituent will lead to weak complexes, as has been shown to be the case for monophosphoric acid esters (section 5.1.1). We expect, however, a similar trend for the triphosphates, but the range of formation constants will most probably be smaller. In order to establish such a relation, it would be interesting to extend the research to the respective mono- di- and tetraphosphates. The range of formation constants should decrease with increasing chain length.

Another interesting relation could be the effect of different substituents on the participation of the different phosphate groups in the complexation. If the substituent is electron-donating, all three phosphate groups should participate in metal binding. In fact, the α phosphate group could be the strongest binding site because it is closest to the substituent. If, on the other hand, the substituent is electron-withdrawing, it seems likely that the α phosphate group is rendered too positive to attract metal ions, and binding should preferably take place at the phosphate groups far from the substituent (the protonation equilibria of fluorotriphosphate (section 4.1.11) illustrate this).

The conclusion of this discussion is that the strength of complexes of polyphosphoric acids can only be interpreted with respect to the electron-donating or electron-withdrawing properties of the substituent if the contribution of the different phosphate groups has been established and is taken into account in the comparison. So far, only few triphosphates have been investigated and considerable work is needed before any relationships between the properties of the substituent groups and the the complex equilibria of the respective triphosphates can be proposed.

5.3 Conclusion

In this thesis I studied the protonation and the metal complexation of some phosphoric acid esters. A correlation between the nucleophilicity of the ester group and the value of the protonation constant has been found, and explained. A similar correlation exists for the stability constants of the copper and zinc complexes. From the data obtained, it cannot be decided whether the formation constants of the calcium complexes of the phosphate esters follow a similar trend. The correlations of the protonation constants as well as the copper and zinc complexation constants with the nucleophilicity of the ester group lead to the assumption that the strength of the respective complexes is governed by electronic induction effects, i.e. by polarisation of the phosphate oxygens by the substituent. The determination of reaction enthalpies for the protonation and copper complexation reactions, however, showed that the complexation was not only dependent on the electronic effects, but that desolvation of the ligands and cations plays an important role. In fact, the main contribution to the protonation and copper complexation heats is the desolvation of the free ligand during the reaction. The electron donating capacity of the ester group is reflected in the protonation heats. The protonation of methyl phosphate is more endothermic than expected because the free ligand is stabilized in solution due to the small size of the substituent. For the same reason the copper complexation heat of methyl phosphate is high, too. The values for the copper complexation heats of α-D-glucose-1′-phosphate, phenyl phosphate, 1-naphthyl phosphate and p-nitrophenyl phosphate are the same within experimental error. The electron donating capacity is thus not the dominant factor for the differences observed in the complexation of these ligands with copper. Solvation effects dominate and "swamp" the electronic induction effects. The copper complexation of glycerol-2-phosphate is highly entropy driven. It remains unclear as to which factors govern the complexation of glycerol-2-phosphate with copper and why it differs so markedly from the structurally related α-D-glucose-1′-phosphate.

It would have been desirable if some more information about the role of hydroxo complexes in the metal ion catalyzed hydrolysis of phosphate esters could have been obtained. This, however, was impossible because of the formation of precipitates in the pH range where hydroxo complexes are expected to exist and in which no hydrolysis studies have been made. It may be worthwhile to conduct a similar investigation as described in

this thesis, but to use trivalent instead of divalent metal ions. Because of their higher charge, trivalent metal ions are expected to form stronger complexes. If a considerable amount of the metal ions is complexed fewer free metal ions remain in the solution. It may be possible that complexation can be studied at higher pH. If a wide range of trivalent metal ions can be studied, it is perhaps possible to find a correlation between the hydrolysis constants of the metal ion and the strength of the ligand-metal or ligand-metal-hydroxo complexes as well as the rates of metal ion catalyzed hydrolysis of phosphoric acid esters.

Another possibility to circumvent the problem of precipitation might be the study of monophosphoric acid esters which contain additional binding sites in their ester moiety. Maybe these compounds chelate divalent metal ions so strongly as to prevent metal-hydroxide precipitation. With chelating ligands one would have the problem to distinguish between the induction effects due to the substituent and the increase in complex stability due to chelation. It may be possible to estimate the increase in complex stability due to chelation by studying the complexation equilibria of ligands which can only complex metal ions via their ester groups, but which cannot bind at their phosphate group. The phosphate group could be blocked by an unreactive functional group, such as e.g. a methyl or phenyl group. The inductive effect of this group must then be taken into account, too.

At the same time, the study of polyphosphoric acid esters should be pursued. The possibility of correlations between the nucleophilicty of the ester group and the formation constant of the metal complexes has been discussed in this thesis. The importance of hydroxo complex formation in the hydrolysis of triphosphates has been indicated in some recent papers [31,32]. The study of polyphosphoric acid esters thus promises to yield some relevant biochemical results. From the purely chemical point of view the variety of the possible reactions is well worth detailed investigations, too. The first step must, however, be the search for new effective procedures for the synthesis of polyphosphoric acid esters.

Appendix A: The role of hydroxo complex formation in the metal ion catalyzed hydrolysis of 8-quinolyl phosphate

It has recently been emphasized that hydroxo complex formation plays an important role in the hydrolysis of triphosphates [31,32], and there are some indications [13,33,34,20] that the same might be valid for monophosphoric acid esters. On the other hand, the mechanism of the catalytic action of metal ions on the hydrolysis of several monophosphoric acid esters has been explained by assuming the formation of a chelate [19,22-24]. For example, the hydrolysis of 8-quinolyl phosphate has been extensively studied in the presence of divalent copper and nickel ions, and the formation of a chelate between copper and 8-quinolyl phosphate, but not between nickel and 8-quinolyl phosphate has been suggested as accounting for the different catalytic action of these two metal ions [22]. In order to explore the possible role of hydroxo complex formation in the hydrolysis of 8-quinolyl phosphate I describe here the results of an extensive equilibrium study of the protonation and metal complexation of 8-quinolyl phosphate. The two related ligands, 1-naphthyl phosphate and 8-quinolyl methyl phosphate, have also been studied. 1-Naphthyl phosphate and 8-quinolyl methyl phosphate differ from 8-quinolyl phosphate in the absence of one potential binding site, namely the quinolyl nitrogen and one of the non-ester oxygens, respectively (figure A.1).

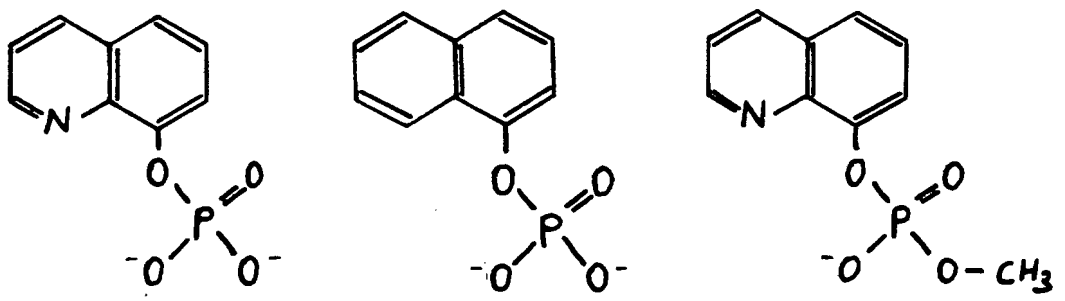

8-quinolyl phosphate, 1-naphthyl phosphate, 8-quinolyl methyl phosphate

Figure A.1: Structures of 8-quinolyl phosphate, 1-naphthyl phosphate and 8-quinolyl methyl phosphate

The study of these related ligands can provide evidence whether or not chelates are formed between 8-quinolyl phosphate and various metal ions. The potentiometric results are summarized in table A1. (for details, see sections 4.1.3, 4.1.8, and 4.1.9, respectively).

Table A1: Formation constants of 8-quinolyl phosphate, 1-naphthyl phosphate and 8-quinolyl methyl phosphate with protons and divalent copper, zinc, nickel and cobalt ions (T=25°C, I=0.15 mol/l NaCl)

cation	species	8-quinolyl phosphate log β	1-naphthyl phosphate log β	8-quinolyl methyl phosphate log β
H^+	LH	6.333	5.740	4.725
	LH_2	10.462		
Cu^{2+}	LM	5.114	2.635	2.523
	LMH_{-1}	-0.910	-3.840	-4.062
Zn^{2+}	LMH	9.695		
	LM	4.870	2.014	1.187
	LMH_{-1}	-1.697	-4.730	-5.531
Ni^{2+}	LM	2.345	1.568	1.724
	LMH_{-1}	-5.469		-5.083
Co^{2+}	LM	1.781	1.681	1.237
	LMH_{-1}			-5.263

Table A1 shows that the complexes of 1-naphthyl phosphate and 8-quinolyl methyl phosphate are weak. The complexes formed between 8-quinolyl phosphate and divalent copper, zinc and nickel ions are considerably stronger. This indicates that both coordination sites, the quinolyl nitrogen and one of the phosphate oxygens, are involved in the binding of the metal ion. In contrast to the postulate of Murakami and Sunamoto [22], 8-quinolyl phosphate acts as a bidentate ligand with both copper and nickel ions, although the complexation with nickel ions is considerably weaker than that with copper ions (table A1). Therefore, chelation cannot be the only requirement in the metal ion catalyzed hydrolysis. As has already been described above hydroxo complex formation is thought to be involved in some hydrolysis processes. In order to decide whether hydroxo-complex formation could play any important role in the hydrolysis of 8-quinolyl phosphate, speciation plots of the copper-8-quinolyl phosphate and nickel-8-quinolyl phosphate system (fig.A.2 and figure A.3) have been calculated.

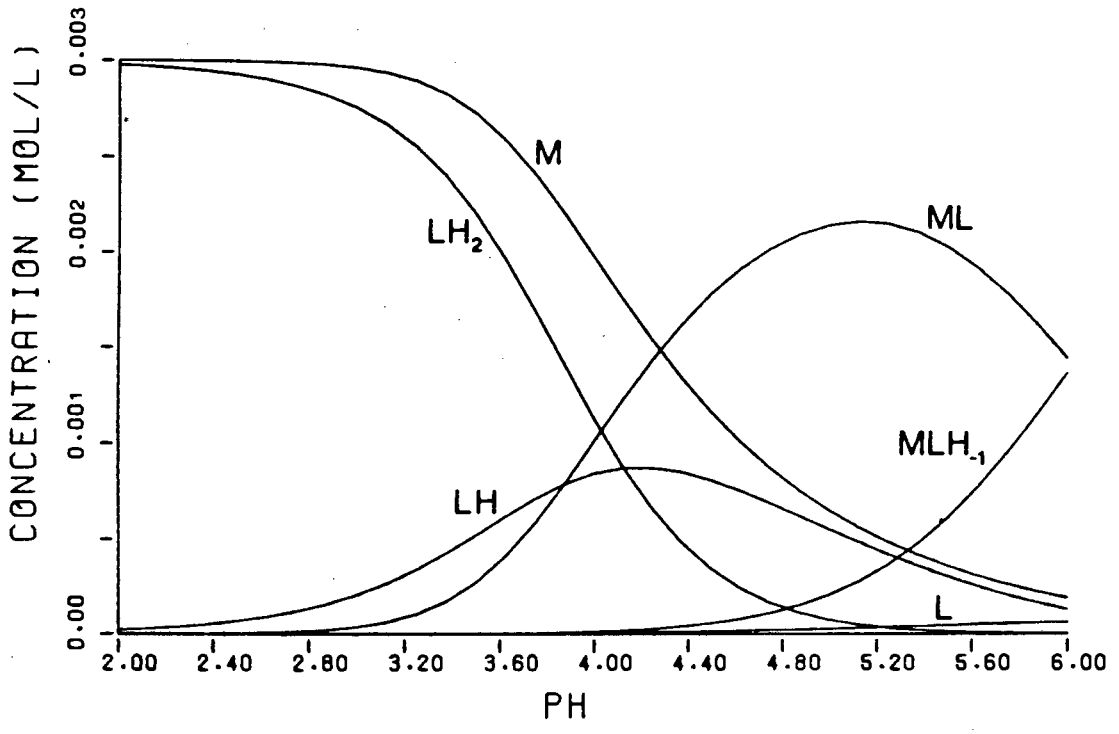

Figure A.2: Concentrations of the various complexes formed between 8-quinolyl phosphate and copper ions as a function of pH. Both ligand and metal concentrations were taken as 0.003 mol/l.

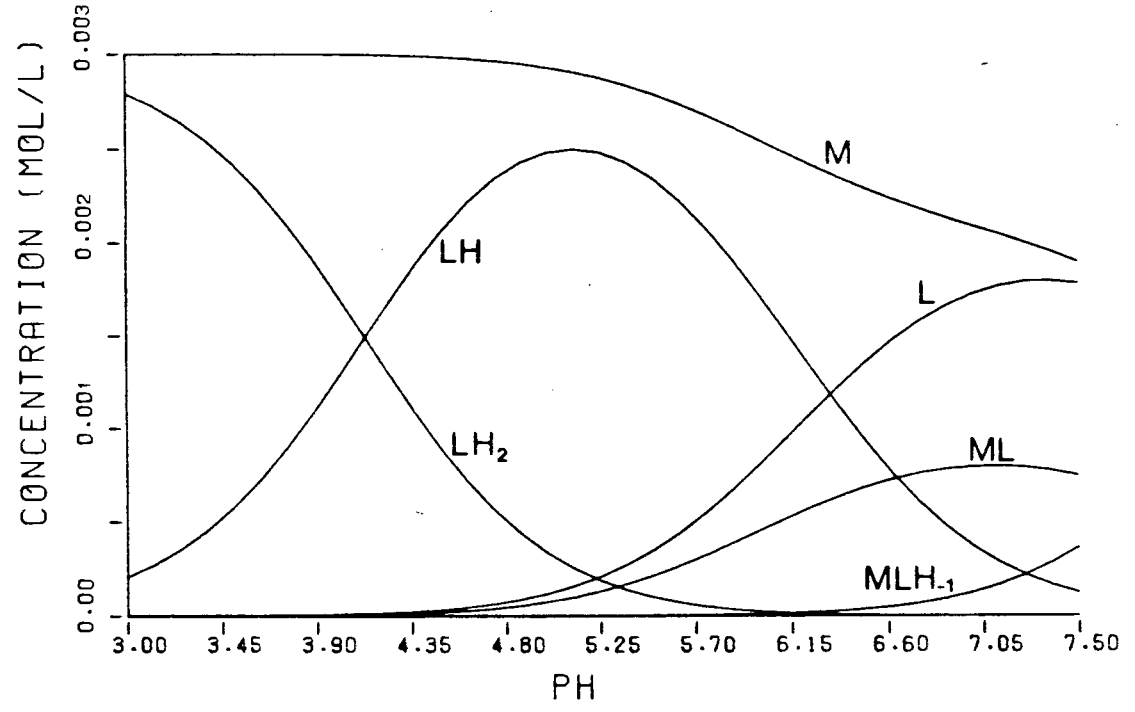

Figure A.3: Concentrations of the various complexes formed between 8-quinolyl phosphate and nickel ions as a function of pH. Both ligand and metal concentrations were taken as 0.003 mol/l.

The hydroxo complex MLH_{-1} is a major species for the copper-8-quinolyl phosphate system, but occurs only in small amounts in the nickel-8-quinolyl phosphate system. It cannot, however, be concluded that the formation of MLH_{-1} is an essential requirement in the metal catalyzed hydrolysis of 8-quinolyl phosphate. Murakami and Sunamoto [22] report catalysis by copper ions in the pH range 2.03 to 3.85, where the concentration of $CuLH_{-1}$ is not significant (fig. A.2). It therefore remains unclear why the catalytic action of copper and nickel ions on the hydrolysis of 8-quinolyl phosphate is so markedly different, and whether or not hydroxo complex formation plays any significant role in this reaction.

Appendix B: The effect of simultaneous refinement of various titration parameters on the precision of stability constants

It has been suggested [97] that the precision of stability constants can be improved by refining formation constants and several titration parameters at the same time. The effects of random errors of all the titration parameters are believed to be absorbed in the refined values of individual titration parameters , which may differ substantially (5-10%) from their original values. The refined formation constants, however, are much closer to their true value. This can be demonstrated as follows:

For a given set of formation constants, titration data are calculated for a set of m titrations and the program ESTA7 is used to impose random errors on all the titration parameters. This is repeated n times, thus creating n sets of m titrations. For each set, an increasing number of titration parameters is refined. The simultaneous optimization of β, E_o, $[H]_{vessel}$ and $[L]_{vessel}$ has been found particularly successful [97]. The formation constants obtained approach the "true" formation constants the more parameters are refined.

This analysis was carried out with the protonation constants of 8-quinolyl phosphate. Ten sets of four titrations each were created and βs only, $\beta + E_o$, $\beta + E_o + [H]_{vessel}$, $\beta + E_o + [H]_{vessel} + [L]_{vessel}$ were refined simultaneously. The results are shown in Figure A.4a and figure A.4b. Indeed, the more parameters are optimized, the smaller is the spread of the results and the deviation from the true value. The same analysis was attempted for a system containing metal ion, but frequently the variables were found to be correlated with the formation constants. The same problem arose with real data. Therefore I decided to refine only formation constants when I analyzed all my real data. The example of the 8-quinolyl phosphate does, however, give an indication of the size of the random error of the formation constants, which seems more reliable than the calculated standard deviations.

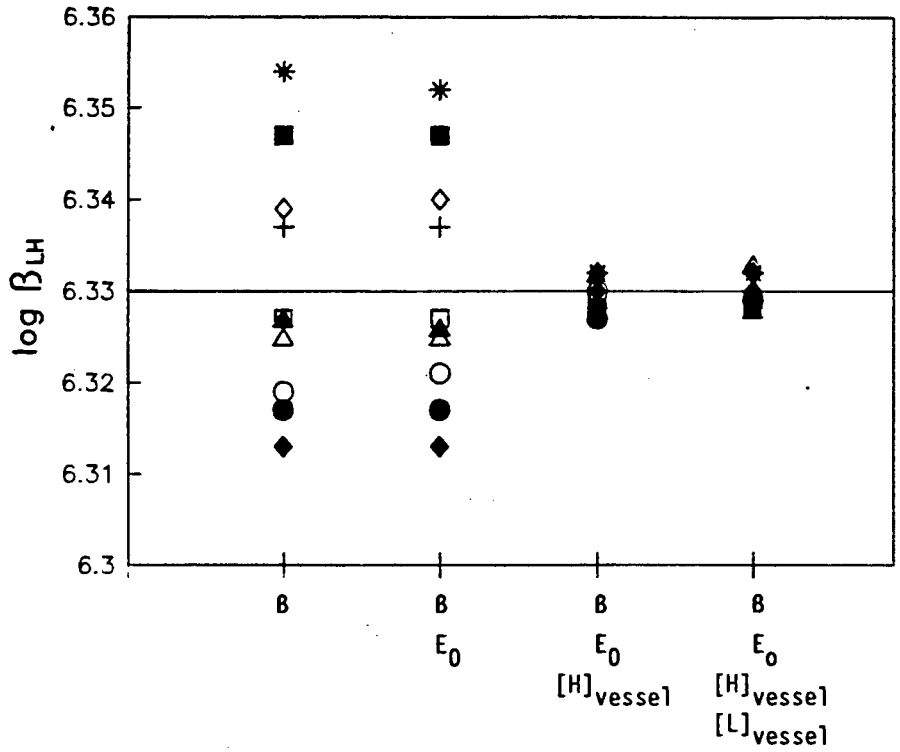

Figure A.4a: Formation constants calculated for the complex LH from the ten sets of synthetic titration data (indicated by different symbols) as a function of the parameters optimized. The solid line denotes the value used in the calculation of the synthetic data.

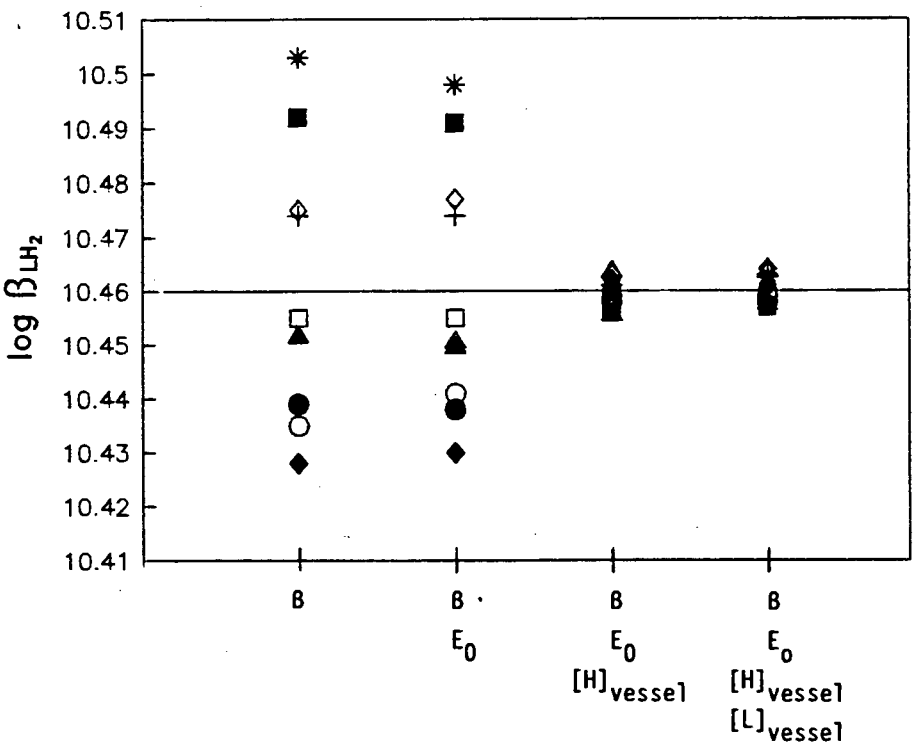

Figure A.4b: Formation constants calculated for the complex LH_2 from the ten sets of synthetic titration data (indicated by different symbols) as a function of the parameters optimized. The solid line denotes the value used in the calculation of the synthetic data.

APPENDIX C: Materials used and synthesis of the ligands

General

The water was deionized and distilled. It was boiled before use to remove carbon dioxide.

Glassware used to make up standard solutions was calibrated just before use by weighing the amount of water needed to fill up the vessel to the mark.

Sodium hydroxide (Merck ampoules) solutions were prepared under nitrogen and protected from atmospheric carbon dioxide by soda lime. Solutions were not kept for longer than five days. They were standardized against dried potassium hydrogen phthalate (Merck p.a. 99.9-100.5%).

Tetramethylammonium hydroxide $(CH_3)_4NOH$: The concentrated stock solution (25% solution, BDH GPR) was filtered and diluted to the desired concentration. It was stored and standardized like sodium hydroxide solutions.

Hydrochloric acid: HCl (Merck ampoules) was standardized against sodium hydroxide or borax [133]. Both methods agreed within 0.1%.

Gran plots were used in all acid-base standardizations to ensure the absence of contaminants, especially carbon dioxide [134].

Sodium chloride: NaCl (BDH Aristar) was dried at 70°C.

Tetramethylammonium chloride: $(CH_3)_4NCl$ (Merck p.a. >98%) was recrystallized according to [135]. The salt is slightly hygroscopic and was stored at 50°C.

Ethylenediaminetetra-acetic acid (EDTA): standard solutions were prepared by weighing out EDTA (Merck Titriplex III p.a. >99%) which had been dried at 80°C for at least 24 hours. Frequent concentration checks by titrations versus standard zinc solutions [133] agreed with the value obtained from weight within 0.2%.

Copper ions: solutions of copper ions were made from $CuCl_2 \cdot 2H_2O$ (Merck p.a. >99%) and standardized against EDTA using murexide indicator [133].

Zinc ions: solutions were prepared by weighing out zinc granules (Merck p.a. >99.9%) and dissolving them in concentrated hydrochloric acid (BDH AnalaR). The acid content of the solutions was determined in titrations against NaOH using Gran plots [134].

Nickel ions: $NiCl_2 \cdot 6H_2O$ (Merck p.a. >98%) was dissolved and standardized against EDTA using murexide indicator [133].

Cobalt ions: solutions containing cobalt ions were prepared from $CoCl_2 \cdot 6H_2O$ (Merck p.a. >99%) and standardized against murexide indicator [136].

Manganese ions: $MnCl_2 \cdot 4H_2O$ (Merck p.a. >99%) was used as the source for manganese ions. Solutions containing manganese ions were standardized against EDTA using solochrome black indicator [133].
Calcium ions: calcium ion solutions were prepared from $CaCl_2$ (ROC/RIC anhydrous salt >99.95%) and standardized against EDTA using methylthymolblue indicator [133].
Trimetaphosphate: $P_3O_9Na_3$ (Sigma, 95-97%) was purified by recrystallization [137].
Phenol: Merck p.a. >99.5%
Potassium fluoride: Merck p.a. >99%
Silver nitrate: BDH AnalaR >99.9%
Concentrated hydrochloric acid and concentrated ammonia: Merck p.a.
Ammonium chloride: Merck p.a. >99.8%
All organic solvents (methanol, ethanol, acetone, chloroform, ether, acetonitrile): BDH AnalaR. Before use organic solvents were always dried and distilled [138]

Ligands

All ligands were examined by proton and phosphorus nmr before use. In addition the orthophosphate content was determined by the very sensitive phosphomolybdate test [101]. The orthophosphate content never exeeded 0.1% of total phosphorus and often was not detectable at all. In addition the orthophosphate content of stock solutions was determined before and after all titrations were performed to ensure that no hydrolysis occurred during the use of these solutions.

1. p-Nitrophenyl phosphate

The purchased $O_2NC_6H_4O\ PO_3Na_2 \cdot 6H_2O$ (Sigma 104) was used without further purification.

Microanalysis:	C	H	N
Calculated:	19.4%	4.3%	3.8%
Found:	19.5%	4.5%	3.8%.

p-Nitrophenyl phosphate is both light and heat sensitive and was stored in a dessicator over silica gel in the freezer. When weighing out samples for the titrations the cold ligand seemed to pick up moisture from the air which was then slowly released. After 30 min a steady balance reading was obtained. Concentrations obtained from weight and

from titration endpoints agreed to better than 0.2%. The concentration obtained from weight was used in all the calculations.

2.1 1-Naphthyl phosphate

The sample of $C_{10}H_7OPO_3H_2$ used was synthesized as part of M.M. Armstrong's M.Sc. thesis [139]. The purity was confirmed by determination of the melting point (159-161°C) (literature : 155-157°C [152].

Microanalysis:	C	H
Calculated:	53.6%	4.1%
Found:	53.6%	4.1%

The compound was used as obtained.

3. Phenyl phosphate

$C_6H_5OPO_3Na_2 \cdot 2H_2O$ (Aldrich, 98%) was used without further purification after it had been dried under vacuum.

Microanalysis:	C	H
Calculated for $C_6H_5OPO_3Na_2$	33.0%	2.3%
Found:	33.0%	2.1%

The ligand is hygroscopic.

Stock solutions (~0.01 mol/l) were freshly prepared daily and standardized against sodium hydroxide after addition of hydrochloric acid.

4. α-D-Glucose-1'-phosphate

It was attempted to characterize the purity of the purchased sample of $C_6H_{11}O_3PO_3Na_2 \cdot 4H_2O$ (Sigma, 98%) by microanalysis. However, results were not entirely satisfactory.

Microanalysis:	C	H
Calculated for:		
$C_6H_{11}O_3PO_3Na_2 \cdot 4H_2O$	19.1%	5.1%
$C_6H_{11}O_3PO_3Na_2 \cdot 3.5H_2O$	19.6%	4.9%
Found:	19.6%	4.0%

The sample was found to be free of phosphate. The proton nmr spectrum showed no peaks other than those expected for the ligand. Therefore the salt was used as obtained. The reason for the discrepancy between calculated and found carbon and hydrogen content is probably the variation of the water content with storage conditions. Stock solutions were prepared daily and standardized in acid-base titration.

5. Glycerol-2-phosphate

$(CH_2OH)_2CHOPO_3Na_2.4H_2O$ (Sigma) was used as obtained after analyzing the freshly obtained sample.

Microanalysis:	C	H
Calculated:	12.5%	5.2%
Found:	12.4%	5.2%

It was found that the water content changed considerably with storage conditions. Therefore stock solutions were prepared daily and standardized in acid-base titrations. It has been shown [140] that solutions of glycerol-2-phosphate are sufficiently stable towards hydrolysis and conversion to glycerol-1-phosphate.

6. Methyl phosphate

The synthesis of $CH_3OPO_3Na_2$ involved two steps:

1. preparation of CH_3OPOCl_2 from $POCl_3$ and CH_3OH:
   To 23 ml $POCl_3$ in 45 ml ether in an ice bath, 10 ml methanol in 20 ml ether were slowly added. The temperature was kept below 10°C. After two hours of stirring at room temperature, the solvent was evaporated on a rotary evaporator and the remaining solution distilled on a water pump. B_p = 64-66°C .
2. reaction of CH_3OPOCl_2 with NaOH to $CH_3OPO_3Na_2$:
   10 g CH_3OPOCl_2 was added dropwise to 120 ml of 2.5 mol/l NaOH solution at room temperature. The mixture was stirred overnight and the water evaporated. A mixture of $CH_3OPO_3Na_2 \cdot 5H_2O$ and NaCl (ratio 1:2) was obtained as a white solid. The purity was confirmed by microanalysis and nmr.

Microanalysis:	C	H
Calculated:	3.31%	3.60%
Found:	3.35%	3.60%

The coupling constant of the CH_3 hydrogens is 11 Hz. The product is slightly hygroscopic.

7. Hydrogen phosphate

Concentrated phosphoric acid (Merck pa, 85%, d=1.71) was diluted to the desired concentration and assayed by acid-base titration.

8. 8-Quinolyl phosphate

8-Quinolyl dihydrogen phosphate was synthesized by M.M. Armstrong [139] and used without further purification.

Microanalysis:	C	H	N
Calculated:	48.01%	3.59%	6.22%
Found:	47.95%	3.65%	6.25%

9. 8-Quinolyl methyl phosphate

The monosodium salt of 8-quinolyl methyl phosphate was synthesized by M.M. Armstrong [139] and used without further purification. The ligand is extremely hygroscopic. Stock solutions of 8-quinolyl methyl phosphate were prepared daily and standardized in acid-base titrations.

Microanalysis:	C	H	N
Calculated:	43.02%	3.98%	5.02%
Found:	42.55%	3.85%	4.80%

10. Triphosphate

Pentasodium triphosphate hexahydrate (Sigma 98+%) $Na_5P_3O_{10}\cdot 6H_2O$ was purified on the day before the titrations were performed by two recrystallizations from water-ethanol mixtures [141]. On the day of the titration the salt was passed through Amberlite IR-120 ion exchange resin to convert the sodium salt to the free acid. This was necessary because of the non-negligible complex formation between sodium and triphosphate ion (K=1.64 I=1.0 T=25°C [142], K=2.58 I=0 T=25°C [121]). Unfortunately, it was found impossible to remove 100% of the sodium in such a short time that no hydrolysis occurred. Therefore, the ion exchange was done such that less than 0.5% of the initial sodium was left. This was confirmed by measuring the sodium content of the solution by atomic emission spectroscopy at 589 nm. Unremoved sodium up to 2% of the initial sodium content only affects the stability constants in the third decimal and can therefore be neglected. This was shown by creating synthetic data from literature constants [35] by means of the program library ESTA. The synthetic data were created assuming a certain amount of sodium to be present. The sodium complexation constant and sodium concentration were then deleted and the remaining stability constants refined as if no sodium was present. In order to obtain the "right" answer, it was found that the acid concentration in the vessel had to be refined at the same time, which accounts for the error caused by the incomplete substitution of sodium by protons. If less than 20% of the sodium was assumed not be removed by ion exchange, a linear drop of the three protonation constants was observed. The decrease of the value for protonation constants was 0.0025 per 1% of unremoved sodium. If the "true" protonation constants were fixed, the same decrease was found if a similar analysis was carried out for the copper complexation. If, however, the protonation constants with the "sodium error" were used, the decrease of log β was slightly higher and also depended on the ligand to metal ratio. The maximum error that occurs due to the incomplete ion exchange is thus of the order of 0.005, which is considered to be tolerable. Initially it was thought that the refined acid concentration could be used as an additional criterion for the choice of the right set of complexes because in the calculations on the synthetic data the refined acid concentration always converged to the right value. This, however, is not true for real data, where all kinds of errors seem to accumulate in the refined acid concentration value. Therefore, it was thought safer to determine the acid concentration at the same time as the ligand concentration by titration with tetramethylammonium

hydroxide. This value was compared with the value obtained from the determination of the sodium content of the solution, which agreed within 0.5%. The values obtained from the titrations were used as input values for ESTA.

11. Fluorotriphosphate

$KAg_3P_3O_9F$ was prepared from potassium fluoride and trimetaphosphate $Na_3P_3O_9$ as described in [123]. 20.7g $Na_3P_3O_9 \cdot 6H_2O$ and 11.6g KF were dissolved in 500ml water. After one week this solution was diluted with 1l water and 500ml methanol. 100ml of $AgNO_3$ (1 mol/l) was then added dropwise with stirring. After 30 min of stirring, $Ag_3KP_3O_9F$ had precipitated. The precipitate was filtered and washed three times with 20ml of water/methanol (1:3) mixture. The product was dried over silica gel for 3 days.

Yield: 6.80g (22% based on $Na_3P_3O_9$).

$KAg_3P_3O_9F$ is light sensitive and was kept in the dark.

$KAg_3P_3O_9F$ is insoluble in water. In order to obtain the soluble salt, $KAg_3P_3O_9F$ was slurried in a solution of KCl or $(CH_3)_4NCl$, respectively. After some stirring AgCl precipitated and was filtered off. No suction must be applied as this was found to destroy the ligand.

All attempts to obtain the solid potassium or tetramethylammonium salt failed. When methanol or acetone was added to a solution of $K_4P_3O_9F$ or $((CH_3)_4N)_4P_3O_9F$ a white precipitate formed, but phosphorus nmr showed that the compound had disintegrated. Evaporation of the water of a solution of $K_4P_3O_9F$ or $((CH_3)_4N)_4P_3O_9F$ gave the same result. (Other workers [143] also failed to isolate salts of fluorotriphosphate although they detected its presence in solution by chromatography).

On the day of the titration $KAg_3P_3O_9F$ was stirred in a solution of $(CH_3)_4NCl$ and applied to Amberlite IR 120 ion exchange resin after removal of the AgCl precipitate.

The solution obtained was analyzed for sodium and potassium by atomic absorption spectroscopy at 589 and 766.5 nm, respectively. No sodium could be detected and more than 99.5% of the initial potassium was removed. A phosphorus-nmr spectrum of fluorotriphosphate is shown in figure A.5.

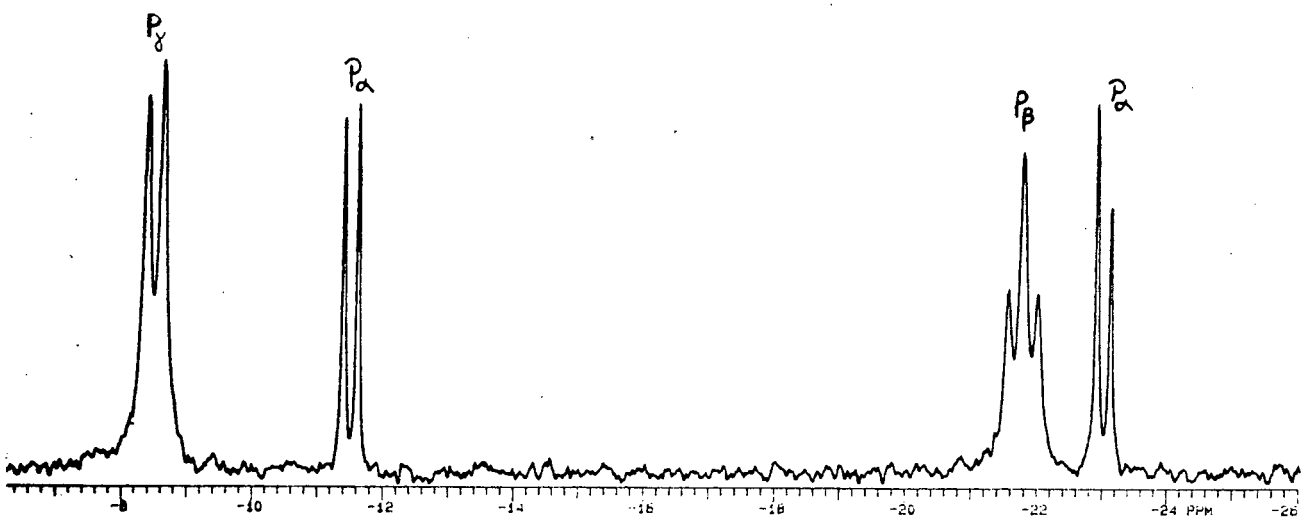

Figure A.5: ^{31}P-nmr spectrum of fluorotriphosphate at pH=5.56

The triplet is assigned to the central phosphate. The doublet at low field corresponds to the terminal or γ phosphate. The strong interaction between fluorine and P_α causes a splitting of the P_α doublet into a doublet of doublets with a coupling constant of 931±2 Hz as is expected for F-P coupling [144]. The spectrum clearly shows the absence of phosphates other than the product. It has been demonstrated [123] that fluorotriphosphate is most stable against hydrolysis in acidic solution. Solutions prepared as described above were therefore kept in acid and used within 5 hours.

12. Methyltriphosphate

Four different approaches were employed in the synthesis of methyltriphosphate:

1. This procedure has been successfully used to synthesize adenosine triphosphate [145] and γ-phenylpropyltriphosphate [146]. The first step was the synthesis of dimethyl phosphoryl chloride from trichlorophosphate and methanol (1:2 molar ratio). Dimethyl phosphoryl chloride was then reacted with morpholine (1:1 molar ratio) in ether below 10°C [147]. Dimethyl phosphoromorpholidate was obtained and purified by destillation (Bp=98-101°C, P=0.7mmHg). The purity was

confirmed by proton nmr and determination of the refractive index (n=1.4550, literature value n=1.4530 [147]). The compound was then treated with an excess of trimethylamine in acetonitrile at 60°C over night to obtain methyl phosphoromorpholidate as the tetramethylammonium salt. The product precipitated out of solution after cooling to room temperature as white needles. The purity was confirmed by proton nmr. This intermediate was added to di-(tri-n-butylammonium) dihydrogen diphosphate in pyridine at room temperature. The reaction was attempted using different ratios between the intermediate and diphosphate. It was followed by both proton and phosphorus nmr, but no sign of a product appeared. A possible reason might be the low solubility of methyl phosphoromorpholidate in pyridine, so that the solution was too dilute. Unfortunately, no better solvent was found, and the approach was abandoned.

2. The successful synthesis of methyltriphosphate from dimethylsulphate and sodium triphosphosphate in alkaline solution has been indicated in the literature without describing the detailed procedure [127]. Different ratios between sodium triphosphate and dimethyl sulfate in water were employed, but the desired product was never obtained. The problem may once again be the choice of the right solvent. No solvent was found that could dissolve both dimethyl sulfate and pentasodium triphosphate. The addition of a small amount of $(C_4H_9)_4NHSO_4$, which was supposed to dissolve some of the pentasodium triphosphate in an organic solvent (benzene, carbon tetrachloride, acetonitrile, dioxane, dimethylsulfoxide) did not lead to any success. Eventually, this attempt was also dropped. For comparison, however, methyl monophosphate was successfully prepared in a test tube experiment from disodium hydrogen phosphate and dimethyl sulfate in water after shaking the mixture for twenty minutes at room temperature. The product was detected by proton-nmr.
3. The third approach involved the reaction of methyl iodide with sodium triphosphate. As a preliminary experiment, it was attempted to fuse methyl iodide with disodium hydrogen phosphate in alkaline solution. Unfortunately, methyl iodide hydrolyzed before any reaction took place. Because the reaction with the sodium triphosphate was expected to be even slower, this approach was not pursued any further.
4. The synthesis of tetrasodium methyltriphosphate from trisodium trimetaphosphate and methanol in alkaline solution is described in the literature [148]. To 25g $Na_3P_3O_9 \cdot 6H_2O$ in 120ml H_2O were added 364ml of methanol and 60ml of NaOH (1 mol/l). This solution was

diluted to 1l and left for three weeks in a stoppered flask. After this time a slight decrease in volume was observed and a white precipitate had formed ($Na_5P_3O_{10}\cdot 6H_2O$) which was discarded. To the solution, 100ml of nitric acid (1 mol/l) was added, upon which the pH dropped to about 4. The pH was then raised to pH=9 by the addition of concentrated ammonia. The precipitate that formed after the addition of 20ml of silver nitrate (1 mol/l) was discarded. The precipitate that formed after the addition of further 180 ml of silver nitrate was collected and washed with methanol-water mixture (1:1), methanol and ether. It was dried over silica gel.

Yield: 7g of $Ag_4P_3O_{10}CH_3\cdot H_2O$

On the next day 10ml NaCl (2 mol/l) was added to a mixture of 3.7g $Ag_4P_3O_{10}CH_3\cdot H_2O$ and 15ml water in an ice bath. Silver chloride precipitated and was filtered off. 200ml of methanol was added to the solution which was then kept in a freezer for three hours. A fine pricipitate formed. 400ml of acetone was added, the precipitate was collected and washed with ethanol and ether. It was dried over silica gel. The product is hygroscopic.

The yields obtained in three different syntheses were always very much lower than the yields reported in the literature. Although phosphorus-nmr showed the right pattern, namely two doublets and one triplet, two doublets instead of one for the CH_3-group were found on the proton-nmr spectrum. This agrees with the fact that the percentage carbon and hydrogen found by microanalysis was always higher than expected. All attempts to recrystallize the hygroscopic product did not remove the impurity.

Finally, the synthesis of methyltriphosphate was given up.

13. Phenyltriphosphate and p-Nitrophenyltriphosphate

A procedure for the synthesis of phenyltriphosphate from phenol and trimetaphosphate in aqueous solution is described in the literature [128] and was followed. To 55.19g of $P_3O_9Na_3\cdot 6H_2O$ in 200ml of water was added 117g of phenol and 50 ml NaOH (1 mol/l). This two-phase mixture was shaken for ten days. During the reaction the organic layer turned dark brown. On the tenth day the two phases (130ml of organic phase, 250ml of aqueous phase) were separated. The aqueous phase, which was yellowish (pH=9), was brought to pH=5 by adding nitric acid (1 mol/l). A small amount of a white precipitate formed and was discarded. The solution was then shaken twice with 480ml of ether and 250ml of ether, respectively, after which the yellow colour had disappeared. 250ml of

water was added to the 250ml of solution and the pH was raised to pH=7 by the addition of ammonia (1 mol/l). 24ml of silver nitrate (1 mol/l) was added, and the white precipitate that immediately started to form was filtered after thirty minutes of stirring. Another 50ml of silver nitrate was added and again, a white precipitate was collected after fourty minutes. The two fractions were washed with ethanol-water mixture (1:1) and subsequently with ethanol, and were air dried.

Yield: 1.4g (1.4% based on trimetaphosphate) of a crude product which could not be identified as the desired compound. Microanalysis yielded low percentages for carbon and hydrogen.

At the same time, the synthesis of p-nitrophenyltriphosphate was attempted by the same procedure, but the reaction time was extended to three month. No product was obtained. One of the reasons is probably the poor solubility of p-nitrophenol in water.

REFERENCES

[1] D.R. Williams, The Metals of Life,
Van Nostrand Reinhold Company, London, 1971

[2] ed. H. Sigel, Metal Ions in Biological Systems, vol.1-19,
Marcel Dekker, Inc., New York and Basel, 1974-1985

[2a] ed. H. Sigel, Metal Ions in Biological Systems, vol.5,
Marcel Dekker, Inc., New York and Basel, 1976

[2b] ed. H. Sigel, Metal Ions in Biological Systems, vol.8,
Marcel Dekker, Inc., New York and Basel, 1979

[2c] ed. H. Sigel, Metal Ions in Biological Systems, vol.13,
Marcel Dekker, Inc., New York and Basel, 1981

[2d] ed. H. Sigel, Metal Ions in Biological Systems, vol.14,
Marcel Dekker, Inc., New York and Basel, 1982

[2e] ed. H. Sigel, Metal Ions in Biological Systems, vol.15,
Marcel Dekker, Inc., New York and Basel, 1983

[3] P.M. Harrison, R.J. Hoare, Metals in Biochemistry,
Chapman and Hall, London, 1980

[4] Ed. A.V. Xavier, Frontiers in Bioinorganic Chemistry,
VCH Verlagsgesellschaft mbH, Weinheim (Germany), 1986

[5] JRJ Sorensen, Chem. Br., Dec. 1984, 1110

[6] R.B. Lauffer, Chem. Rev. 87, 901, 1987

[7] S.J.R. Phillips, Chem. Rev. 66, 501, 1966

[8] ed. J.N. Hawthorne, G.B. Ansell, New Comprehensive Biochemistry
vol4: Phospholipids, Elsevier Biochemical Press 1982

[9] J.R. Cox, O.B. Ramsay, Chem. Rev. 64, 317, 1964

[10] F.H. Westheimer, Chem. Rev. 81, 313, 1981

[11] N. Bourne, A. Williams, J. Org. Chem. 49, 1200, 1984

[12] M.T. Skoog, W.P. Jencks, J. Am. Chem. Soc. 106, 7597, 1984

[13] D. Herschlag, W.P. Jencks, J. Am. Chem. Soc. 108, 7938, 1986

[14] C.A. Bunton, E.J. Fendler, E. Humeres, K. Yang,
J. Org. Chem. 32, 2806, 1967

[15] Y. Murakami, J. Sunamoto, J. Chem. Soc. Perkin II, 1235, 1973

[16] Ed. M. Florkin, E.H. Stolz,
Comprehensive Biochemistry, vol.15, ch.4, Elsevier, 1964

[17] J.A. Gerlt, Chem. Rev. 87, 1079, 1987

[18] Ed. P.D. Boyer, The Enzymes, vol.2, ch.9,
Academic Press New York, 1970

[19] C.M. Frey, J.E. Stuehr, J. Am. Chem. Soc. 94, 8898, 1972

[20] J.J. Butzow, G.L. Eichhorn, J. Inorg. Biochem. 28, 21, 1986

[21] R.C. Phillips, P. George, R.J. Rutman,
J. Biol. Chem. 244, 3330, 1969
[22] Y. Murakami, J. Sunamoto, Bull. Chem. Soc. Jpn. 44, 1827, 1971
[23] Y. Murakami, M. Takagi, J. Am. Chem. Soc. 91, 5130, 1969
[24] Y. Murakami, M. Takagi, Bull. Chem. Soc. Jpn. 42, 3478, 1969
[25] S.J. Benkovic, L.K. Dunikoski, J. Am. Chem. Soc. 93, 1526, 1971
[26] R. Hofstetter, Y. Murakami, G. Mont, A.E. Martell,
J. Am. Chem. Soc. 84, 3041, 1962
[27] R.W. Hay, A.K. Basak, Inorg. Chim. Acta 79, 255, 1983
[28] Y. Murakami, M. Tanaka, Bull. Chem. Soc. Jpn. 39, 122, 1966
[29] F. Ramirez, J.F. Maracek, J. Szamosi, J. Org. Chem. 45, 4748, 1980
[30] M. Watanabe, M. Matsuura, T. Yamada,
Bull. Chem. Soc. Jpn. 54, 738, 1981
[31] R.M. Milburn, M. Gautam-Basak, R. Tribolet, H. Sigel,
J. Am. Chem. Soc. 107, 3315, 1985
[32] P.R. Norman, P.F. Gilletti, R.D. Cornelius,
Inorg. Chim. Acta 82, L5, 1984
[33] E. Bamann, W. Mütterlein, Chem. Ber. 91, 471, 1958
[34] E. Bamann, W. Mütterlein, Chem. Ber. 91, 1322, 1958
[35]-A.E. Martell, R.M. Smith, Critical Stability Constants,
vol.1: Amino Acids, Plenum Press, New York, 1974
-R.M. Smith, A.E. Martell, Critical Stability Constants,
vol.2: Amines, Plenum Press, New York, 1975
-A.E. Martell, R.M. Smith, Critical Stability Constants,
vol.3: Other Organic Ligands, Plenum Press, New York, 1977
-R.M. Smith, A.E. Martell, Critical Stability Constants,
vol.4: Inorganic Complexes, Plenum Press, New York, 1976
-A.E. Martell, R.M. Smith, Critical Stability Constants,
vol.5: First Supplement, Plenum Press, New York, 1982
[36]-J. Bjerrum, G. Schwarzenbach, L.G. Sillen,
Stability Constants of Metal-ion Complexes,
Part 1: Organic Ligands, The Chemical Society (London),
Special Publication No. 6, 1957
-J. Bjerrum, G. Schwarzenbach, L.G. Sillen,
Stability Constants of Metal-ion Complexes,
Part 2: Inorganic Ligands, The Chemical Society (London),
Special Publication No. 7, 1957
-J. Bjerrum, G. Schwarzenbach, L.G. Sillen,
Stability Constants of Metal-ion Complexes,
The Chemical Society (London), Special Publication No. 17, 1964

-L.G. Sillen, A.E. Martell,
Stability Constants of Metal-ion Complexes, Supplement No. 1,
The Chemical Society (London), Special Publication No. 25, 1971

[37]-E. Högfeld, Stability constants of metal-ion complexes,
Part A: Inorganic Ligands, Pergamon Press, 1982
(IUPAC Chemical data series No. 21)
D.D. Perrin, Stability constants of metal-ion complexes,
Part B: Organic Ligands, Pergamon Press, 1979
(IUPAC Chemical data series No. 22)
-D.D. Perrin, Ionisation constants of inorganic acids and bases
in aqueous solution,
Pergamon Press, 1982 (IUPAC Chemical data series No. 29)

[38] H. Sigel, J. Inorg. Nucl. Chem. 39, 1903, 1977

[39] T.A. Glassman, C. Cooper, L.W. Harrison, T.J. Swift,
Biochemistry 10, 843, 1971

[40] R.D. O'Brian, Insecticides-Action and Metabolism,
Academic Press, New York, 1967

[41] L.G. Nickell, Plant Growth Regulators, Springer Verlag, 1982

[42] Mellor's Comprehensive Treatise on Inorganic and Theoretical
Chemistry, vol. 8, supplement 3: Phosphorus, Longman, 1971

[43] Chemical Abstracts, Subject Index

[44] C. Yuan, S. Li, H. Long, Phosphorus Sulfur 18, 323, 1983

[45] M. Tetas, J.M. Lowenstein, Biochemistry 2, 350, 1963

[46] F. Tafesse, R.M. Milburn, Inorg. Chim. Acta 135, 119, 1987

[47] K. Murray, P.W. Linder, J. Soil Sci. 35, 217, 1984

[48] P.W. Linder, A. Voye, J. Coord. Chem, in press

[49] R.M. Garrels, M.E. Thompson, Am. J. Sci. 260, 57, 1962

[50] L.G. Sillen, Chem. Br., 291, July 1967

[51] R.E. McDuff, F.M.M. Morel, Environ. Sci. Technol. 14, 1182, 1980

[52] F.F.M. Morel, J.C. Westall, C.R. O'Melia, J.J.Morgan,
Environ. Sci. Technol. 9, 756, 1975

[53] P.W. Linder, J.C. Little, Inorg. Chim. Acta 123, 137, 1986

[54] P.M. May, P.W. Linder, D.R. Williams,
J. Chem. Soc. Dalton, 588, 1977

[55] C.D. Johnson, The Hammett Equation, Cambridge University Press 1980

[56] D.D. Perrin, B. Dempsey, E.P. Serjeant, pK_a Prediction for Organic
Acids and Bases, Chapman and Hall, London, 1981

[57] L.G. Van Uitert, W.C. Fernelius, J. Am. Chem. Soc 76, 379, 1954

[58] Z.L. Ernst, F.G. Herring, Trans. Faraday Soc. 61, 454, 1965

[59] J.G. Jones, J.B. Poole, J.C. Tomkinson, R.J.P. Phillips, J. Chem. Soc. 2001, 1958
[60] H. Irving, J.J.R.F. Da Silva, J.Chem. Soc., 3308, 1963
[61] M.S. Sun, D.G. Brewer, Can. J. Chem. 45, 2729, 1967
[62] H.M.N.H. Irving, M.G. Miles, J. Chem. Soc. (A), 1268, 1966
[63] H. Irving, H. Rossotti, Acta Chem. Scand. 10, 72, 1956
[64] E. Nieboer, W.A.E. McBryde, Can. J. Chem. 48, 2549, 1970
[65] E. Nieboer, W.A.E. McBryde, Can. J. Chem. 48, 2565, 1970
[66] E. Nieboer, W.A.E. McBryde, Can. J. Chem. 51, 2512, 1973
[67] S. Ehrenson, R.T.C. Brownlee, R.W. Taft, Prog. Phys. Org. Chem. 10, 1, 1973
[68] R.D. Hancock, F. Marsicano, Inorg. Chem. 17, 560, 1978
[69] R.D. Hancock, F. Marsicano, Inorg. Chem. 19, 2709, 1980
[70] L.P. Hammett, Physical Organic Chemistry, ch.7, McGraw-Hill, New York 1940
[71] T.A. Mastryukova, M.I. Kabachnik, J. Org. Chem. 36, 1201, 1971
[72] O. Mäkitie, S. Mirttinen, Acta Chem. Scand. 25, 1146, 1971
[73] A.I. Rezvukhin, G.N. Dolenko, S.A. Krupoder, Magn. Res. Chem. 23, 221, 1985
[74] N.S. Isaacs, Physical Organic Chemistry, Longman Scientific & Technical, 1987
[75] R.M. Izatt, J.H. Rytting, L.D. Hansen, J.J. Christensen, J. Am. Chem. Soc. 88, 2641, 1966
[76] R. Gut, E. Schmid, J. Serrallach, Helv. Chim. Acta 54, 593, 1971
[77] Chemical Abstracts 46: 9953a
[78] CRC Handbook of Chemistry and Physics, 68th edition, 1987
[79] J.J. Christensen, J.H. Rytting, R.M. Izatt, J. Chem. Soc. (B), 1646, 1970
[80] R.M. Izatt, J.H. Rytting, L.D. Hansen, J.J. Christensen, Am. Chem. Soc. J. 88, 2641, 1966
[81] P. De Maria, A. Fini, Tetrahedron 33, 553, 1977
[82] S.D. Hamann, M. Linton, J. Chem. Soc. Faraday I, 70, 2239, 1974
[83] M.M. Fickling, A. Fischer, B.R. Mann, J. Packer, J. Vaughan, J. Am. Chem. Soc. 81, 4226, 1959
[84] W.A.E. McBryde, Can. J. Chem. 46, 2385, 1968
[85] A.G. Desai, R.M. Milburn, J. Am. Chem. Soc. 91, 1958, 1969
[86] C.F. Baes, R.M. Mesmer, The Hydrolysis of Cations, John Wiley & Sons, New York, 1976
[87] I. Qvarfort-Dahlman, Chem. Scr. 8, 112, 1975

[88] F. Rossotti, H. Rossotti, The Determination of Stability Constants, McGraw Hill, London, 1961

[89] F.R. Hartley, C. Burgess, R. Alcock, Solution Equilibria, Ellis Horwood Limited, 1980

[90] P.M. May, K. Murray, D.R. Williams, Talanta 32, 483, 1985

[91] A. Sabatini, A. Vacca, P. Gans, Talanta 21, 53, 1974

[92] A.K. Covington, Ion-selective Electrode Methodology, vol. 1 and 2, CRC Press, 1979

[93] J.R. Van Wazer, E.J. Griffith, J.F. McCullough, J. Am. Chem. Soc. 74, 4977, 1952

[94] A. Albert, D. Serjent, Ionisation Constants of Acids and Bases, p.20, Methuen, 1962

[95] P.W. Linder, K. Murray, Talanta 29, 377, 1982

[96] W.C. Hamilton, Acta Cryst. 18, 502, 1965

[97] K. Murray, P.M. May, Anal. Proc. 21, 364, 1984

[98] J.J. Christensen, J.W. Garner, D.J. Eatough, R.M. Izatt, Rev. Sci. Instrum. 44, 481, 1973

[99] Tronac operationg instructions for the calorimeter

[100] J.J. Christensen, L.D. Hansen, R.M. Izatt, Handbook of Proton Ionization Heats and related Thermodynamic Quantities, John Wiley and Sons, New York, 1976

[101] P.S. Chen, T.Y. Toribara, H. Warner, Anal. Chem. 28, 1756, 1956

[102] D. Herschlag, W.P. Jencks, J. Am. Chem. Soc. 109, 4665, 1987

[103] J.D. Chanley, E.Feageson, J. Am. Chem. Soc. 77, 4002, 1955

[104] J.I. Watters, E.D. Loughran, S.M. Lambert, J. Am. Chem. Soc. 78, 4855, 1956

[105] O. Mäkitie, V. Konttinen, Acta Chem. Scand. 23, 1459, 1969

[106] W.E. Trevelyan, P.F.E. Mann, J.S.Harrison, Arch. Biochem. Biophys. 39, 419, 1952

[107] J.H.Ashby, H.B. Clarke, E.M. Crook, S.P.Datta, Biochem. J. 59, 203, 1955

[108] C.F. Cori, S.P. Colowick, G.T. Cori, J. Biol. Chem. 121, 465, 1937

[109] B.E. Doody, E.R. Tucci, R. Scruggs, N.C. Lee, J. Inorg. Nucl. Chem. 28, 833, 1966

[110] H.B. Clarke, S.P. Datta, Biochem. J. 64, 604, 1956

[111] J.H. Ashby, E.M. Crook, S.P. Datta, Biochem. J. 56, 198, 1954

[112] C.A. Bunton, D.R. Llewellyn, K.G. Oldham, C.A. Vernon, Chem. Soc. J. 3574, 1958

[113] H. Brintzinger, Helv. Chim. Acta 48, 47, 1965

[114] C.W. Childs, Inorg. Chem. 9, 11, 2465, 1970
[115] H. Sigel, K. Becker, D.B. McCormick,
Biochim. Biophys. Acta 148, 655, 1967
[116] G. Anderegg, Helv. Chim. Acta 57, 1340, 1974
[117] G.E. Jackson, K.V.V. Voyi, S. Afr. J. Chem. 41, 17, 1988
[118] G. Anderegg, Helv. Chim. Acta 48, 1712, 1965
[119] H. Ellison, A.E. Martell, J. Inorg. Nucl. Chem 26, 1555, 1964
[120] R.R. Irani, C.F. Callis, J. Am. Chem. Soc. 64, 1398, 1960
[121] J.A. Wolhoff, J.Th.G. Overbeek, Rec. Trav. Chim. 78, 759, 1959
[122] S.J. Rehfeld, H.F. Loken, Thermochim. Acta 18, 265, 1977
[123] W. Feldmann, Z. Anorg. Allg. Chem. 338, 235, 1965
[124] Chemical Abstracts 105: 214715x
[125] H. Irving, H. Rossotti, Acta Chem. Scand. 10, 72, 1956
[126] F. Franks, Water, vol.3, page 55, Plenum Press New York 1973
[127] P.W. Schneider, H. Brintzinger, H. Erlenmeyer,
Helv. Chim. Acta, 47, 993, 1964
[128] W. Feldmann, Chem. Ber. 99, 3251, 1966
[129] D.L. Miller, F.H. Westheimer. J. Am. Chem. Soc., 88, 1514, 1966
[130] W. Feldmann, E. Thilo, Z. Anorg. Allg. Chem. 328, 113, 1964
[131] P.R. Mitchell, H. Sigel, Eur. J. Biochem. 88, 149, 1978
[132] M.E. Heyde, L. Rimai, Biochemistry 10, 1121, 1971
[133] Vogel's Textbook of quantitative inorganic analysis,
4th edition, Longman Group Limited, New York 1981
[134] F.J.C. Rosotti, H. Rosotti, J. Chem. Ed. 42, 7,375, 1965
[135] P.L. Pickard, W.E.Neptune, Anal. Chem. 27, 1358, 1955
[136] Merck AG: Complexometric Assay Methods with Titriplex, 3rd edition
[137] J.I. Watters, S. Kalliney, R.C. Machen,
J. Inorg. Nucl. Chem. 31, 3817, 1969
[138] A.I. Vogel, Practical Organic Chemistry, 3rd edition, Longman 1967
[139] M.M. Armstrong, M.Sc. thesis, University of Cape Town, 1984.
[140] Bull. Soc. Chim. France 9, 314, 340, 405, 421, 1942
[141] O.T. Quimby, J. Phys. Chem. 58, 603, 1954.
[142] J.I. Watters, E.D. Loughran, S.M. Lambert,
J. Am. Chem. Soc. 79, 3651, 1957
[143] M.H. Grunze, I. Grunze, Bull. Soc. Chim. France, 1675, 1968.
[144] J. Emsley, D. Hall, The Chemistry of Phosphorus, Ch. 3,
Harper and Row, London, 1976
[145] J.G. Moffatt, H.G. Khorana, J. Am. Chem. Soc., 83, 649, 1961.
[146] D.L. Miller, F.H. Westheimer, J. Am. Chem. Soc. 88, 1514, 1966.

[147] J. Cheymol, P. Chabrier, M. Selim, T.N. Thanh,
Compte Rendue de l'Academie des Sciences Paris, 249, 1240, 1959

[148] W. Feldmann, Chem. Ber. 100, 3850, 1967.

[149] S. Cabani, J. Chem. Soc. 5271, 1962

[150] A.Avdeef, D.L. Kearney, J.A. Brown, A.R. Chemotti, Anal. Chem. 54, 2322, 1982

[151] G.J. Lloyd, B.S. Cooperman, J. Am. Chem. Soc. 93, 4883, 1971

[152] O.M. Friedman, A.M. Seligman, J. Am. Chem. Soc. 72, 624, 1950.

10 AUG 1989